RESEARCH FOR ABATEMENT OF
LEAKS FROM UNDERGROUND STORAGE TANKS
CONTAINING HAZARDOUS SUBSTANCES

U.S. E.P.A. CONTRACT NO.   68-03-3409

DRAFT
FINAL REPORT

PHASE 1 OF
MODELING VAPOR PHASE MOVEMENT
IN RELATION TO
UST LEAK DETECTION

EPA WORK ASSIGNMENT NO. 1-4
25 FEBRUARY 1988

CAMP DRESSER & McKEE, INC.

DISCLAIMER

This report is an external draft for review purposes only and does not constitute Agency policy. Mention of trade names or commercial products does not constitute endorsement or recommendation for use.

CDM

environmental engineers, scientists,
planners, & management consultants

CAMP DRESSER & McKEE INC.

One Center Plaza
Boston, Massachusetts 02108
617 742-5151

February 25, 1988

Mr. Philip Durgin
Technical Project Monitor
US EPA/EMSL
944 East Harmon
Las Vegas, Nevada 89109

Subject: "Modeling Vapor Phase Movement in Relation to
UST Leak Detection."
Work Assignment No.: 1-4
EPA Contract No.: 68-03-3409

Dear Mr. Durgin:

We are pleased to submit this Draft Final Report on Phase 1 of
"Modeling Vapor Phase Movement in Relation to UST Leak Detection." We
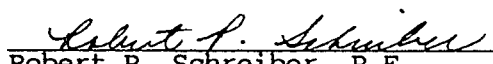look forward to meeting with you to discuss the findings in the
report.

Very truly yours,   APPROVED:

CAMP DRESSER & McKEE INC.   CAMP DRESSER & McKEE INC.

Myron S. Rosenberg   Robert P. Schreiber, P.E.
Deputy Project Director   Work Assignment Manager

Enclosure

RESEARCH FOR ABATEMENT OF
LEAKS FROM UNDERGROUND STORAGE TANKS
CONTAINING HAZARDOUS SUBSTANCES

U.S. E.P.A CONTRACT NO. 68-03-3409

DRAFT
FINAL REPORT
ON PHASE 1 OF
MODELING VAPOR PHASE MOVEMENT
IN RELATION TO
UST LEAK DETECTION

EPA WORK ASSIGNMENT NO. 1-4

Prepared by: _~Robert P. Schreiber~_ Date __2/25/88__
Robert P. Schreiber, P.E.
Work Assignment Manager
Camp Dresser & McKee Inc.

Approved by: _~Myron Rosenberg~_ Date __2/25/88__
Myron S. Rosenberg, Ph.D., P.E.
Deputy Project Director

Approved by: _~David F. Doyle~_ Date __25 February '88__
David F. Doyle, P.E.
Project Director

ABSTRACT

Diffusive transport of hydrocarbon vapors in the soil from a leaking underground storage tank (UST) was simulated with a three-dimensional groundwater flow model. This modeling was performed by analogy between Fick's Second Law of diffusion and the confined groundwater flow equation.

A model of a cylindrical UST, emplaced in backfill and surrounded by native soils, was designed. The tank was 6 feet in diameter by 12 feet in length and was surrounded on all sides by backfill to a thickness of 2 feet. The ground surface was assumed to be paved and impervious to vapors.

A synthetic gasoline blend, incorporating commonly occurring chemical constituents of commercial gasolines, was devised for the vapor transport simulations. Physicochemical properties, such as air diffusion coefficients and equilibrium vapor concentrations, were taken from the literature. Soil-air diffusion coefficients for the gasoline blend incorporated a formulation for porous medium tortuosity given by Millington and Quirk (1961).

Simulations were designed to examine the importance of moisture content and total porosity in the native soils and backfill. These properties were varied from "average" conditions in gravel backfill and sandy soil to "wet" or "very wet" conditions in low porosity materials.

The model results indicated that decreasing the soil-air diffusion in the native soil would be expected to have an insignificant influence on diffusion, under the same backfill conditions. Similar changes in the backfill, however, strongly influenced diffusive transport. These results, while hardly surprising, underscore the importance of understanding the physical properties of the backfill.

Additional simulations were performed to test the effects of an unpaved surface. They showed that an unpaved surface is expected to have an insignificant influence on sensor response.

Results of the simulations also indicated that low molecular weight alkanes (e.g., isobutane, n-butane, isopentane, n-pentane) are predicted to be detected much earlier by external, passive vapor sensors at the same threshold vapor concentration than would aromatic compounds (e.g., benzene, toluene, xylene) or heavy molecular weight compounds (C_9-C_{12} aliphatics). This result argues for the development of sensors specific to those compounds in gasoline having high vapor concentrations and diffusion coefficients. Furthermore, analysis with an expression based on Henry's Law indicated that those compounds such as the C_4-C_5 alkanes are expected to suffer little attenuation due to water-air phase partitioning.

i

Simulation results were presented as time histories of vapor concentrations in the backfill, and as time histories of the vaporized gasoline. It was found that, even under the most conservative simulation conditions, total gasoline hydrocarbon concentrations of 500 parts per million were predicted to reach halfway across the backfill by one month. Under "average" conditions, this threshold concentration was reached at all points within the backfill by less than one month.

The modeling also predicted that vaporization rates of about 10^{-4} gallons per hour would be detected by vapor sensors in the backfill within one month. This compares favorably to in-tank detection methods that may achieve detection at rates of 0.2 gallons per hour, with allowable sampling intervals of several months. The early detection time afforded by external, passive vapor sensors translates into low liquid gasoline volumes lost to vaporization, providing a high degree of "protection" about an UST.

Recommendations on sensor network design were made, considering the effects of soil conditions and temperatures. For the simulated hypothetical UST, a plot of sensor distance from the leak versus volume of vaporized gasoline before detection occurs showed an "optimum" sensor spacing of about 10 feet.

Further investigations should include an improved characterization of the leakage source of vapors, and the quantification of the effects of density-driven vapor transport.

ACKNOWLEDGEMENTS

CONTENTS

LIST OF APPENDICES

LIST OF FIGURES

NOTE: All figures are found at the end of their corresponding section, following the text and preceding the tables.

NOTE: All figures are found at the end of their corresponding section, following the text and preceding the tables.

LIST OF TABLES

Note: All tables are found at the end of their corresponding section,
       following the figures.

1.0 OBJECTIVES

1.1 OVERVIEW

The objectives of this work assignment are to use modeling of vapor phase contaminants emanating from a leaking Underground Storage Tank (UST) to improve the understanding of vapor transport in the vicinity of a leaking UST. Modeling is used to simulate and analyze the sensitivity of contaminant vapor concentrations, measured at sensor sampling points, to variations in the parameters governing vapor transport.

The processes that govern vapor transport in the excavation zone underlie the selection of simulation modeling and analysis tools. Using information from other portions of EPA's UST research program, (e.g., the testing of sensor detection capabilities), the modeling of vapor transport helps identify the parameters of vapor transport most critical to network design. Also, this work yields results that can be used to guide the design of field programs for the testing of vapor sensors.

1.2 CONCEPTUAL APPROACH

This research effort provides technical information on the transport of vapors in the UST excavation zone from a leak source to an external vapor sensor. The findings aid in understanding external leak detection methods and network design. In its proposed UST regulations, EPA's Office of Underground Storage Tanks (OUST) has expressed a preference for adopting method-specific performance requirements, partly because soil vapor sensing and subsurface vapor transport were considered to be poorly-understood. Since vapor sensors may act, however, as "early warning" devices, EPA/OUST did not want external detection to be excluded from consideration prior to more study. This report is directed at this need.

This project was designed to produce technical information consistent with EPA's "four-parameter" approach to setting regulations for leak detection systems. The four parameters are:

- release rate;
- probability of detection (P_D);
- probability of false alarms (P_{FA});
- and frequency of testing.

Each of these is discussed separately below.

Release Rate

The release rate was addressed in this research effort through the development of a methodology, called "base" volatilization, in which the UST leak was treated as a point source at the bottom of the tank. By assuming that there is sufficient leaking product to maintain a constant concentration source of vapor which diffuses into the excavation zone, the simulation model yielded estimates of instantaneous, time-varying leak rates based on the ability of the excavation zone and native soil to transport the diffusing vapors. When integrated over time, the vaporization rates provided estimates of the minimum volume of leaked product lost to vaporization from initiation of the leak until detection. These estimates were made for different combinations of soil conditions, temperatures, and leaked products.

Probability of Detection

The probability of detection, P_D, is comprised of a sensor-related component, and for vapor monitors, another component that is determined by network design and vapor transport processes and parameters. The component related to the sensor performance is being investigated by Radian Corporation under a separate work assignment.

The P_D component determined by network design and vapor transport phenomena was addressed by the vapor transport modeling described herein. For example, spacing vapor sensors 5 feet apart rather than 10 feet has been shown to yield a higher P_D as expected. The effects of varying the location and density of vapor sensors were analyzed with the modeling techniques. Plots of concentration versus time at potential sensor locations were produced by the simulation model, and were used as the basis for comparing sensor performance under different conditions of soil moisture, soil properties, and temperature.

Probability of False Alarm

The probability of false alarm (P_{FA}) is assumed to be primarily a function of the detector hardware, although background vapor concentrations in the subsurface can also contribute to P_{FA}. The probability of false alarm, however, was not included in this study at this time.

Sampling Frequency

The fourth regulatory parameter, sampling frequency, is a key variable in designing a leak detection network. Vapor transport modeling has provided estimates of vapor movement rates, from which diffusive rates from a leak to a sensor were estimated directly. Other types of modeling results presented herein illustrate vapor concentration versus time at a given point in space. These results, in conjunction with the network design work at the Environmental Research Center of the University of Nevada at Las Vegas (UNLV/ERC) and the device testing by Radian Corporation, are intended to provide EPA with the basis for selecting suggested sampling frequencies for vapor sensors.

In summary, the overall objective of this work assignment is to build the technical foundation, based on modeling, for understanding the aspects of subsurface vapor transport that are important to vapor

monitoring network design. From this foundation, EPA will be in a better position to promulgate method-specific performance requirements for vapor detection systems, and ultimately general performance standards for all leak detection methods, including vapor sensors.

1.3 PHASE 1 REPORT OBJECTIVES

This report was intended to provide an initial understanding and estimation of possible vapors sensor performance, assuming diffusion-dominated transport of vapors from a single leaking UST. Recommendations for further work, by including investigations of leak characterization and modeling of leaking pipeline systems are made, including simulation of "sandbox" vapor experiments now being conducted by the Oregon Graduate Center.

The purpose of this Phase I Final Report is to present and discuss the results of the UST vapor transport simulations performed under this work assignment. Section 2 of this report describes the development of a typical, or "generic" UST, which was used as the basis for the modeling, presenting the simulation methodology and analytical techniques that were developed and used. Section 3 includes graphical depictions of the modeling results, emphasizing the changes in vapor transport due to variations in soil conditions and temperature. Discussions of the implications of the simulation results appear in Section 4 with recommendations for Phase 2 activities.

The appendices to this report provide the technical foundation for this study, and they can serve as a valuable source of information for investigators. The appendices provide other researchers sufficient information to reproduce the results presented in this report. The appendices include: a glossary; a variable dictionary; a presentation of the governing equations used in the vapor transport modeling; a discussion of how CDM's DYNFLOW model was used for vapor transport simulations; estimation of physicochemical properties of gasolines;

development and presentation of equations used to estimate the modeling parameters; an analysis of the potential effects of vapor-water partitioning; verification of the DYNFLOW model versus an analytical solution; a comparison of DYNFLOW and the U.S. Geological Survey's MODFLOW program; a listing of the simulated UST conditions; and listings of the simulation model command files and simulated time histories of vapor concentrations and volatilized volumes.

2.0 TECHNICAL APPROACH

2.1 SYSTEM CONCEPTUALIZATION

Development of a conceptual model was the first step in modeling vapor transport from a leaking UST. This system conceptualization formed the basis for the mathematical model of the system.

In formulating the system conceptualization, important processes to vapor transport were included, whereas unimportant ones were neglected. The conceptualization addressed such issues as tank and sensor configuration, source characterization, hydrological conditions, and fate and transport processes. This system conceptualization represents an abstraction of a hypothetical leaking UST, including important features of the system, from which a generic model of the UST system and surrounding excavation zone was developed. The generic UST model was then used to perform vapor transport simulations.

2.1.1 FATE AND TRANSPORT PROCESSES

The various processes which govern the fate and transport of contaminant vapors in the vicinity of a leaking UST are described in detail in reports by EPA (1987) and CDM (1986). In summary, the migration of contaminants released from underground storage tanks is governed by a complex combination of processes involving multi-phase transport. That is, the contaminant can be transported as a dissolved component in water, as a volatile component in air, or as a separate immiscible liquid.

When a leak starts, an immiscible fluid phase consisting of one or more petroleum constituents leaks from the tank and migrates downward through the excavation zone due to gravity. Capillary forces cause the downward migrating liquid to spread laterally. Due to volatilization of the lighter constituents, a gaseous envelope of contaminant vapor will surround the immiscible fluid phase.

This contaminant vapor may diffuse or be advected and dispersed into the porous media. In addition, if the vapor is denser than the surrounding air, it will sink due to gravity.

Several natural processes retard the migration of the contaminant vapors, including biodegradation and adsorption of chemical constituents to the soil matrix. In addition, chemicals may partition between the vapor phase and the residual soil moisture.

If the leak is of sufficient size, the immiscible fluid will eventually reach the water table. If the fluid is lighter than water, it will travel under its own pressure gradients in the capillary fringe zone above the water table and may depress the water table to some extent. If the fluid is heavier than water, it will tend to sink through the saturated groundwater zone.

It is important to realize that a large percentage of the immiscible fluid can be trapped by capillary forces in the pores of the unsaturated zone. This trapped fluid, filling as much as 30% of the soil pore volume (J.T. Wilson, 1987), can serve as a source of contaminant vapor. In addition, it may serve as a source for dissolved contaminants for infiltrating rain water or a rising water table.

2.1.2 MAJOR ASSUMPTIONS

The primary purpose of the system conceptualization was to reduce the complexity of the processes summarized above by making assumptions allowing analysis and simulation of vapor transport while still preserving the essential aspects of the processes. The following paragraphs list these assumptions, and provide further explanations as appropriate.

- Only a single UST was investigated. Although most UST's are found in groups of 2 or 3 or more, with piping and fill systems that may also leak, the assumption of using only one tank was made to keep the simulations simple and straightforward. More complex arrangements can be analyzed in FY88, although the results presented here will not vary with multiple tanks.

- The UST was assumed to be cylindrical, and located in a homogeneous and isotropic backfill, with the geometry and vapor transport properties as defined in Section 2.2.2.

- Conceivably, it is possible to consider the influence of interfering sources (e.g., adjacent UST systems, surface spills), existing background contamination, and the presence of man-made or natural obstacles to measurement. It was decided, however, that these factors would not be considered; only a "clean" system was assumed.

- Gasoline and its chemical components were selected for simulation. A discussion of the physiocochemical properties of the simulated blend is found in Section 2.1.2, with a more complete presentation of properties for different blends in Appendix D. This assumption was made because of the prevalence of gasoline in UST's. Other fuels and chemicals, however, can be considered and simulated in the future; results may also be inferred from information presented here.

- The ground surface was assumed to be paved and therefore impermeable to vapors. This is a valid assumption because most UST's, in general, are located below paved areas. One simulation of an open, unpaved surface was performed.

- The water table was assumed to be below the excavation zone. This is generally the case at most UST's where vapor sensors would be used.

- Although the presence of the water table below the excavation zone indicates unsaturated conditions, moisture content of the excavation zone and surrounding native soils was varied to examine the effects of reduced air-filled porosity or vapor transport. The moisture content was assumed to be homogeneous throughout the backfill and native soils, with different values possible for the backfill versus the native soil.

- Several factors influencing vapor transport were assumed to be insignificant, based on literature reviews, simple calculations, and consideration of the influence of the paved surface (CDM, 1986). These factors are:

    - wind over a ground surface
    - barometric pressure fluctuations
    - water table fluctuations
    - rainfall infiltration
    - temperature gradients

- Although it was assumed that there were no horizontal or vertical temperature gradients across the UST site, temperature was a factor in the vapor simulations. Temperature strongly affects the equilibrium vapor pressure (i.e., maximum vapor concentration) of gasoline vapors in the air-filled pores. Consequently, variation in the equilibrium vapor pressure of gasoline due to temperature changes, (presented in Appendix D), was used as a key model variable.

- Vapor density will most likely have a significant effect on gasoline vapor transport because gasoline vapors are roughly 50% heavier than air (See Appendix F). For this study, however, gravity-driven advection was neglected. This means that the modeling results presented herein may overestimate the time-to-detection for sensors placed deep in an UST excavation zone, and conversely underestimate the time-to-detection for shallow sensors. The future research should include investigations into the quantitative effects of gravity-driven vapor advection.

- Diffusion was assumed to be the dominant vapor transport process. Also, it was determined that simulation of diffusion in three dimensions were required to estimate realistically the movement of vapors. Two-dimensional radial simulation of diffusion, it was determined, could significantly underestimate the time for vapors to reach a sensor. Capturing the geometries of the UST and its excavation zone, and their influence on three-dimensional aspects of vapor movement, was essential.

- Advection due to artificially-induced pressure gradients was not considered. This is a conservative approach, because suction wells or active (pumping) sensors will draw in vapors sooner, in general, that would occur under static air pressure.

- It was assumed that biological and chemical degradation were slow when compared to the time scale of interest, which is hours to days (Corapcioglu and Baehr, 1987). Also, given that pea gravel backfill, for example, is unlikely to possess a high organic matter content, the degree of sorption was assumed to be insignificant.

- Spurious pathways for vapor movement were not considered, because they are highly dependent on individual UST site conditions and thus difficult to assign in a generic representation.

- For purposes of presenting estimated times for sensors to reach alarm or detection levels, sensor response to total vapor hydrocarbons at 500 ppm levels were investigated. These numbers can be easily modified to reflect the results of on-going sensor testing. Also, sensor specificity to chemicals can be incorporated because the simulation models can produce estimates for not only a gasoline blend, but for individual chemical components as well.

- Partitioning between the vapor phase and water in the subsurface was assumed to have a negligible effect on diffusion. The validity of this assumption is examined in Appendix E.

- Changes in diffusion of gasoline vapors due to temperature variations are small compared to the effects of soil moisture content and porosity. Also, vapor diffusion rates do not vary significantly between the constituitive chemicals of gasoline. The small variability of vapor diffusion with temperature or constituents justified using a single vapor diffusion coefficient

2-4

for gasoline for the vapor transport simulations. Appendix D tabulates the average and individual vapor diffusion coefficients for selected gasoline blends and their constituents.

By making the assumptions listed above, the problem of simulating vapor transport from an UST leak was made tractable. The key parameters that were then varied, in performing the vapor simulations, were:

- Vapor diffusion coefficients of the backfill and surrounding native soils, as affected and determined by the moisture content, air-filled porosity, and total porosity of the soils;

- Temperature, which effects the equilibrium vapor pressure of the leaked gasoline according to the chemical properties of the constituents of the gasoline blend;

- Ground surface conditions, with one simulation performed with an open, unpaved surface, and all the others a paved, impervious surface.

2.2 DESCRIPTION OF SIMULATED UST

Based on the system conceptualization, a generic model of an UST excavation zone and surrounding native soil was developed. It incorporates all of the key parameters and considerations that were identified, and it is based on the assumptions described above that make the problem tractable.

The following text describes the typical gasoline blend and the physicochemical properties of it and its components (Section 2.2.1), and the geometry and hydrogeologic properties of the excavation zone and native soil (Section 2.2.2). This conceptualization of the UST and the leaking product was then transformed into a numerical model, as described in Section 2.3.

2.2.1 PRODUCT CHARACTERISTICS

A typical gasoline blend (Table 2-1) was developed to represent an average mixture of the various chemical constituents of gasoline. This synthetic gasoline was used for all of the simulations in this report and is similar to one of the gasoline blends suggested by K. Stetzenbach (1987). See Appendix D for further information on synthetic gasoline blends.

The physiocochemical properties of this blend and its component chemicals were estimated based on literature values, chemical estimation techniques, or literature-reported estimation equations, as discussed in Appendix C. A summary of the average properties for the typical gasoline blend, as affected by temperature variations, appears in Table 2-2. A comparison of the properties for individual components to the average properties for the blend is shown in Table 2-3. Similar tables for other synthetic blends are listed in Appendix D.

Tables 2-2 and 2-3 show how vaporization varies significantly with temperature. Vapor transport simulations therefore included vapor pressures at temperatures of 0°, 10°, and 20°C for the synthetic gasoline blend. This wide temperature range, from freezing to 68°F, is intended to bracket the more typical range of about 45°F to 60°F. The constituitive chemicals of the gasoline blend also exhibit a wide variation in vapor pressure; thus, simulations were produced for a compounds with a low vapor pressure,, (e.g., benzene, toluene, and xylene), and for two with high vapor pressures, (i.e., isopentane and isobutane).

The estimate diffusion coefficients do not vary significantly with component or with temperature. Therefore, a diffusion coefficient equal to the average diffusion coefficient for the synthetic gasoline blend at 10°C was used in performing the simulations.

2.2.2 UST SYSTEM GEOMETRY AND HYDROGEOLOGIC CHARACTERISTICS

The geometry of the single UST used for the simulations is depicted in Figure 2-1. The tank and excavation zone have the following dimensions:

- The tank is cylindrical, 12 feet long, and 6 feet in diameter;

- The top of tank is 2 feet deep below ground surface;

- The excavation zone is rectangular in plan view and in cross-section, surrounding the tank with at least 2 feet of backfill. Further simulations in Phase 2 will include 1:1 or 2:1 side-slopes, as required for safely excavating the native soils.

The excavation zone is assumed to be backfilled with coarse sand or pea gravel, while the native soil ranged from clay to coarse sand. The ranges of hydraulic and hydrogeologic properties for the backfill and native soil used to bracket the different simulation conditions are listed in Table 2-4.

2.3 SIMULATION METHODOLOGY

2.3.1 "BASE CASE" VOLATILIZATION SCENARIO

The representation of the UST leak itself was based on the assumption that diffusion alone transports vapors away from the leak, and that the loss of the diffused mass is exactly balanced by the vaporization of liquid product. The leak was assumed to be a "point" at the far bottom end of the tank. Based on the mathematics of the simulation model, the leak source at "time zero" of the simulations was approximated as a cube of vapors, varying linearly from 100 percent saturation at the center (leak) to zero concentration at the edge, 1 foot from the leak. It is recognized that the liquid-vapor interface location is a difficult and complex problem to describe and solve; this source geometry approximation, however, was necessary at this time. Further analysis of the source representation should be performed in future work.

This volatilization scenario is called "base case," because the volatilizing leak is confined to a point source, instead of a line or plane source, which produces the minimum volume of vapors that can be detected. The vapor transport model can do this because it simulates the spreading of vapors from the point source, and thus time-varying concentrations at sensor locations are predicted. When the vapor concentration at a sensor point reaches the detection level, there is a distributed amount of vapor around the leak and the total mass can be computed. The "base case" volatilized volume can be estimated for any potential sensor location within the excavation zone.

2.3.2 SELECTION OF SIMULATION MODEL

Because diffusion was to be the only vapor transport process to be simulated, it was determined that the most accurate representation of the three-dimensional nature of that process would be attained by using a simulation model. The most suitable was the DYNFLOW ground water flow simulation mode, which solves the diffusion equation by analogy. Appendix H provides a description of the diffusion-groundwater flow analogy, as well as background information on DYNFLOW. The work assignment team has had extensive experience with DYNFLOW, and the work assignment manager was a co-developer of the program.

Although several three-dimensional confined ground water flow or heat conduction models could have been used in the assignment, the advantages of DYNFLOW to the work assignment team were familiarity, and the availability of powerful software for grid generation and multi-color graphics display.

A test simulation of a preliminary UST scenario was also performed using MODFLOW from the U.S. Geological Survey, as described in Appendix L. Reasonable agreement between MODFLOW and DYNFLOW was shown, demonstrating that any three-dimensional groundwater flow model could be used to address this problem.

2.3.3 DESCRIPTION OF MODEL GEOMETRY AND BOUNDARY CONDITIONS

The generic UST was transformed into a three-dimensional numerical model as shown in Figures 2-2 through 2-5. Because the simulation results are symmetrical about the longitudinal centerline of the tank, only half of the tank, surrounding backfill, and native soils was simulated. Simulating only half the volume of the site reduces computer computation and storage charges that would be necessary for a full representation.

The sides and bottom of the native soil portion of the model were placed far enough from the tank so that significant vapor concentrations would not reach the edges of the model before concentrations at sensors in the excavation zone would reach detection limits. The bottom of the model can be likened to a water table that is 24 feet from the ground surface.

The leak was represented as a fixed concentration at 100 percent of equilibrium vapor concentration. The tank leak was simulated as a constant 100 percent concentration in the model, at the node point located at the bottom left end of the tank. The model elements at this location are 1 foot in width. The DYNFLOW model interpolates concentrations linearly across each element. Thus, the concentration gradient at the leak source point at the beginning of the first simulation time step was an abrupt linear drop from 100 percent to 0 percent across the surrounding elements.

The bottom and top of the model were no-flow boundaries, except in one simulation with an open top surface which had concentrations fixed at zero to simulate diffusion through the top surface. The lateral sides were held at a fixed concentration of zero so that vapors would not build up and cause concentrations in the backfill zone to be overestimated.

The sensor locations depicted in Figure 2-6 and listed in Table 2-5 are the points at which model results were tabulated for the time history plots presented in Section 3. These locations were selected to represent "nearby," "intermediate," and "distant" locations from the source. In actuality, simulation results for any point in the model can be tabulated and plotted.

2.3.4 DEFINITION OF SIMULATION MATRIX

A set of seven simulation runs was defined, with the input parameters for each run selected to represent various soil moisture and porosity values. Table 2-6 is a summary of the simulation matrix; Appendix K contains a complete listing of the conditions simulated. Run number 1 is considered the "average soil conditions" run because it represents what may be considered the most typical situation. This is a dry sand native soil surrounding a dry gravel backfill.

The simulation matrix contains "pairs" of backfill/soil conditions. The first run in each pair has the same backfill as the native soil; the second run in each pair has a contrast, testing the effects of decreased diffusion in the native soil. Run number 7 is not in a "pair," but was rather designed to test the effects of an open surface.

The only parameter that varied from run to run was the effect diffusion coefficient. This term incorporates the influences of porosity and moisture content. Therefore, a single simulation run can represent more than just the single combination of properties listed in the simulation matrix, as long as the combination of properties results in the same effective diffusion coefficient.

2.3.5 TRANSFORMING RESULTS FOR DIFFERENT PRODUCT CHARACTERISTICS

To interpret the output from the simulation runs, in which all concentrations are expressed as "percent of equilibrium vapor concentration," the concentrations and vapor flux (or minimum volatilization rate) predictions were multiplied by the equilibrium vapor concentration (in ppm) and divided by 100 (correction for percentage). The vapor fluxes were also transformed into the equivalent liquid volume of the volatilized and diffused vapors through a similar transformation process, described in Appendix G, that is also based on the equilibrium vapor concentration. In this way, the results from a single run were used to tabulate and plot predicted results for different volatilized products and temperatures.

Table 2-7 is a listing of the equilibrium vapor concentrations for selected gasoline components, and for the synthetic gasoline blend, that were used for transforming model results into more meaningful concentration units. This listing gives a good indication of how sensor response may be expected to vary according to temperature, and how predicted vapor diffusion would be expected to vary by gasoline component.

2.3.6 CREATING AND PERFORMING THE SIMULATIONS

A set of seven simulation runs, defined in Table 2-6 and Appendix K, was formulated as DYNFLOW command files, which are listed in Appendix M. Each command file was run against DYNFLOW Version 4B, with output from the program stored on computer files for later display and analysis of results.

The simulation time-frame was from time zero, when the volatilization started, to 28 days afterwards. Simulation results were saved every three-and-a-half days.

Time histories of simulated concentrations at the sensor point locations are listed in Appendix N, as well as time histories of simulated vapor influx at the leak. Transformed versions of these time histories appear in some of the graphs contained in Section 3.

Additional simulation results, besides the output listed in Appendix N, were sued to prepare the contour plots and some of the "sensor response," or "alarm time" plots shown in Section 3. The results were extracted from the computer output files, which were too extensive to list in this report.

Plan View

12 ft.

Leak

Tank

2 ft.

6 ft.

2 ft.

Pavement

**Longitudinal
Cross Section**

Tank

2 ft.

Leak

2 ft.

Pavement

**Lateral
Cross Section**

Tank

2 ft.

2 ft.
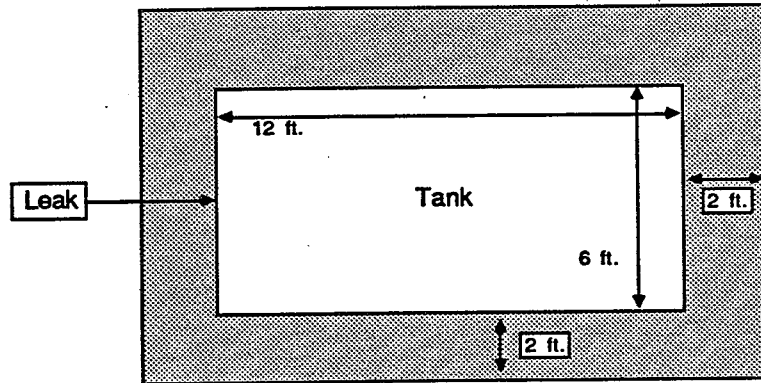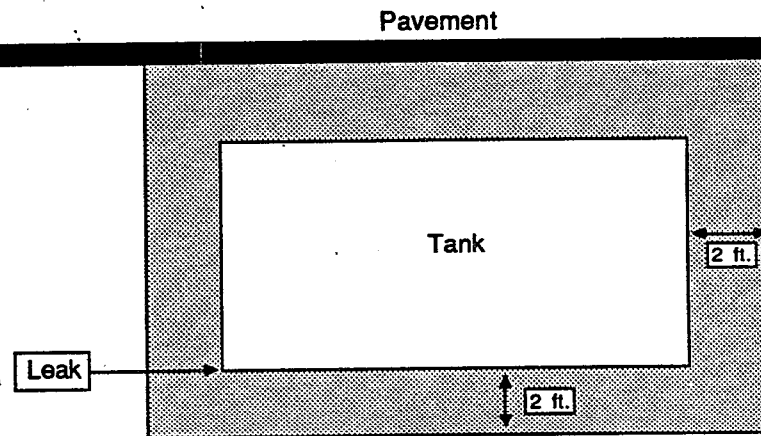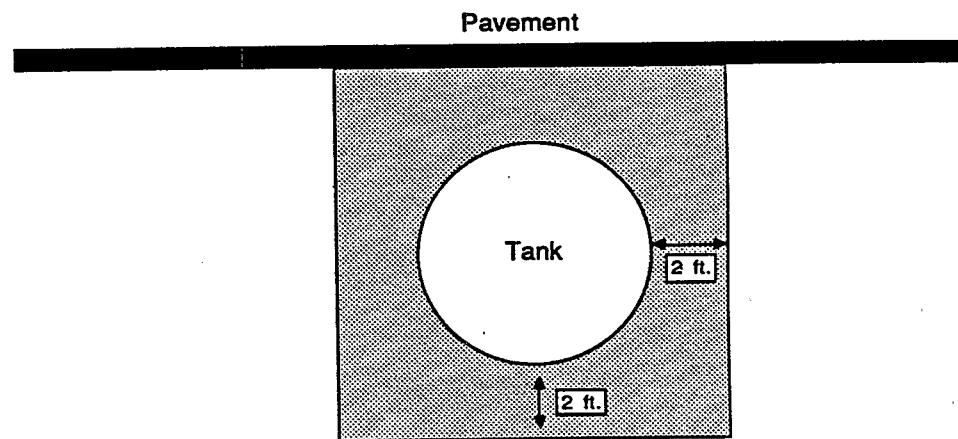
Figure 2-1. Geometry of the "Generic" UST
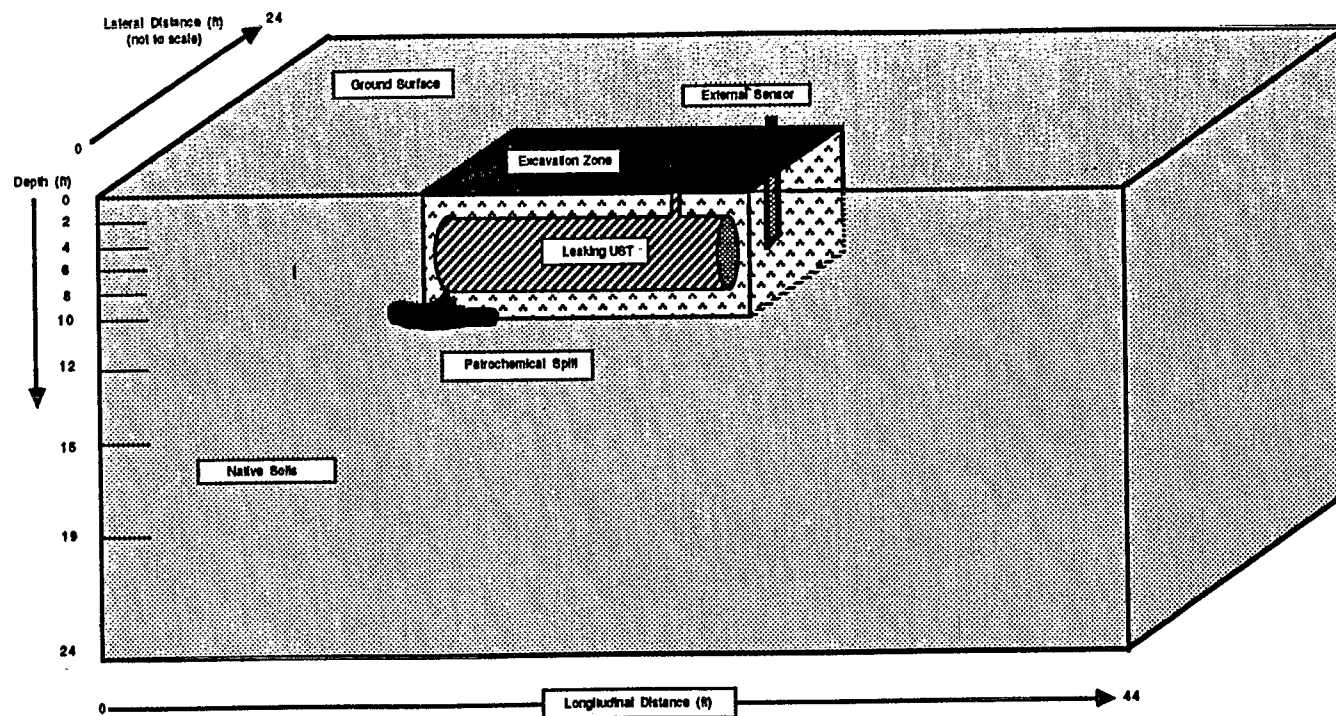
Figure 2-2. Cut-Away Isometric View of the Vapor Diffusion Model.
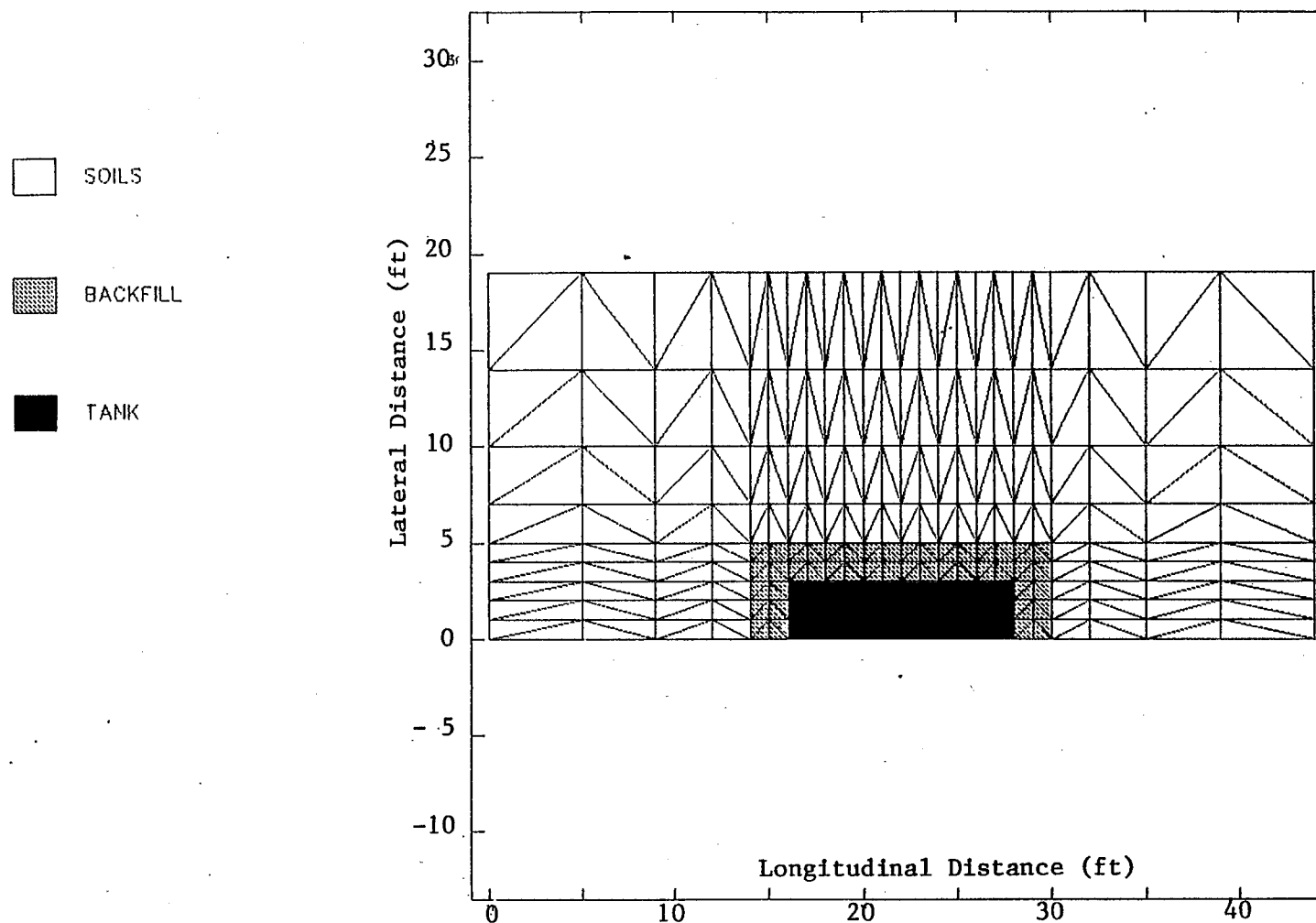
Figure 2-3. Plan View of the Vapor Diffusion Model.
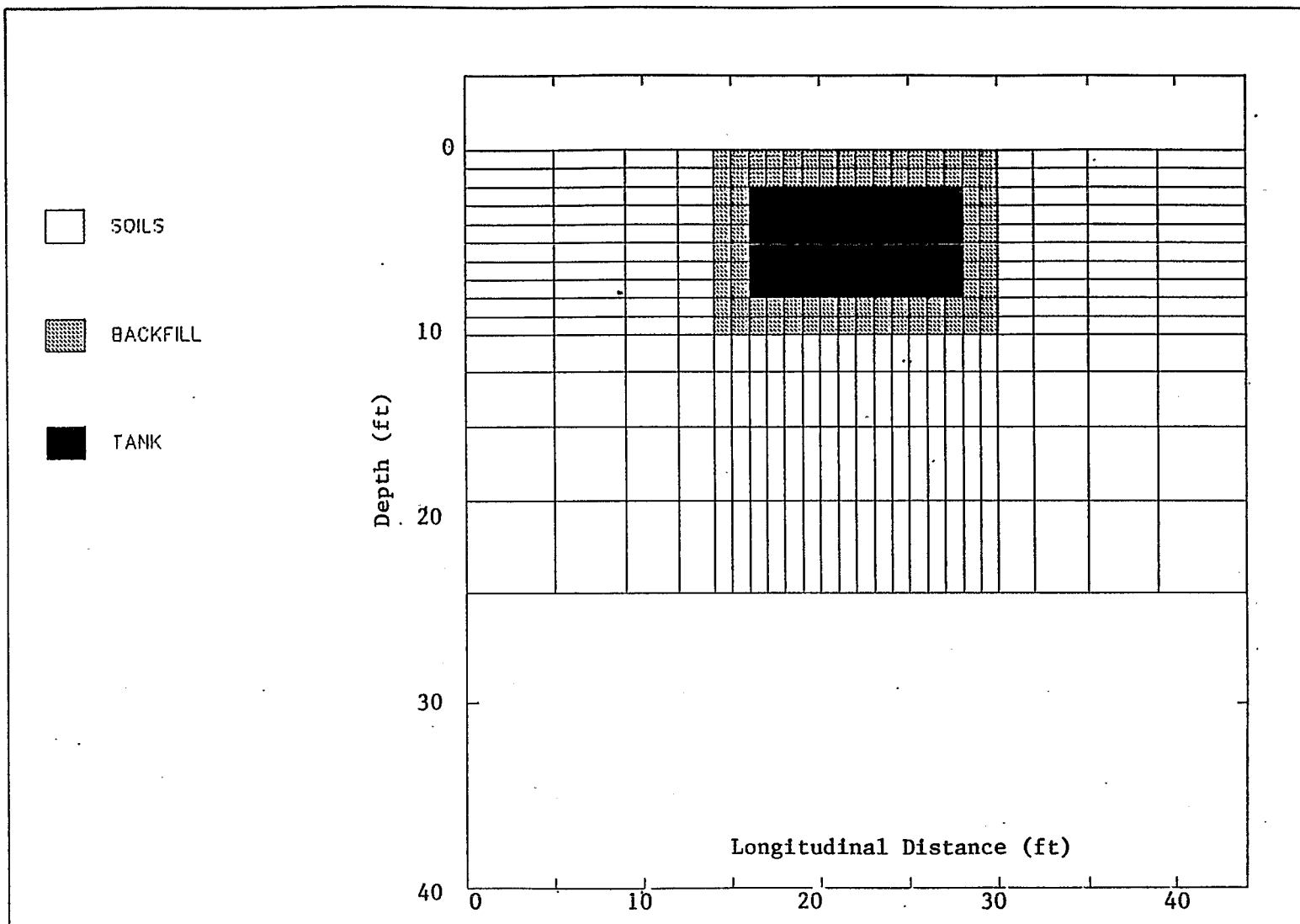
Figure 2-4. Longitudinal Cross-Section of the Vapor Diffusion Model.
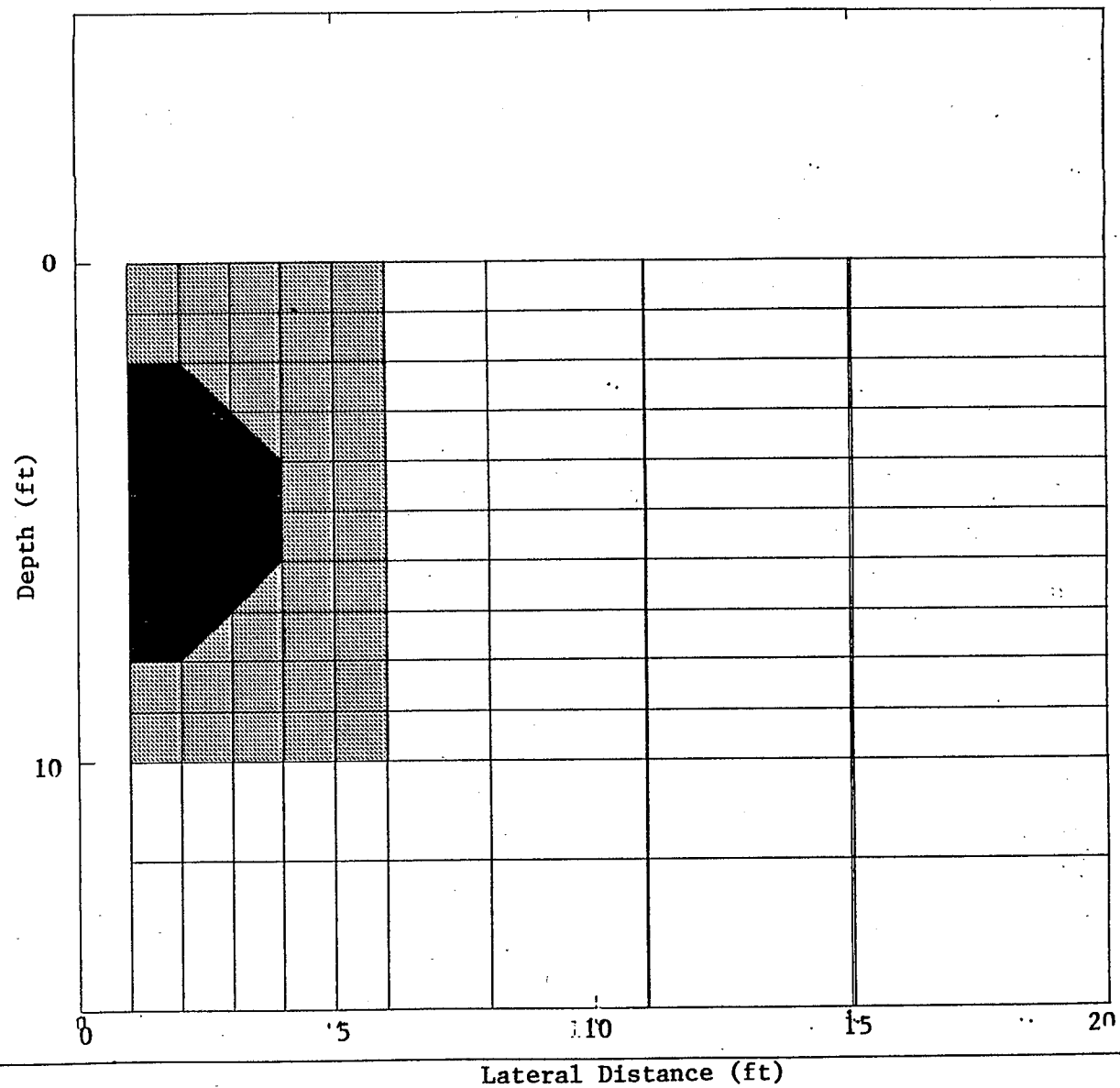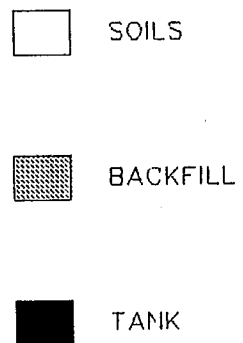
Figure 2-5. Lateral Cross-Section of the Vapor Diffusion Model.
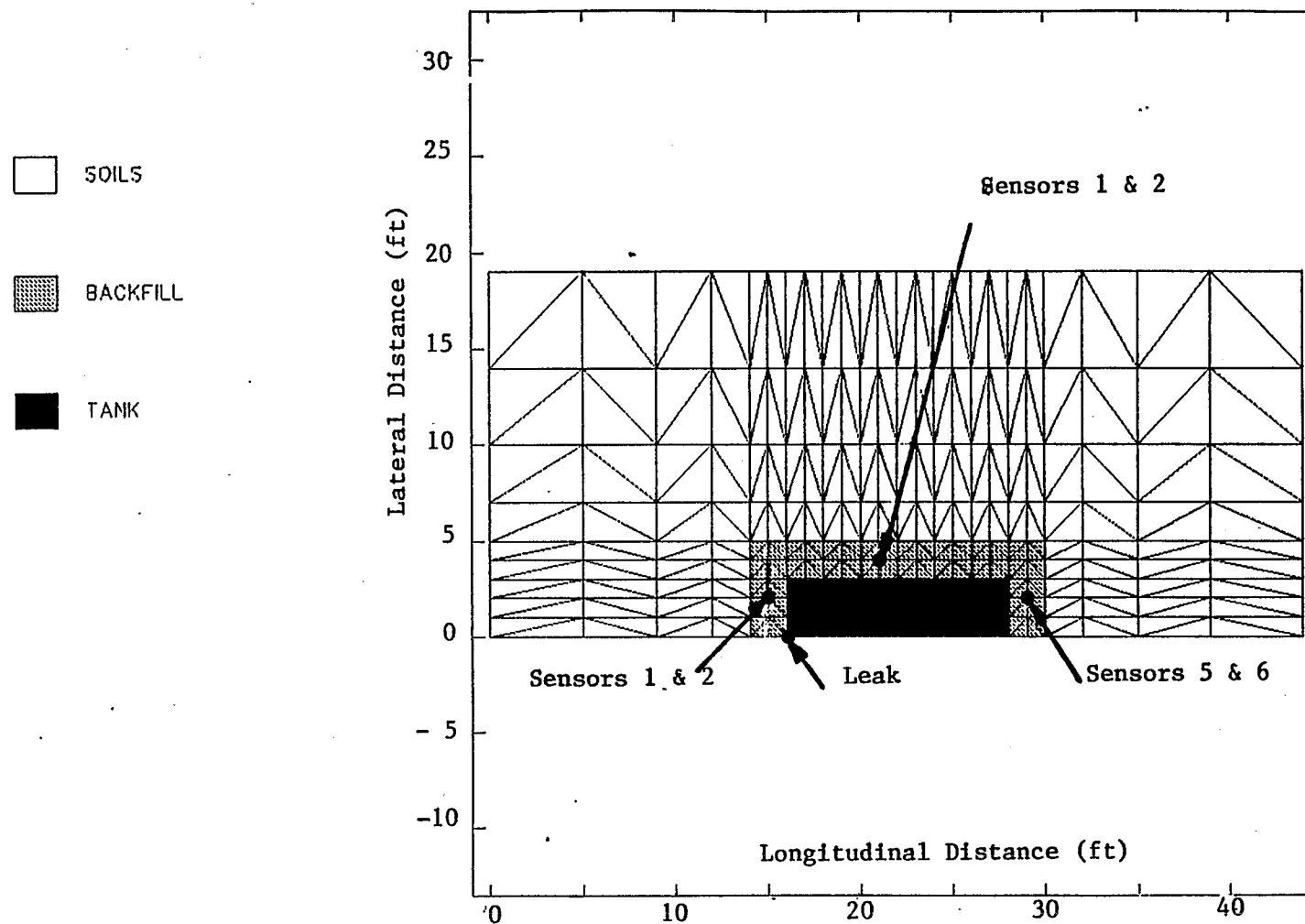
Figure 2-6. UST Leak and Vapor Sensor Locations in the Vapor Diffusion Model.

TABLE 2-1
COMPONENTS OF THE SIMULATED GASOLINE BLEND

COMPONENT OF BLEND	PERCENTAGE ($\%w/w$)
Isopentane	14
C_{12}-aliphatic	10
n-Hexane	9
2,4-Dimethylhexane	8
2-Methylpentane	8
m-Xylene	7
Toluene	5
2-Methylhexane	5
1,4-Diethylbenzene	5
1,3,5-Trimethylbenzene	5
Cyclohexane	3
Benzene	3
n-Pentane	3
Isobutane	2
Ethylbenzene	2
2,2,4-Trimethylhexane	2
2,2,5,5-Tetramethylhexane	1.5
n-Heptane	1.5
1-Pentene	1.5
1-Hexene	1.5
n-Butane	1
n-Octane	1
Methylcyclohexane	1
Total	100%

TABLE 2-2
AVERAGE PHYSICOCHEMICAL PROPERTIES OF THE SIMULATED GASOLINE BLEND AT DIFFERENT TEMPERATURES

	Temperature		
	0°C	10°C	20°C
Average Gram Molecular Weight of Gasoline Vapors(g /mol)	68.34	68.92	69.48
Average Liquid Density of Gasoline Components (g /cm^3)	0.7358	0.7271	0.7182
Equilibrium Vapor Concentration of Pure Gasoline Vapor in Air (ppm)	165,976	248,191	360,661
Average Air Diffusion Coefficient of Gasoline Components (cm^2/sec)	0.0642	0.0684	0.0726

Table 2-3. Physicochemical Properties of Individual Chemicals
versus the Simulated Gasoline Blend at 10° Centigrade,

REPRESENTATIVE CHEMICAL	PERCENT COMPOSITION	GRAM MOL. WEIGHT (GM/MOL)	LIQ. PHASE MOL FRACT.	AIR DIFFUSION COEFFICIENT (CM^2/SEC)	LIQUID DENSITY (GM/CM^3)	PURE CHEMICAL VAPOR PRESSURE (mm Hg)	PARTIAL PRESSURE OVER GASOLINE (mm Hg)	PURE CHEMICAL VAPOR DENSITY (GM/M^3)	CONCENTRATION OVER LIQUID GASOLINE (ppm)	BOILING POINT (deg. K)	HENRY'S LAW CONSTANT (dim.)	GAS VISCOSITY (uPOISE)
Isobutane	2	58.12	0.0326	0.0857	0.5728	1647.77	53.7745	5423.76	70755.9	261.25	3259.64	67.62
n-Butane	1	58.12	0.0163	0.0857	0.5931	1112.75	18.1571	3662.69	23890.9	272.65	2521.65	68.48
Isopentane	14	72.15	0.1840	0.0769	0.6311	392.47	72.2231	1603.70	95030.4	300.95	3387.63	66.54
n-Pentane	3	72.15	0.0394	0.0769	0.6364	283.84	11.1925	1159.80	14727.0	309.15	2977.29	61.67
n-Octane	1	114.23	0.0083	0.0563	0.7096	5.63	0.0468	36.43	61.5	398.75	5200.06	58.98
Benzene	3	78.11	0.0364	0.0851	0.8957	45.53	1.6583	201.40	2182.0	353.25	11.32	69.76
Toluene	5	92.14	0.0515	0.0776	0.8759	12.43	0.6397	64.86	841.7	383.75	12.60	71.49
Xylene (a)	7	106.17	0.0625	0.0629	0.8701	3.26	0.2039	19.61	268.3	466.25	11.83	51.89
n-Hexane	9	86.18	0.0990	0.0669	0.6676	75.70	7.4976	369.48	9865.2	341.85	3461.34	56.50
2-Methylpentane	8	86.18	0.0880	0.0669	0.6620	109.55	9.6446	534.70	12690.2	333.35	3765.69	57.37
Cyclohexane	3	84.16	0.0338	0.0677	0.7884	47.51	1.6060	226.44	2113.2	353.85	376.99	68.11
n-Heptane	1.5	100.20	0.0142	0.0620	0.6914	20.66	0.2933	117.23	385.9	371.55	4459.78	52.35
2-Methylhexane	5	100.20	0.0473	0.0620	0.6867	30.94	1.4642	175.57	1926.5	343.15	6962.93	53.12
Methylcyclohexane	1	98.19	0.0097	0.0627	0.7789	21.45	0.2071	119.26	272.6	374.05	797.24	54.09
2,4-Dimethylhexane	8	114.23	0.0664	0.0581	0.7071	13.30	0.8833	86.03	1162.2	382.55	5808.15	50.42
Ethylbenzene	2	106.17	0.0179	0.0690	0.8748	3.77	0.0673	22.66	88.6	409.25	13.65	52.16
1-Pentene	1.5	70.14	0.0203	0.0780	0.6513	359.48	7.2909	1427.99	9593.3	303.05	977.71	64.23
2,2,4-Trimethylhexane	2	128.26	0.0148	0.0572	0.7240	6.18	0.0915	44.92	120.3	399.65	6214.17	48.08
2,2,5,5-Tetramethylhexane	1.5	142.29	0.0100	0.0543	0.7264	3.40	0.0340	27.37	44.7	410.55	21405.95	46.47
1,4-Diethylbenzene	5	134.22	0.0353	0.0559	0.8683	0.32	0.0113	2.43	14.9	456.85	19.24	45.98
1-Hexene	1.5	84.16	0.0169	0.0677	0.6821	94.87	1.6036	452.20	2110.1	336.55	917.75	58.44
1,3,5-Trimethylbenzene	5	120.20	0.0394	0.0591	0.8718	0.84	0.0333	5.74	43.8	437.85	9.02	48.49
C12-aliphatic	10	170.00	0.0558	0.0493	0.8656	0.03	0.0016	0.27	2.1	489.15	7742.54	39.99
Total	100	102.20	1.0000		0.7457		188.6252		248191.2		3202.673	

Temperature = 283.15 deg. K
Pressure   =   760 mm Hg
Gas Constant =
        0.06236 mm Hg*m^3/mol*K
Molecular Weight
of Air =   28.96 gm/mol
Average Molecular
Weight of Gasoline
Vapors =   68.92 gm/mol
Molecular weight
of Gasoline-Air
Mixture =   38.00 gm/mol

Vapor Density
of Gasoline-Air
Mixture =   1673.38 gm/m^3

Weighted average
air diffusion
coefficient =   0.0684 cm^2/sec
Weighted average
liquid density   0.7271 gm/cm^3
Weighted average
gas density   736.25 gm/m^3

TABLE 2-4
VAPOR TRANSPORT PROPERTIES OF
EXCAVATION ZONE BACKFILL AND NATIVE SOILS

BACKFILL

Material: Gravel or Sand

Total Porosity: 20% to 40%

Saturation: 30% to 75%

NATIVE SOILS

Material: Sand, Silty Sand, or Clay

Total Porosity: 20% to 45%

Saturation: 30% to 84%

TABLE 2-5
SENSOR LOCATIONS IN THE VAPOR DIFFUSION MODEL

Sensor Number	Depth (ft)	Vertical Distance From Source (ft)	Longitudinal Distance From Source (ft)	Lateral Distance From Source (ft)	Direct Horizontal Distance from Source (ft)	Approximate Travel Distance (ft)
1	8	0	1	2	2.2	2.2
2	2	6	1	2	2.2	6.4
3	8	0	5	4	6.4	6.4
4	2	6	5	4	6.4	12.0
5	8	0	13	2	13.1	13.1
6	2	6	13	2	13.1	19.1

TABLE 2-6

SUMMARY OF SIMULATION MATRIX

Simulation Run Number	Surface Condition	Backfill Material	Native Soil	Effective Diffusion Coefficient (cm^2/sec)	
				Backfill	Native Soil
1	Paved	Dry Gravel	Dry Silty Sand	0.017	0.017
2	Paved	Dry Gravel	Moist Silty Sand	0.017	0.008
3	Paved	Moist Sand	Moist Sand	0.005	0.005
4	Paved	Moist Sand	Wet Silty Sand	0.005	0.001
5	Paved	Wet Sand	Wet Sand	0.002	0.002
6	Paved	Wet Sand	Wet Clay	0.002	0.0008
7	Open	Dry Gravel	Dry Silty Sand	0.017	0.017

TABLE 2-7

EQUILIBRIUM VAPOR CONCENTRATIONS
USED IN TRANSFORMING SIMULATION RESULTS

Temperature	Component	Equilibrium Vapor Concentration (ppm)
0° Celsius	Benzene	1262
	Isopentane	62785
	Isobutane	50423
	Gasoline Blend	165976
10° Celsius	Benzene	2182
	Isopentane	95030
	Isobutane	70756
	Gasoline Blend	248191
20° Celsuis	Benzene	3604
	Isopentance	139200
	Isobutane	96734
	Gasoline Blend	360661

3.0 NUMERICAL SIMULATION RESULTS

3.1 "BASE CASE" VOLATILIZATION OVER TIME

The vapor diffusion model predicts minimum liquid gasoline volatilization rates (see Figure 3-1). Figure 3-1 shows a decline with time of the rate of volatilized liquid gasoline entering the UST model. This decline in the influx rate of volatilized liquid gasoline occurs as a consequence of the reduced vapor concentration gradient away from the leak with time.

Figure 3-1 also shows the effect of increasing moisture content in the backfill on the influx rate of volatilized liquid gasoline. The rate of volatilization of liquid gasoline declines with increasing water content of the backfill from Run 1 (water saturation percent = 30%) to Run 3 (water saturation percent = 63%) to Run 5 (water saturation percent = 75%). See Appendix K for a tabulation of the total porosity, air-filled porosity, and moisture content values used in the numerical simulations. The increased moisture content of the backfill reduces the air-filled porosity through which volatilized liquid gasoline may diffuse, thereby reducing the "base case" volatilization rate of the leaking gasoline.

Figure 3-2 depicts the cumulative volume of liquid gasoline lost to volatilization. Increasing the moisture content from Run 1 to Run 3 to Run 5 reduces the volume of leaked gasoline that may enter the excavation zone in a volatile state.

Simulations were performed to examine the effect of increasing moisture content in the surrounding native soils. In each of the simulation pairs (i.e., Run 1 and 2, Run 3 and 4, and Run 5 and 6), the moisture content of the native soils within each simulation pair was increased, holding the backfill properties constant. The simulations demonstrated that increasing moisture content in the native soils had little effect on "base case" volatilization. Figure 3-1 and 3-2 show the effects of variation in backfill properties only for Runs 1, 3, and 5.

Another interesting and related aspect of these plots is that the rate of "base case" volatilization reached a steady value soon after volatilization had started, because the excavation zone was still filling with vapors. The rate of "filling" was apparently balancing the volatilization. Because sensors would have responded well before the excavation zone was filled with enough vapors to slow down diffusion at the leak, none of the simulations were extended long enough to demonstrate this effect.

Figure 3-3 demonstrates the strong effect of temperature on the "base case" volatilization. Results of Run 1, plotted in Figure 3-3 at 0°, 10°, and 20°C, show an increase in volatilization rate with temperature. The effect of temperature on the pure chemical vapor pressure and vapor concentration of gasoline can be seen in equation C-6 of Appendix C and in Table 2-7 and Tables D-1, D-7, and D-3 of Appendix D.

The cumulative volumes of vaporized product for three constituents of gasoline (i.e., isopentane, isobutane, and benzene) are plotted versus time in Figure 3-4. The differences in the results for isopentane, isobutane, and benzene are due to differences in equilibrium vapor concentration between the three compounds (see Table 2-7). The equilibrium vapor concentrations of isopentane and isobutane are about ten times higher than that of benzene, for the synthetic gasoline used in these simulations.

Figure 3-4 shows the effect of the larger vapor pressure values on the volume of volatilized gasoline. More pure product of isopentane and isobutane will be lost to volatilization and diffusion than benzene under the same physical conditions, and at the same time. The implication of Figure 3-4 is that if a benzene-specific external sensor is placed within the backfill, a longer time-to-detection of vapors will result than if the sensor was sensitive to a more volatile compound such as isopentane. The result of the increased detection time from a benzene-specific sensor is to increase the volume of liquid gasoline lost to leakage and volatilization prior to detection.

As a final point concerning Figure 3-4, the volume of volatilized gasoline is greater than any of the volumes for isopentane, isobutane, or benzene. This is because each of these three compounds are constituitive compounds of gasoline, and so their individual volumes are all less than the total volume of gasoline.

3.2 VAPOR SPREADING THROUGHOUT BACKFILL AND NATIVE SOIL

Contours of gasoline vapor concentrations have been plotted to demonstrate the spreading of vapors away from the leak. The "pair" of simulation runs 1 and 2, representing "average conditions" and "dry backfill with moist native soil," were used to show the effect of a contrast between the backfill and native soil. As shown in Figures 3-5 and 3-6, an increased moisture content in the native soil caused the vapors to diffuse preferentially into the backfill materials.

Another contour plot (Figure 3-7) shows the vapor spreading at a depth of two feet for Run 1. Comparison of the gasoline vapor concentration contours at depth of 8 feet (Figure 3-5) and 2 feet (Figure 3-7) show the reduced vapor concentration at the shallower depth. This is primarily due to the increased vertical distance from the source. The presence of the UST as a no-flow boundary also impedes the vertical diffusion of vapors, thereby reducing vapor concentrations in Figure 3-7.

3.3 SENSOR LOCATION VAPOR CONCENTRATIONS

The simulation results were tabulated as time histories at six sensor locations (see Figure 2-6 and Table 2-5), and then plotted with respect to time.

Figure 3-8 shows vapor concentrations at each of the six sensors for the "average conditions" simulation. The effects of sensor distance and depth are apparent, with the "nearby" and "intermediate" sensors responding within 8 days. This analysis assumes that a sensor can respond to total gasoline hydrocarbons at about 500 parts per million. Even the most distant, shallow sensor is predicted to respond within about one month.

Figure 3-9 shows predicted vapor concentrations at the deep, "intermediate" sensor. As in the plots of leakage rates and volumes (Figures 3-1 and 3-2), the effects of decreasing air-filled porosity outweigh the effects of contrasting backfill/soil conditions. Figure 3-9 does, however, demonstrate how decreased porosity in the surrounding soils enables the vapors to spread more quickly in the backfill.

3.4 DETECTION TIME VERSUS SENSOR LOCATION

Assuming that a sensor can detect 500 parts per million of total gasoline hydrocarbons, plots of detection time versus potential sensor locations were developed. These plots were based on the definition of "sensor distance," as depicted in Figure 3-10. "Sensor distance" was defined based on the assumption that sensors driven into an existing backfill zone would have to be placed at least one foot from the edge of the tank in plan view. "Sensor distance" is thus the distance from the leak along the line defined by this one-foot spacing.

Figure 3-11 depicts the variation in "sensor distance" with alarm time at a 500 ppm total hydrocarbon vapor concentration threshold. Figure 3-11 indicates the closest "sensor distance" at which an external sensor must be placed to detect the leak at a given alarm time.

The effects of increasing the water content in the backfill on the "alarm sensor distance" is also depicted in Figure 3-11. An increase in moisture content in the backfill reduces the distance at which a sensor are predicted to detect 500 ppm of total hydrocarbon vapor at a given alarm time. In other words, as the moisture content of the backfill increases, sensors must be placed more closely to the leak in order to detect the leak at the same required alarm time.

Figure 3-11 indicates that increasing moisture content of the native soils (e.g., from Run 1 to Run 2) has little effect. The same general observation may be made for Figure 3-12, except that the shallow sensors of Figure 3-12 require closer placement to the leak to enable detection at the same alarm time.

Increasing temperature increases the "sensor distance" at which external sensors are predicted to detect vapors at the 500 ppm level by a given alarm time (see Figure 3-13). The increased vapor concentrations at higher temperatures indicates that sensors may be placed further from the leak for a required alarm time.

Figure 3-14 shows the effect of sensor threshold on the sensor distance at a required alarm time. Increasing the sensor threshold, from 250 to 500 to 750 ppm of total hydrocarbon vapors, reduces the distance at which external sensors are predicted to detect vapors at a given alarm time. At sites where background vapor concentrations are high or sensor thresholds are high, Figure 3-14 indicates that the sensors must be placed more closely to the leak to detect the leak at a required alarm time.

Figures 3-12, 3-13, and 3-14 exhibit a slope break at about 17 feet of "sensor distance," becoming near-vertical. This is because those sensors placed beyond 17 feet of "sensor distance" (see Figure 3-10) from the vapor source are not increasing in radial distance from the source. Consequently, there is little change in alarm time in the portion of the curves beyond 17 feet of "sensor distance."

3.5 VOLUME OF LEAKAGE AT DETECTION TIME

Combining the time histories of "base case" volatilized liquid volume and the simulated detection times versus "sensor distance" yielded the plot shown in Figure 3-15. This plot shows how much gasoline is simulated to have vaporized by the time a sensor responds, as a function of the distance a sensor is placed away from the leak.

3.6 EFFECTS OF OPEN SURFACE

Opening the ground surface and allowing the free escape of vapors had little effect on the simulated leakage or spread of gasoline vapors. This is shown in Figure 3-16, which is a plot of vapor concentrations from the "average condition" simulation at the deep, "intermediate" sensor. The

time history of "base case" volatilization, when plotted, showed no discernible differences over the time scale of the simulation. Differences in "base case" volatilization under conditions of open and closed top surface are predicted to become more evident as the leak continues beyond one month.

Having an open top surface with a zero vapor concentration at the top surface is physically equivalent to an unpaved land surface with a stiff wind blowing across it. The wind removes any diffusing contaminant vapors from the land-air interface. The wind keeps the vapor concentration at the interface at zero throughout time. The effect of this zero concentration at the land-air interface is to maximize the flux of contaminant vapors diffusing through the top of the model to the atmosphere. As a result, the volume of vapors lost through the open top surface (i.e., Run 7), and plotted in Figure 3-14, represents a maximum volume loss. A non-zero vapor concentration at the air-land interface, such as might occur under conditions of intermittent wind removal, would reduce the loss of vapors through the open top surface.
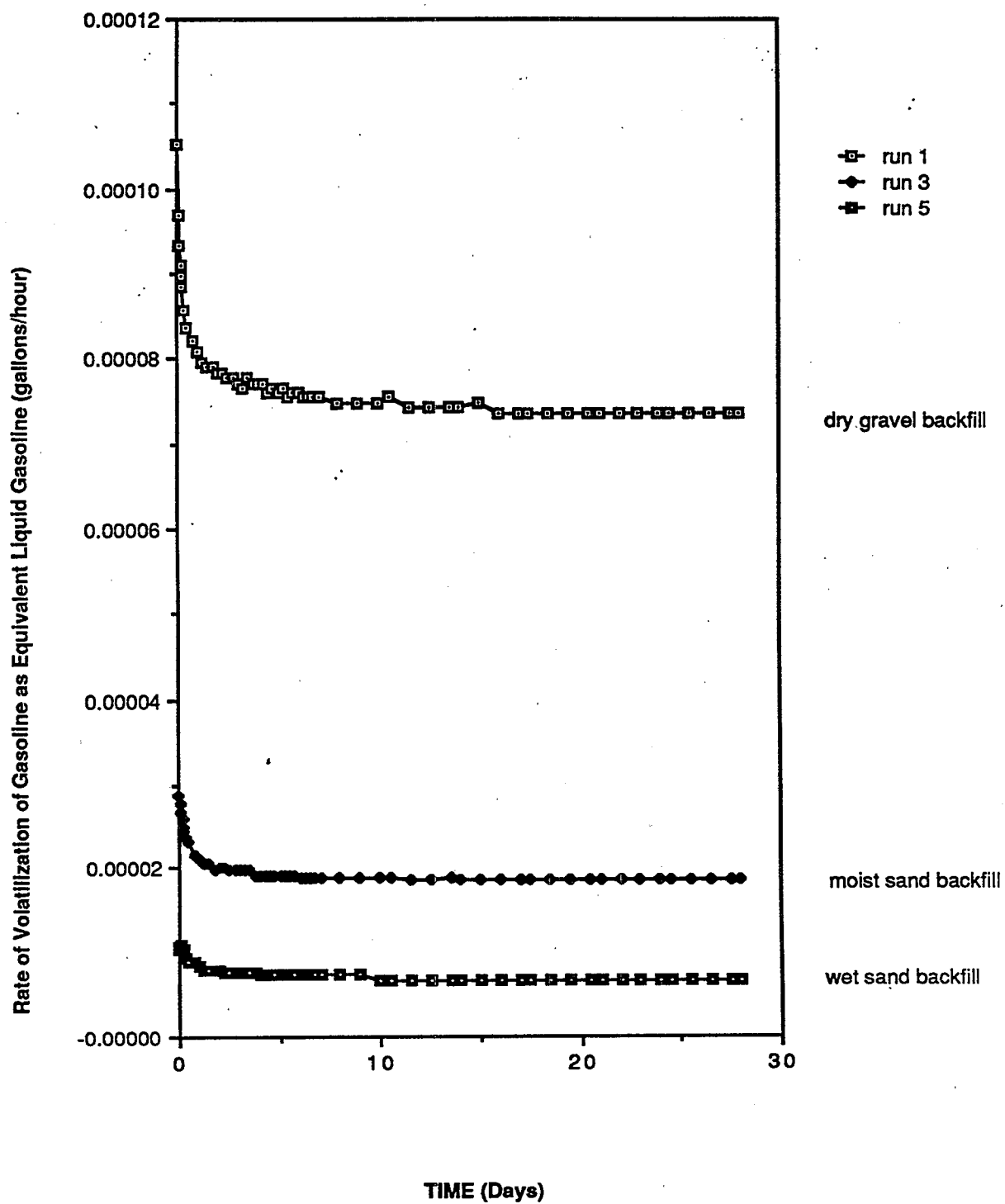
Figure 3-1. Time History of Simulated Gasoline Volatilization Rate
for Different Soil Conditions at 10 deg. C.
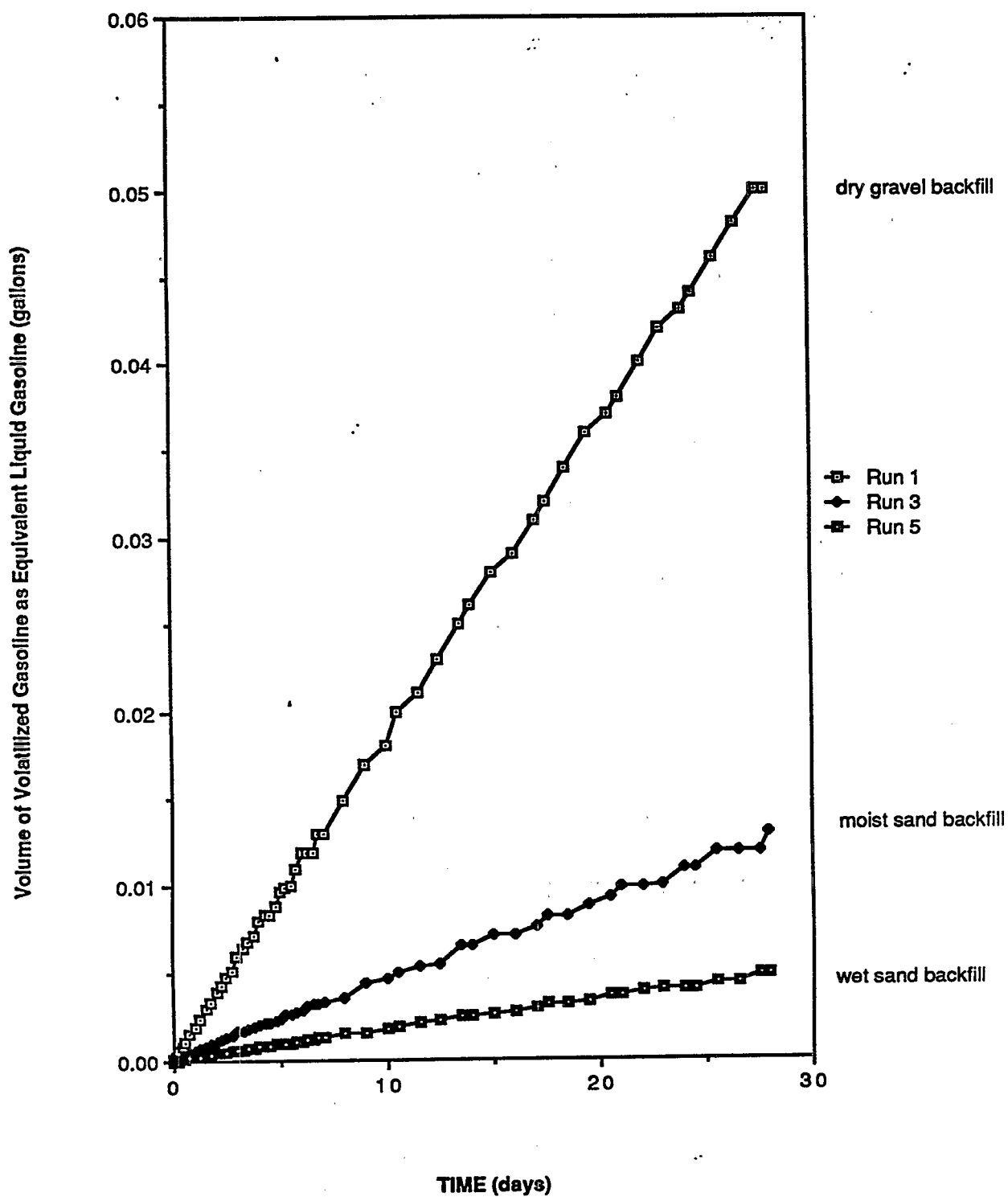
Figure 3-2. Time History of Simulated Gasoline Volatilized Volume
for Different Soil Conditions at 10 C.
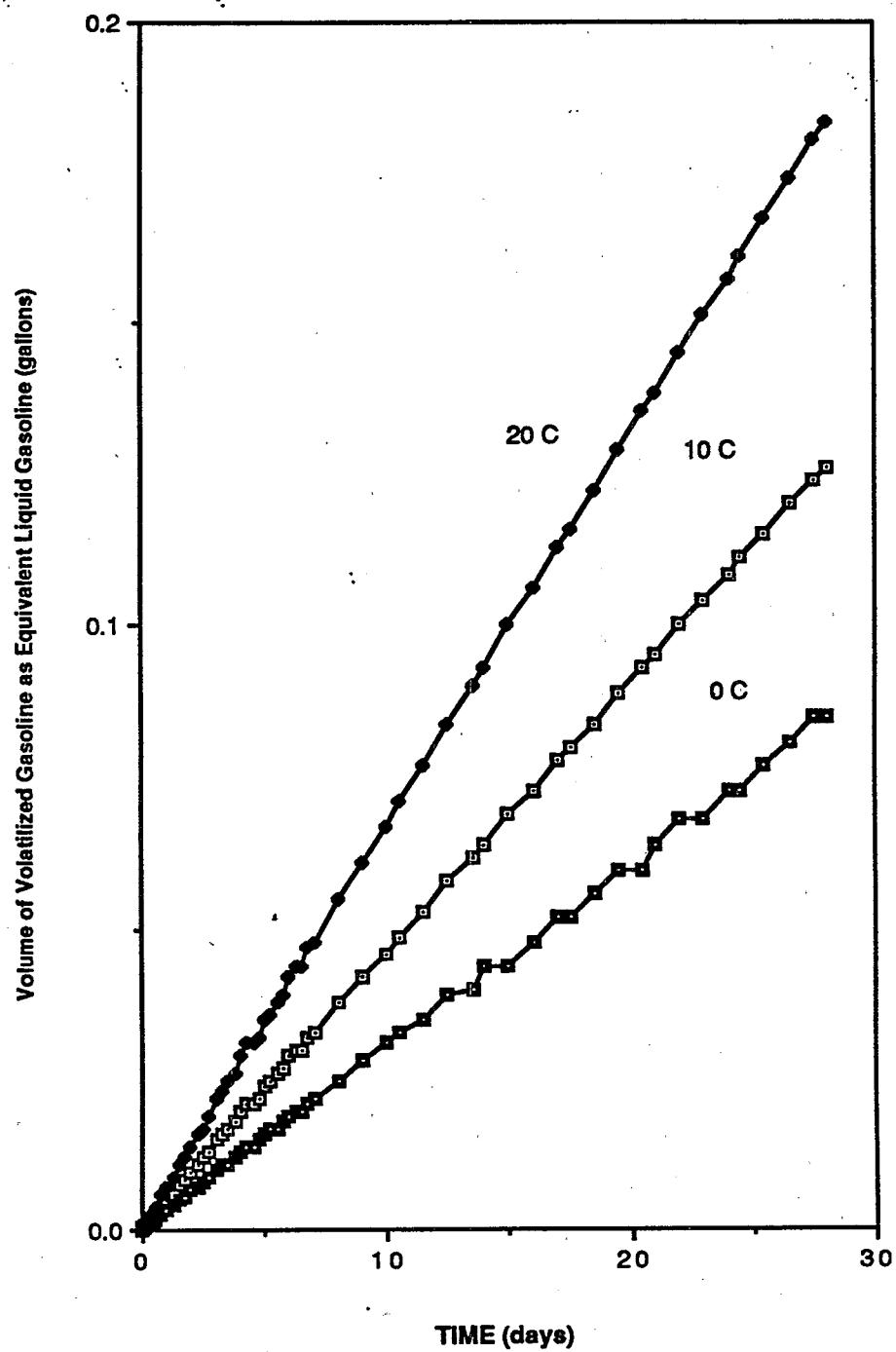
Figure 3-3. Time History of Simulated Gasoline Volatilized Volume for Average Soil Conditions at Different Temperatures
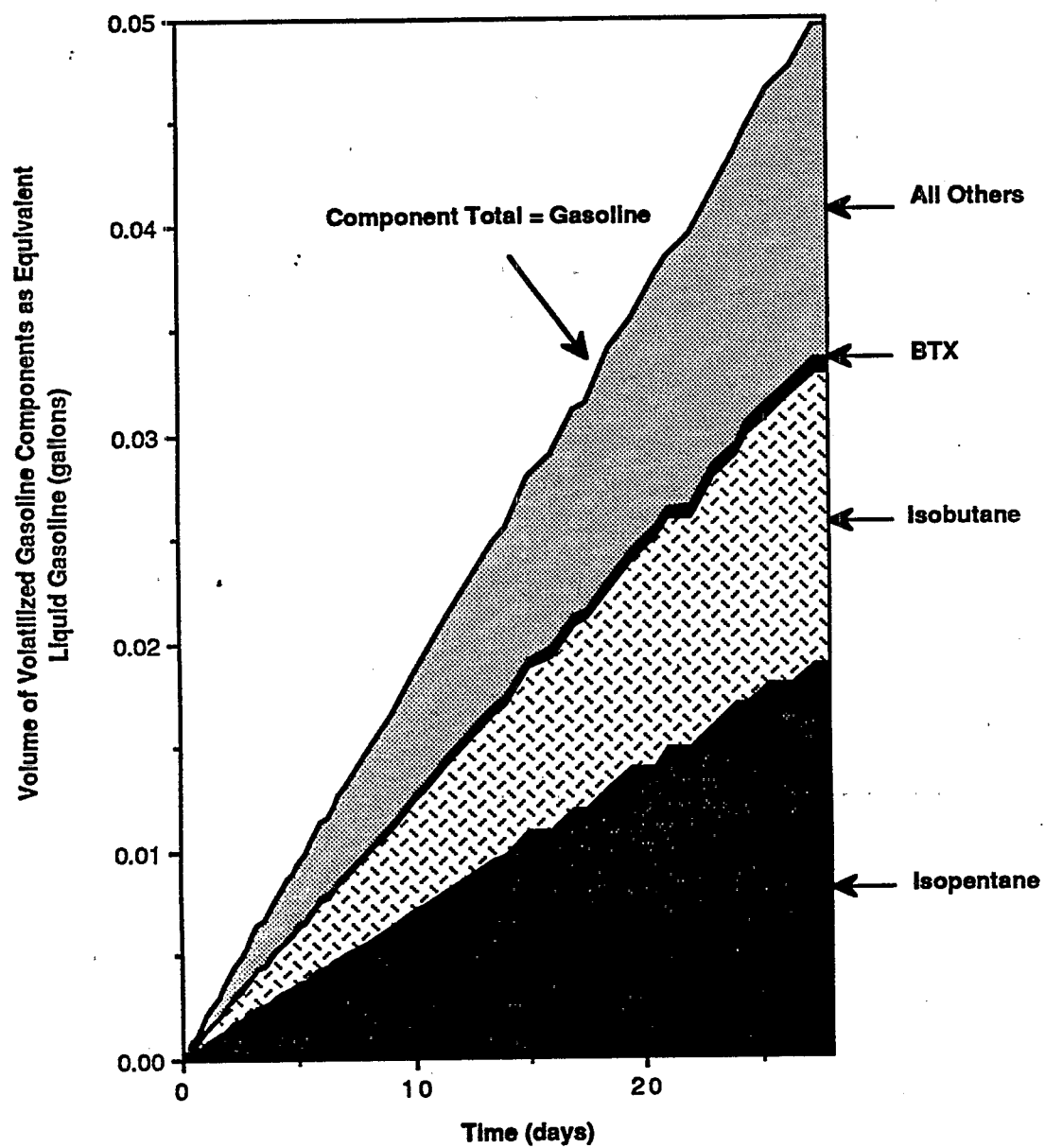
Figure 3-4. Time History of Simulated Volatilized Volume of Different Gasoline Components for Average Soil Conditions at 10. deg. C.

Legend:
- SOILS
- BACKFILL
- TANK

Lateral Distance (ft.)

Longitudinal Distance (ft.)

Values are Gasoline Vapor Concentrations in parts per million.

Contour labels: 250, 500, 750, 1,000, 5,000, 10,000, 50,000, 100,000
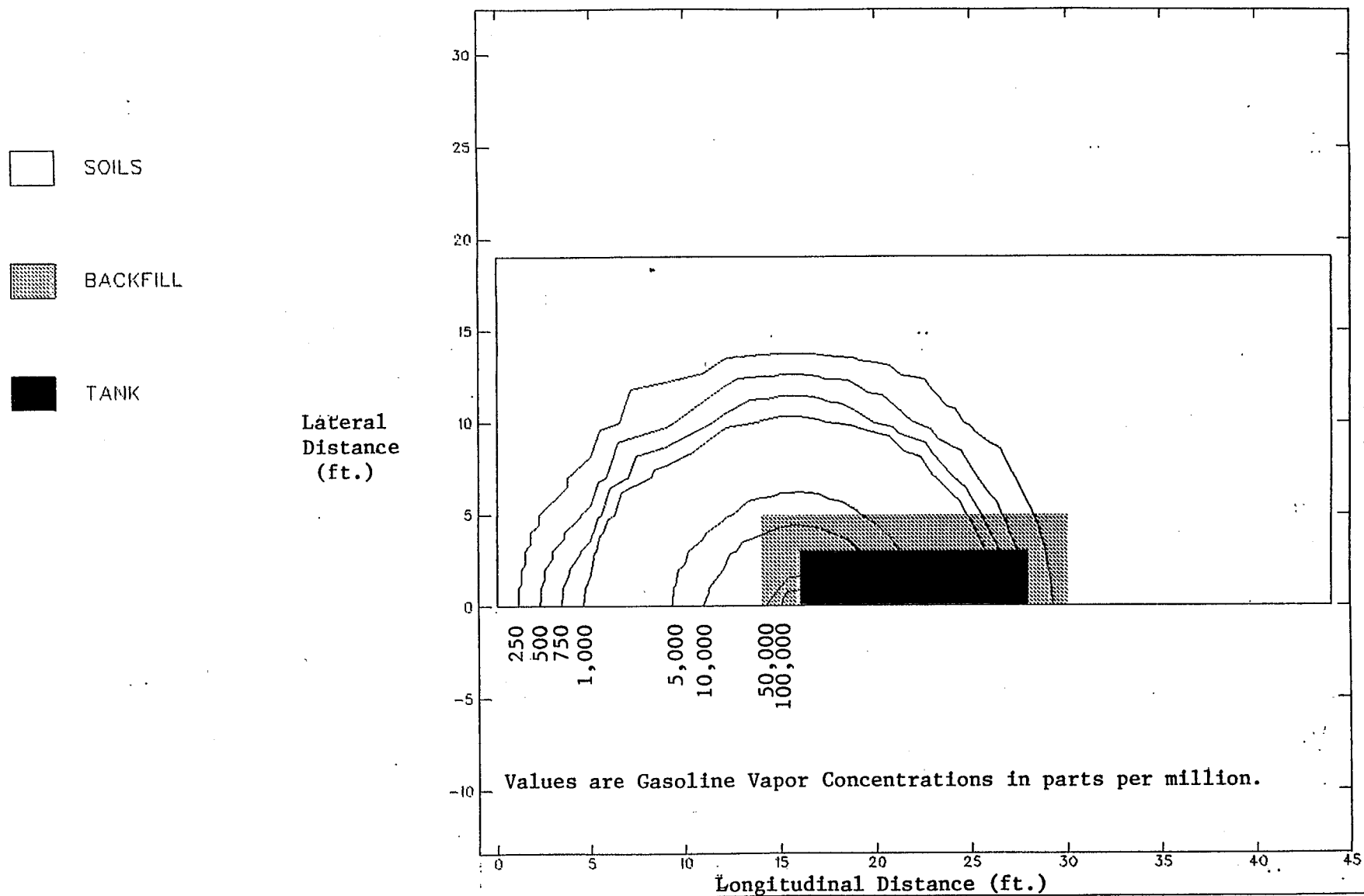
Figure 3-5. Contour Plot of Simulated Vapor Concentrations at 8 Foot Depth for Average Soil Conditions at 10°C and 14 Days Since Leak Started.
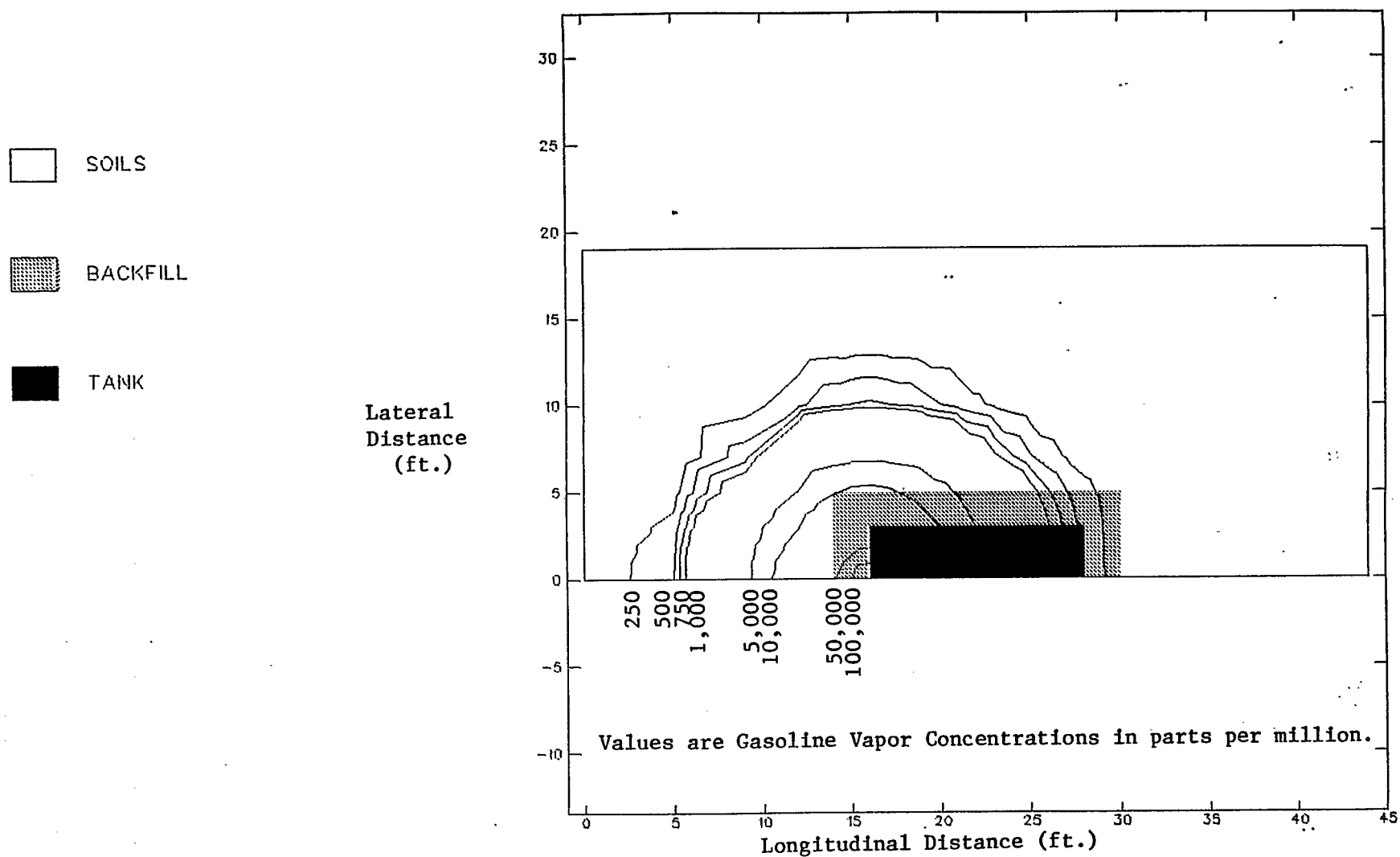
Figure 3-6.   Contour Plot of Simulated Vapor Concentrations at 8 Foot Depth for
Dry Gravel Backfill, Dry Silty Sand Native Soil Conditions at 10°C
and 14 Days Since Leak Started.
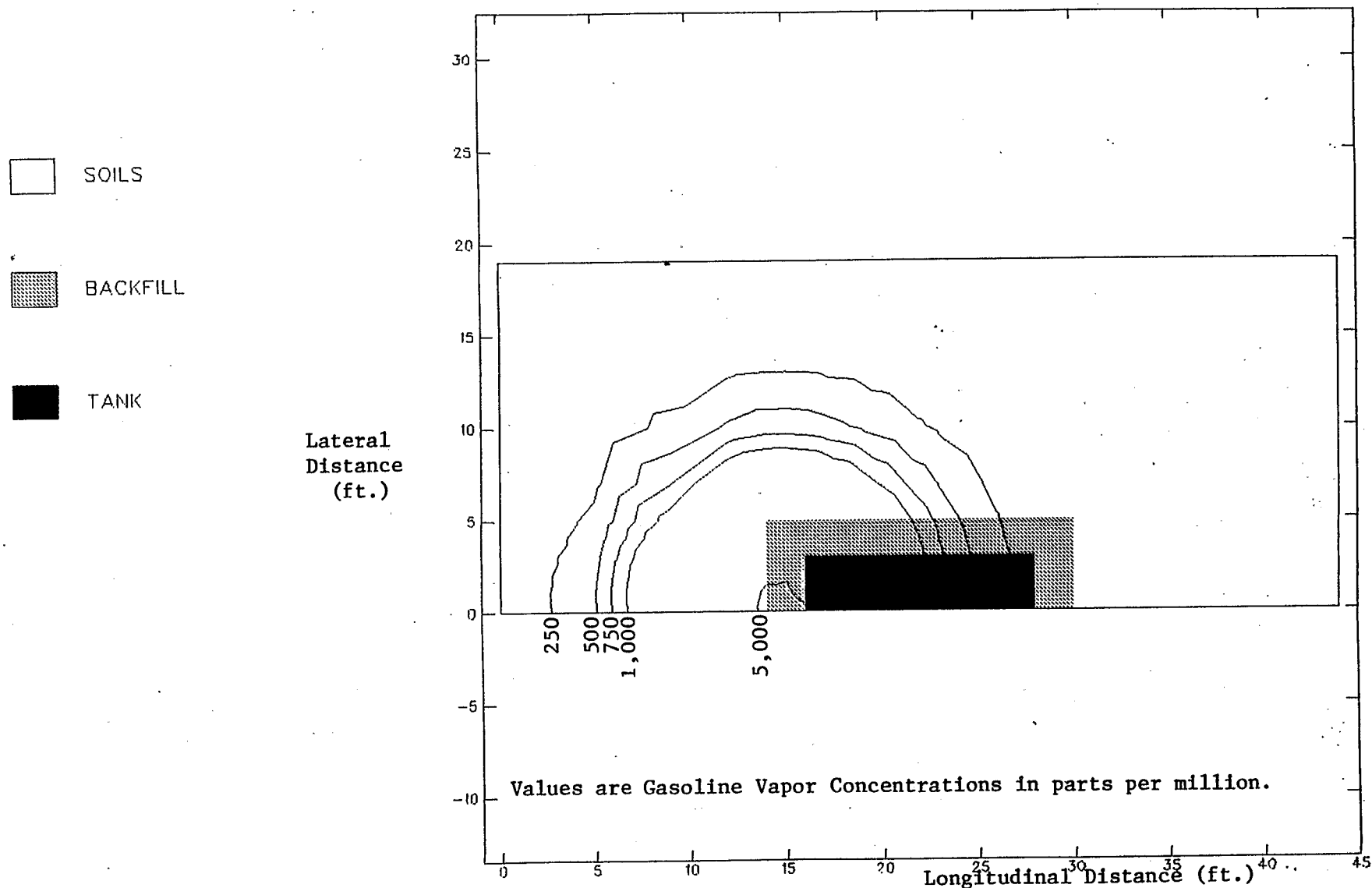
Figure 3-7. Contour Plot of Simulated Vapor Concentrations at 2 Foot Depth for
Average Soil Conditions at 10°C and 14 Days since Leak Started.
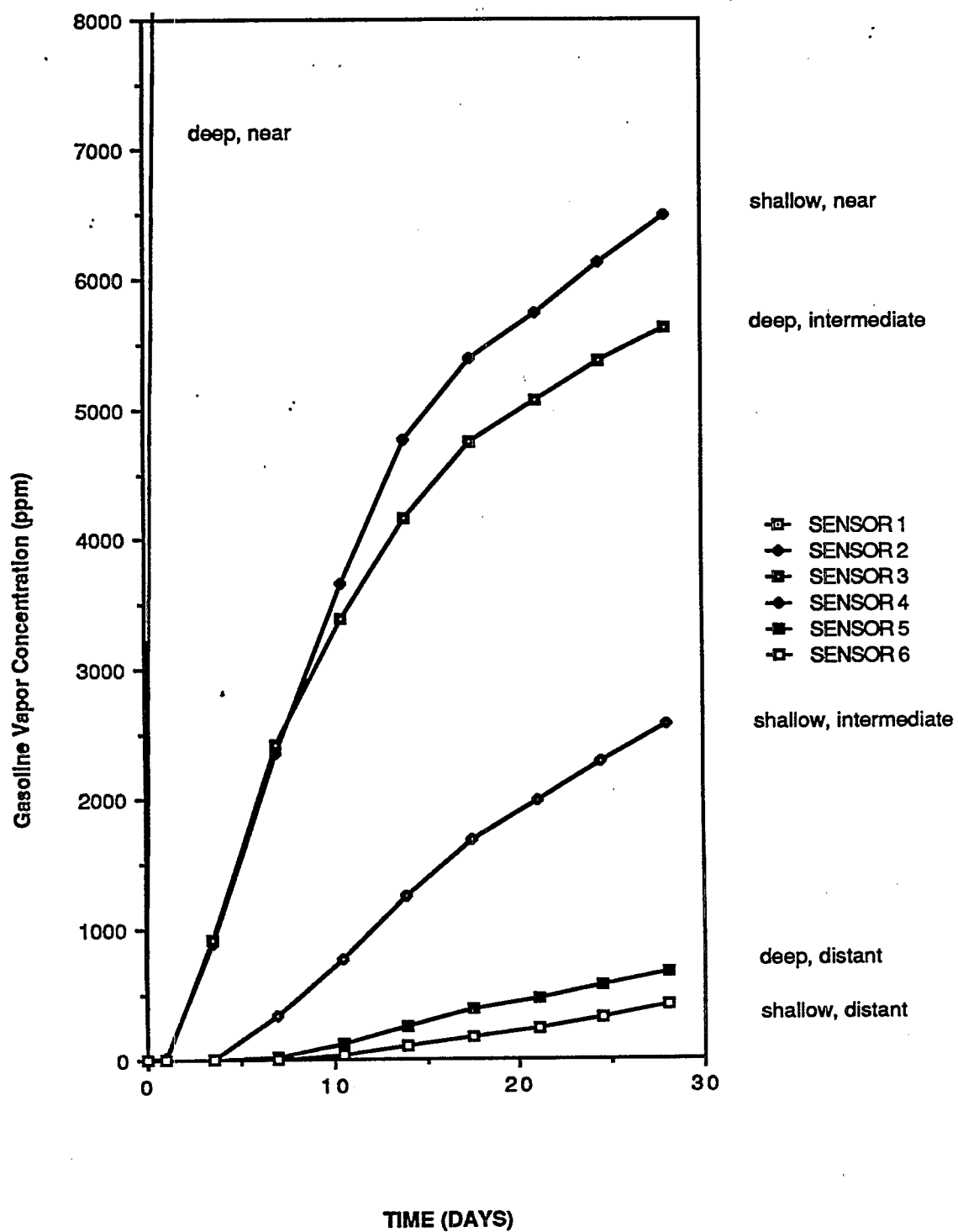
Figure 3-8. Time History of Simulated Vapor Concentrations at Various Sensor Locations for Average Soil Conditions at 10 deg. C.
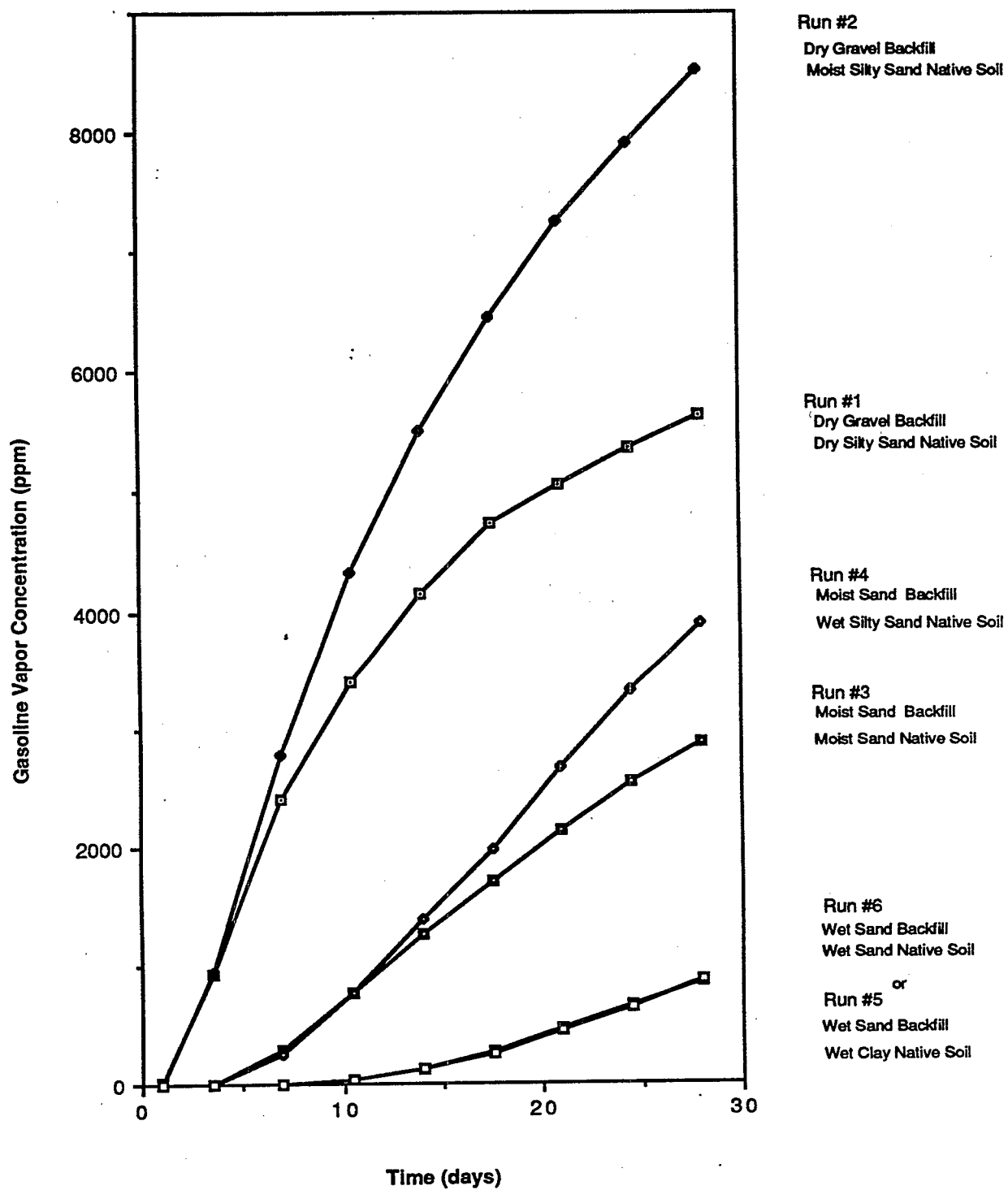
Figure 3-9. Time History of Simulated Vapor Concentrations at a Deep, "Intermediate" Sensor for Different Soil Conditions at 10 deg. C.
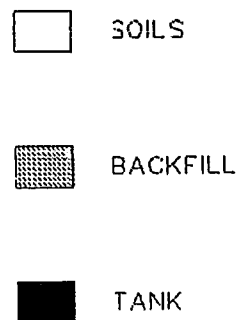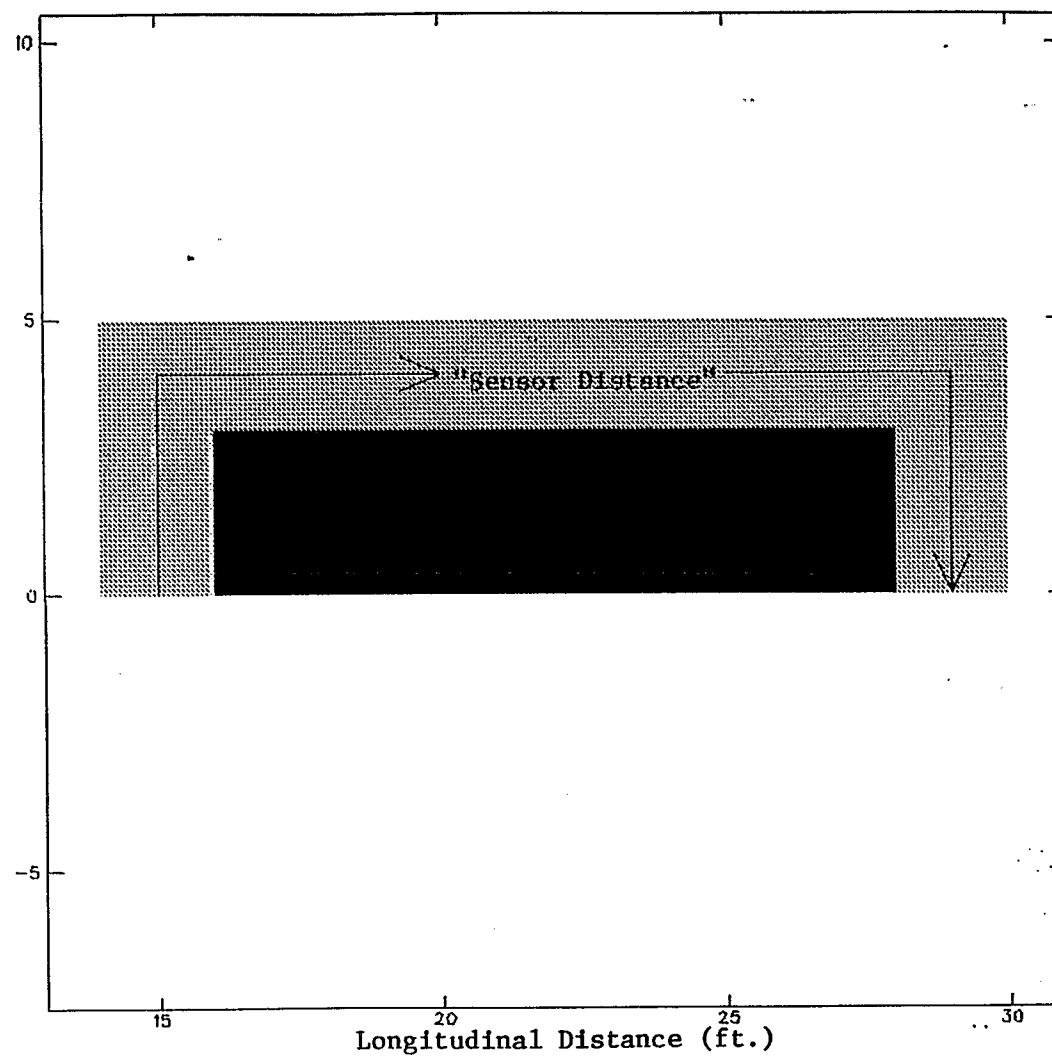
Figure 3-10. "Sensor Distance" Definition.
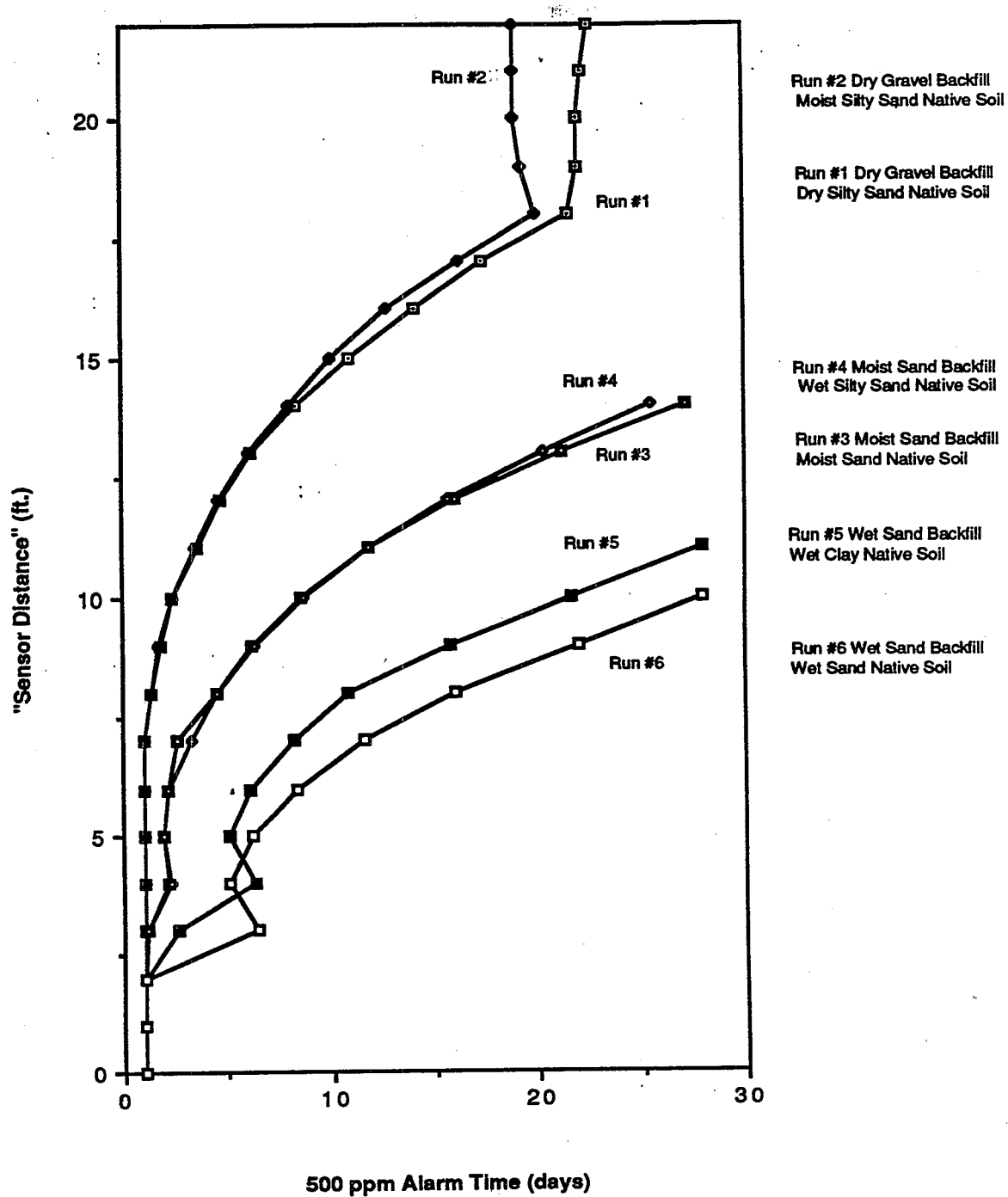
Figure 3-11. Alarm Time Versus "Sensor Distance" for Deep Sensors
and different Soil Conditions at 10 deg. C.
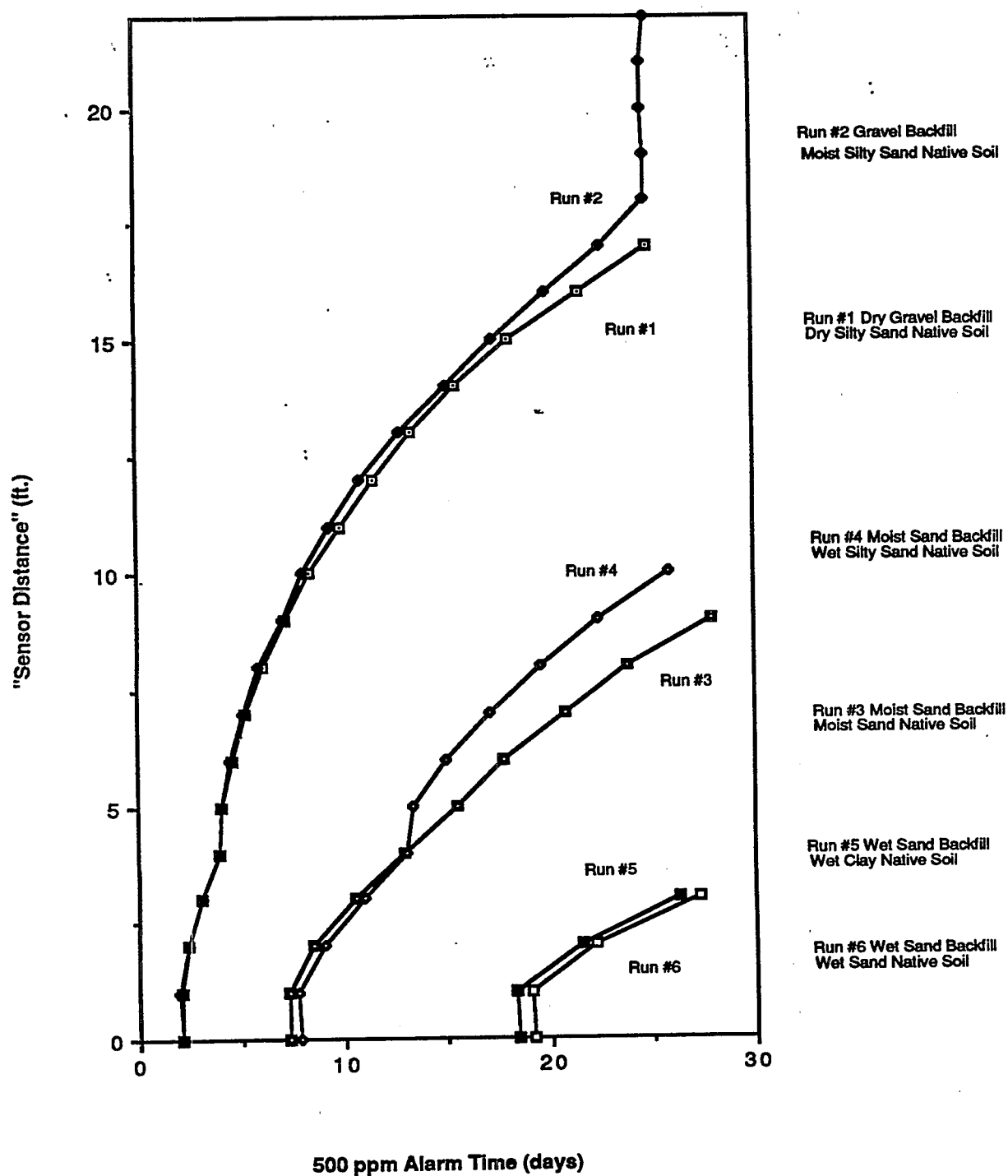
Figure 3-12. Alarm Time Versus "Sensor Distance" for Shallow Sensors and Different Soil Conditions at 10 deg. C.
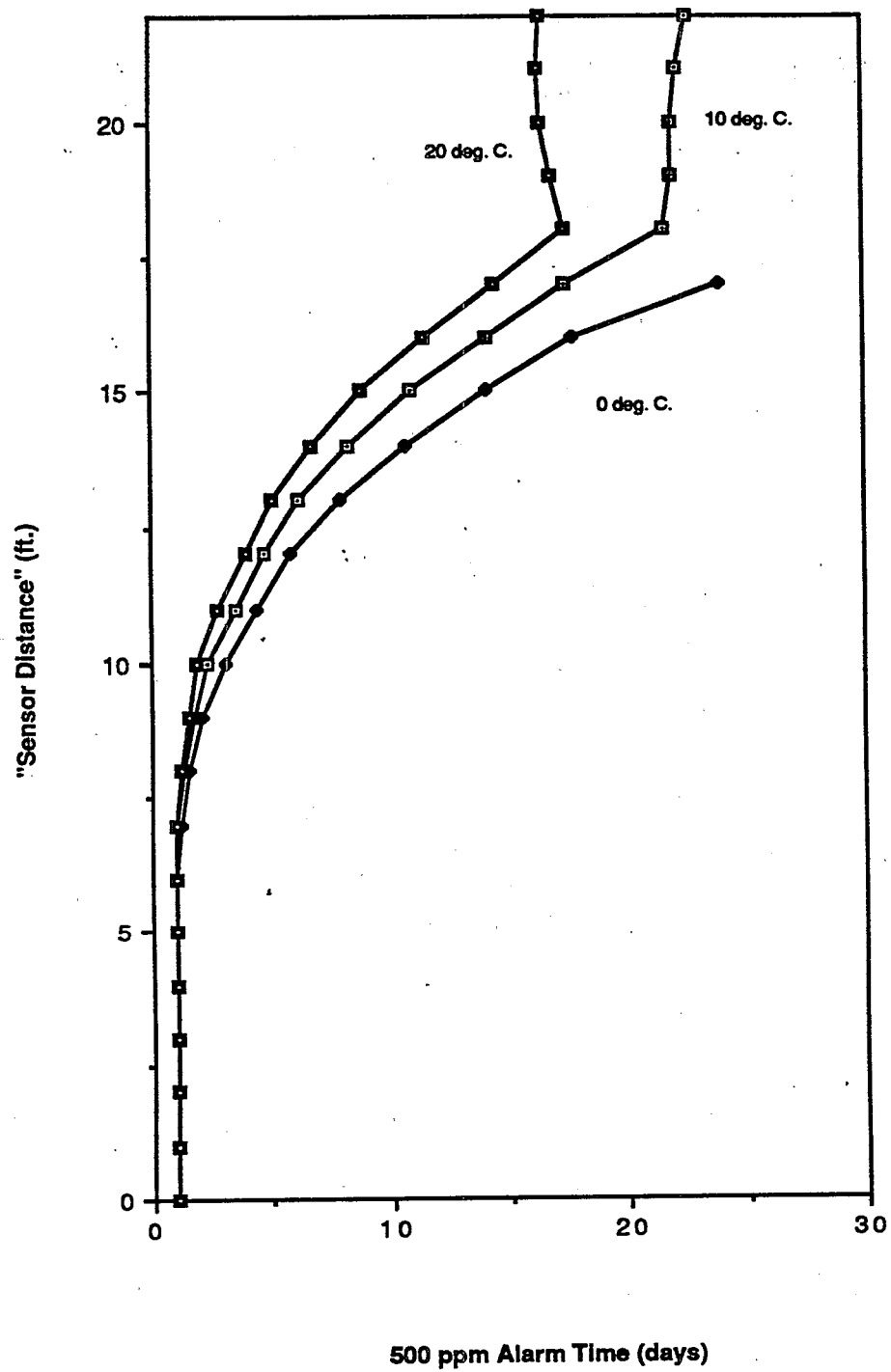
Figure 3-13. Alarm Time Versus "Sensor Distance" for Deep Sensors
and Average Soil Conditions at Various Temperatures
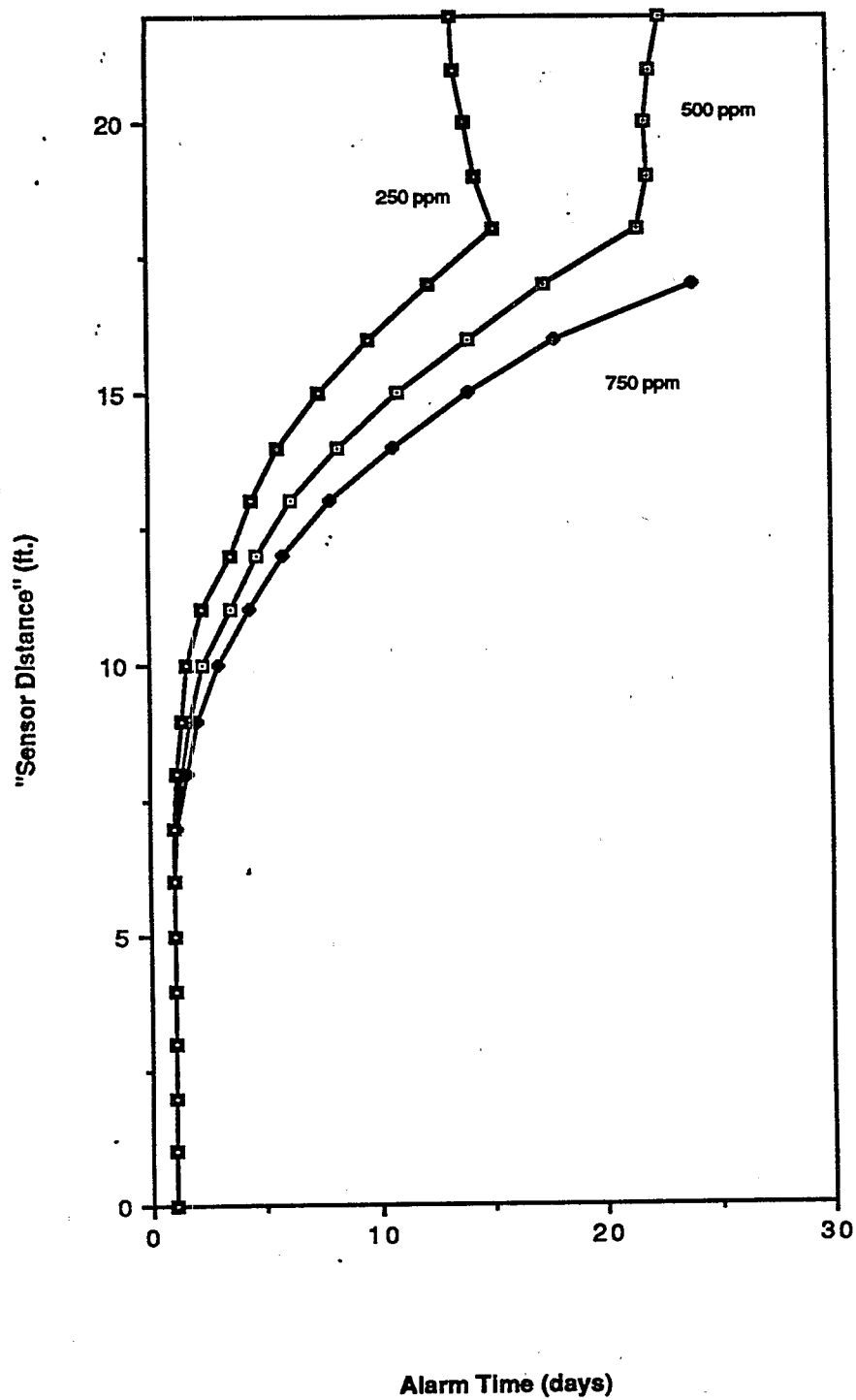
Figure 3-14. Alarm Time Versus "Sensor Distance" for Deep Sensors with Different Alarm Levels Under Average Soil Conditions at 10 Deg. C.
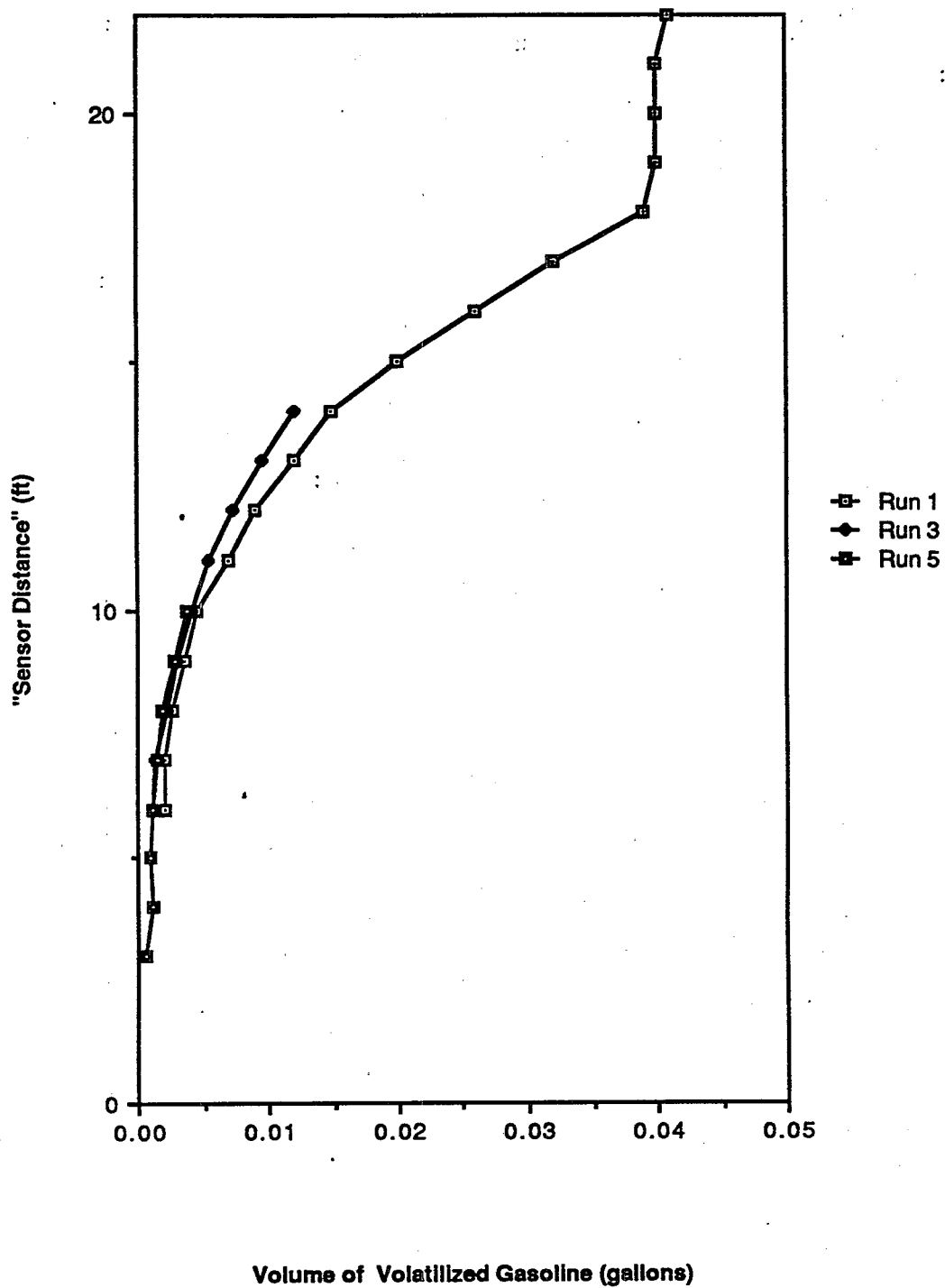
Figure 3-15. Volatilized Liquid Volume at Detection Time Versus "Sensor Distance" for Deep Sensors and Different Soil Conditions at 10 deg. C.
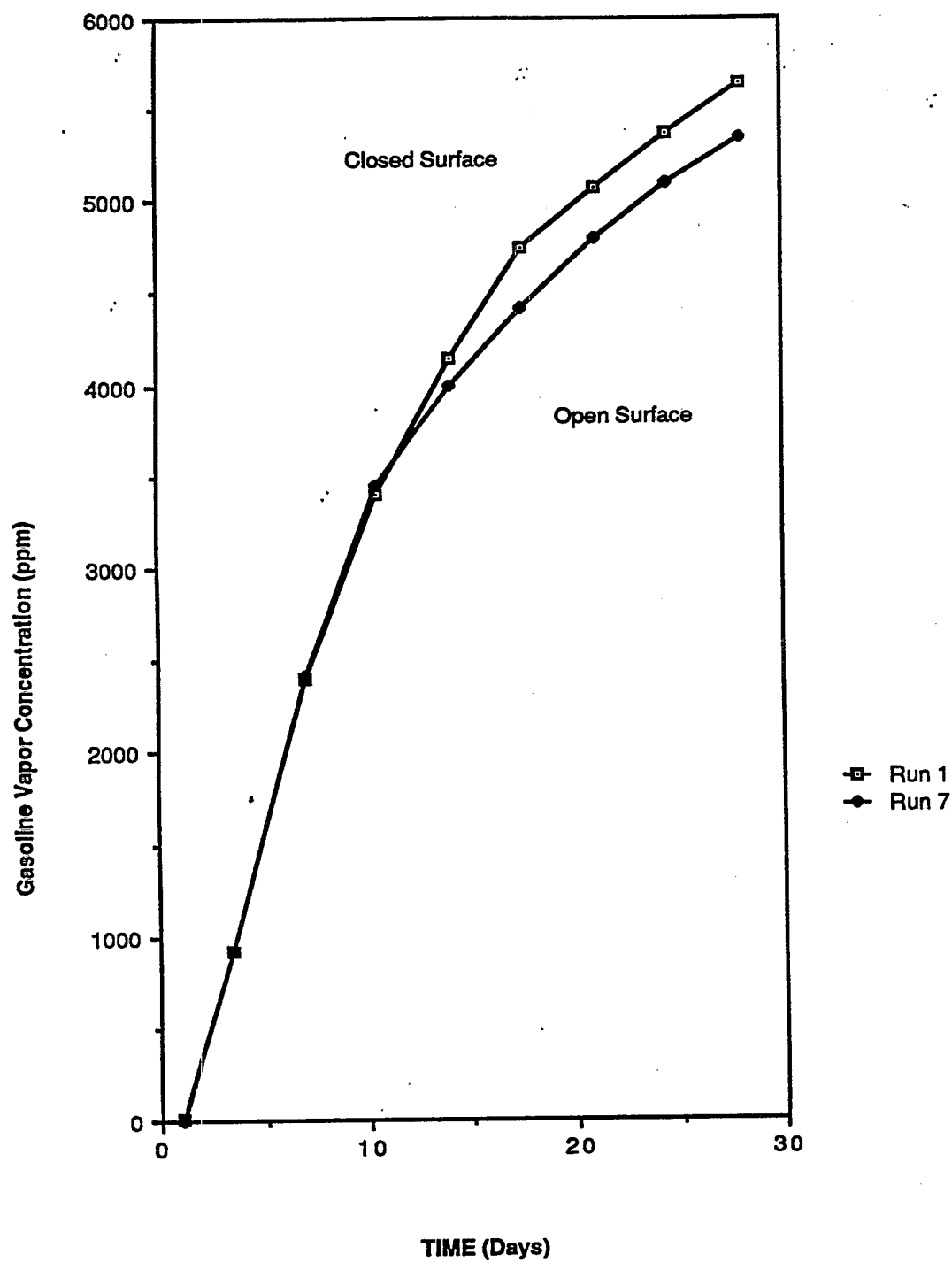
Figure 3-16. Open Versus Closed Surface: Time Histories of Vapor Concentrations at an "Intermediate" Deep Sensor.

4.0 DISCUSSION AND CONCLUSIONS

4.1 VAPOR SENSORS AS EARLY-WARNING DEVICES

The most significant finding of the vapor transport modeling is that, under
a variety of soil and temperature conditions, external vapor detectors,
responding to total hydrocarbons in the 500 parts per million range, are
predicted to act as well as in-tank sensors as good early warning devices.
The vapor transport simulations predicted that, for average conditions, a
shallow vapor sensor on the opposite side of the tank from the leak will
detect the volatilized product within approximately 30 days. Sensors
halfway across the excavation zone were predicted to respond within about 8
days.

Moreover, the minimum amount of volatilized product that can be detected
with external sensors is far lower than the minimum volume of leak that
would be detectable with in-tank methods. For example, if regulations
allow 12 months between in-tank tests and they stipulate the ability to
detect 0.2 gallons per hour, then as much as 1,752 gallons could leak
before detection. For the simulated case with the lowest air-filled
porosity, in which the native soil was a clay at 50 percent of saturation,
and the backfill was a wet sand, vapors from the leak were predicted to be
at detectable (500 parts per million) concentrations at a sensor halfway
across the excavation zone before 0.004 gallons had vaporized. For the
"average" conditions, with dry gravel backfill and dry sand native soil,
the "base case" volatilized volume at detection, by a shallow sensor on the
opposite end of the excavation zone, was estimated to be about 0.05
gallons.

The high volatility and high diffusion rate of the gasoline hydrocarbons
produces early detection times, and therefore a low volume of vaporized
gasoline escapes before detection.

4-1

4.2 IMPLICATIONS FOR MONITORING NETWORK DESIGN

The vapor transport simulations provide information that can guide the conceptualization of sensor network design. Primarily, the simulations predict that a single sensor, in an excavation zone in which diffusion of vapors is the most important transport mechanism, can out-perform in-tank leak detection methods. Sensible network designs for multi-tank systems could then be based on predicted "zones of detection," a concept analogous to the "zones of influence" of ground water pumping wells in an aquifer.

Commonsense would also lead the designer to strive to place the vapor sensors as close to the leak as possible. Not knowing in advance where this is, the designer should anticipate where leaks are likely to occur and where they would be most difficult to detect. Leaks are more likely to occur from the tank bottom, since that area of the tank is in contact with pure product more often than the tank's top or sides. Thus, if leaks can be expected to be at the tank bottom, this would indicate that sensors should be placed lower in the excavation zone, and preferably at or around the depth of the tank or excavation zone bottom. This is the most difficult and expensive monitoring depth, but according to the vapor transport simulations, a shallower sensor at the same plan view location, will respond substantially later. Even shallow sensors, however, perform quite well as evidenced in Section 3.

Although density effects were not simulated, they would have produced an even greater differential between deeper vapor monitors and shallow ones. This is because most of the gasoline components are denser then air. But, again, such consideration even for sensors placed near the surface would not imply "poor" performance overall.

Advection effects, or the movement of vapors due to pressure gradients, could influence the design of a sensor network. Gradients caused by active pumping sensors should enhance the ability to detect vapors, and so a continuous, powerful air suction device would be anticipated to serve one or more tanks. On the other hand, pressure gradients could cause a single passive sensor to miss sensing the vapors. For example, warm basements in

the winter induce a subsurface "wind" that moves vaporized product away from the sensor. In anticipation of this possibility, a four point network, as an example, would provide good coverage against predominating advection currents. The sensors would be placed with two on opposite (longitudinal) ends of the tank, and two straddling the middle (laterally).

With regard to sensor spacing, the vapor modeling has predicted that under static air pressure conditions (i.e., negligible pressure gradients), total hydrocarbon sensors will respond within days of each other whether 12 feet or 4 feet from the leak. Thus, the issues of density and pressure-induced flow would be the only ones that would indicate the need for multiple sensors at an individual tank.

The modeling investigation also illustrated how sensor specificity plays a role in the network design process; the characterization of the leakage source included the calculation of saturation concentrations of typical gasoline components for several representative blends. In particular, it was determined that components such as isopentane and isobutane typically comprise the highest percentage or most volatile portion of the blends and will therefore have the highest hydrocarbon concentration at the sensors. Sensors that are specific or sensitive to these compounds, and to the other chemicals that have similar saturation concentrations as shown in Appendix D, will be the most successful at detecting gasoline UST leaks. Sensors that are specific to benzene, toluene, and xylenes (BTX) will be less successful, unless such sensors are capable of achieving detection at much lower thresholds.

Network design issues such as sensor location, spacing, and specificity will be affected if typical background vapor concentrations are found to approach the concentrations that the vapor modeling showed would be reaching the sensors. In this case, false alarms could be avoided, in theory, by raising the detection concentration threshold above the expected background interference and spacing the detectors more closely together. The vapor transport modeling results can be re-interpreted easily for higher detection limits, to investigate how high background concentrations could affect the timing of sensor response.

4-3

4.3 IMPLICATIONS FOR VAPOR DETECTOR REGULATIONS

Vapor transport modeling has demonstrated that external vapor sensors in the tank excavation zone can be expected to act as good early warning devices. Vapor sensors in a properly designed network are predicted to be capable of detecting vaporizing leaks on the order of 10^{-4} gallons per hour within days or weeks, based on the speed with which vapors from leaks are expected to diffuse throughout the backfill and soils surrounding the UST. This promising evaluation of vapor sensors should be tempered by recalling that the modeling results were based on a generic, single UST, assuming diffusion-dominated transport. Actual conditions vary from site to site. The modeling results, however, are a good first step in the assessment of the expected performance of vapor detectors.

4.4 VAPOR TRANSPORT ANALYSIS AND MODELING RECOMMENDATIONS

The next round of vapor transport analysis and modeling should be designed to focus on the most pressing issues raised by the results reported herein. Several aspects of the generic UST representation could be modified or refined, including:

o Leaking product — other fuels and chemical components could be evaluated;

o Number of tanks — multiple tanks, including the piping network, could be simulated;

o Tank geometry — a different tank size or geometric shape could be defined;

o Excavation zone — its shape and size could be modified;

o Pressure gradients — ambient gradients and sensor-induced suction could be simulated;

o Density effects — this could be investigated further by analysis and modeling;

o Validation of the diffusion model could be accomplished, using laboratory or field data;

o. Background interference – current work on determining background levels could be incorporated as boundary conditions in the model to investigate false alarms versus detection limits;

o Sensor Performance – the work on defining sensor characteristics could be incorporated;

o Leak Representation – the complex dynamics of the leak "source" term in the model could be investigated; and

o Hydrogeologic Conditions – other soil and temperature conditions could be simulated.

Future research should concentrate on refining the leak representation, in advance of performing additional simulations with the diffusion-based UST model. This would be accomplished through a combination of analytical and numerical model-based investigations.

Also to be included in future research on the UST vapor modeling and analysis should be simulation of leakage from pipeline systems. It is anticipated that a simple geometric configuration, similar to the single UST simulated in this report could be used. The bulk of the efforts could be comprised of sensitivity analyses, testing the effects of leak characterization, temperature, soil conditions, or other phenomena, as appropriate.

Future research should also include validation of the diffusion model using data from "sandbox" experiments being conducted by the Oregon Graduate Center. This would involve simulation of the experimental apparatus, in a three-dimensional model grid similar to the UST model described herein. The comparison of computer model results to laboratory data is expected to yield information on the effects of gravity, the significance of vapor-water partitioning, and the importance of diffusion with respect to other fate and transport processes. Further research of the significance of gravity-driven advection through the use of modeling is recommended.

5.0 REFERENCES

Alberton, M., 1979.
"Carbon Dioxide Balancing the Gas-Filled Part of the Soil, Demonstrated
at a Podzol" (in German), Zeitschrift Pflanzenernaeher.
Bodenkd., 147, 39-56.

Allan, R.E., 1986.
"Modeling and Sensitivity Analysis of Vapour Migration in Soil from
Spilled Volatile Liquids", M.S. Thesis, University of Waterloo.

Arthur D. Little, Inc., 1987.
"The Installation Restoration Program Toxicology Guide," V.3, Prepared
for the Aerospace Medical Division Air Force Systems Command, Wright
Patterson Air Force Base, OH, Available from NTIS, ch. 65, 6/87.

Bruell, C., 1987.
University of Lowell, Personal Communications.

Buckingham, E., 1904.
"Contribution to Our Knowledge of the Aeration of Soils," Bull. 25,
52 pp., USDA Bur. of Soils, Washington, DC.

Camp, Dresser & McKee Inc., 1984.
"DYNFLOW: A Three-Dimensional Finite Element Groundwater Flow Model,
Description and User's Manual."

Camp, Dresser & McKee Inc., 1986.
"Interim Report: Fate and Transport of Substances Leaking from
Underground Storage Tanks." Boston: Camp Dresser & McKee, prepared for
the Office of Underground Storage Tanks, U.S. Environmental Protection
Agency.

Camp, Dresser & McKee Inc., 1986.
"Fate and Transport of Substances Leaking from Underground Storage
Tanks,; Volume II — Appendices," Interim Report on Contract No.
68-01-6939 Submitted to U.S. Environmental Protection Agency, Office of
Underground Storage Tanks.

CHEMEST is a Computerized Chemical Property Estimation System Developed by
W. Lyman and R. Potts at Arthur D. Little, Inc., Details are available
from W. Lyman, Camp Dresser & McKee, Inc., One Center Plaza, Boston, MA
02108.

Corapcioglu, M.Y. and A.L. Baehr, 1987.
"A Composition Multiphase Model for Groundwater Contamination by
Petroleum Products, I. Theoretical Considerations," Water Resources
Research, 23(1), 191-200.

Environmental Protection Agency, 1987.
"Processes Affecting Subsurface Transport of Leaking Undergound Tank
Fluids." EPA Report No. 600/6-87/005. Las Vegas: Environmental
Monitoring Systems Laboratory.

"Handbook of Chemistry and Physics," 1980.
R.C. Weast, ed., CRC Press.

Huyakorn, P.S. and G.F. Pinder, 1983.
"Computational Methods in Subsurface Flow," Academic Press, London,
473 pp.

Kirk-Othmer, 1973.
"Encyclopedia and Chemical Technology", 2nd ed., J. Wiley and Sons.

Lugg, G.A., 1968.
"Diffusion Coefficients of Some Organic and Other Vapors in Air,"
Analytical Chemistry, 40(7): 1072-1077, 1968.

Lyman, W. J., W.F. Reehl, and D.H. Rosenblatt, 1982.
"Handbook of Chemical Property Estimation Methods," McGraw-Hill Book Co.

MacKay, D. and W.Y. Shiu, 1981.
"A Critical Review of Henry's Law Constants for Chemicals of
Environmental Interest", Journal of Physical Chemistry Ref. Data, 10(4):
1175-99.

McDonald, M.G. and A.W. Harbaugh, 1984.
"A Modular Three-Dimensional Finite-Difference Ground-Water Flow Model",
U.S. Geological Survey Open File Report 83-875, 528 pages.

Metcalfe, D.E., 1982.
"Modeling Gas Transport from Waste Disposal Sites," M.S. Thesis,
University of Waterloo.

Millington, R.J., 1959.
"Gas Diffusion in Porous Media," Science, 130, 100-102.

Millington, R.J. and J.M. Quirk, 1961.
"Permeability of Porous Solids," Transactions of the Faraday Society,
57: 1200-7.

Penman, H.L, 1940.
"Gas and Vapour Movements in the Soil, 1. The Diffusion of Vapours
through Porous Solids," Journal of Agricultural Science, 30, 347-462.

Perry, R.H. and C.H. Chilton, 1973.
"Chemical Engineer's Handbook," 5th ed., McGraw-Hill Book Co.

Reid, R.C., J.M. Prausnitz, and T.K. Sherwood, 1977.
"The Properties of Gases and Liquids," 3rd ed., McGraw-Hill Book Co.

Robbins, G.A., 1987.
   "Influence of Pore Air/Water Exchange on the Diffusion of Volatile
   Organic Vapors in Soil," Presented at NWWA Conference, Petroleum
   Hydrocarbons and Organic Chemicals in Groundwater, November 17-19,
   Houston, TX.

Stetzenbach, K., September, 1987.
   "Memorandum on Gasoline Composition," and "Memorandum on Standard
   Gasoline Vapor Mixture," University of Nevada at Las Vegas/Environmental
   Research Center. Written to P. Durgin, U.S. Environmental Protection
   Agency/Environmental Monitoring Systems Laboratory.

U.S. Environmental Protection Agency, May, 1986.
   "Underground Motor Fuel Storage Tanks: A National Survey, Volume 1,
   Technical Report," EPA 560/5-86-03, Office of Pesticides and Toxic
   Substances, Washington, D.C.

U.S. Environmental Protection Agency, 1987.
   "Processes Affecting Subsurface Transport of Leaking Underground Tank
   Fluids." EPA Report No. 600/6-87/005. Las Vegas: Environmental
   Monitoring Systems Laboratory.

Wilson, J.T., 1987.
   "Summary: Some Physics and Chemistry of Movement of Organics in the
   Vadose and Saturated Zone," Presented at E.P.A. Seminar on the
   Evaluation of Corrective Action Technologies for Leaking Underground
   Storage Tanks, 10/7/87.

APPENDIX A

GLOSSARY

This appendix is a glossary of terms used in this document. The definitions are related to the problem of vapor transport as presented in this report, and in many cases are not generalized definitions. A consistent set of Systeme Internationale (S.I.) units is used in the definition of physical and chemical parameters and variables. Related terms are cross-referenced.

Defined Terms

Advection
Anisotropy
Backfill
Background Concentration
Capillary Fringe
Density
Diffusion
Dynamic Viscosity
Effective Diffusion Coefficient
Excavation Zone
Fick's First Law
Fick's Second Law
Henry's Law
Heterogeneity
Moisture Content
Organic Matter Content
Partial Pressure
Pea Gravel
Phreatic Surface
Porosity
Raoult's Law
Residual Oil Saturation
Saturated Zone
Solubility
Specific Yield
Surface Tension
Tortuosity
Unsaturated Zone
Vadose Zone
Vapor Pressure
Volatilization
Water Table
Wettability

Definitions

Advection

The process of transfer of vapors through a geologic formation in response to a pressure gradient which may be caused by changes in barometric pressure, water table levels, wind fluctuations, or rainfall percolation. Advection can result from a thermal gradient caused by a heat source.

Anisotropy

The variation of a property of a porous medium according to the direction of measurement. For example, hydraulic conductivity in a stratified deposit will be higher in the horizontal plan than in the vertical direction.

Backfill

The material emplaced around an UST in an excavation zone for support. Clean, well-sorted sand or gravel is the backfill material recommended by the American Petroleum Institute. See pea gravel.

Concentration

The initial level of contamination existing in the subsurface at a site preceding a leak of contaminants at the site.

Capillary Fringe

The zone above the water table characterized by saturated voids within which water pressure is less than atmospheric. The capillary fringe is thicker in fine-grained materials than in coarse materials and depends on the size distribution of grains.

Density

The amount of mass of a substance per unit volume of the substance, having units of mass per volume (g/cm^3).

Diffusion

The process whereby the molecules of a compound in a single phase equilibrate to a zero concentration gradient by random molecular motion. The flux of molecules is from regions of high concentration to low concentration and is governed by Fick's First Law. See Fick's First Law, effective diffusion coefficient.

Dynamic Viscosity

The measure of internal friction of a fluid that resists shear within the fluid; the constant of proportionality between a shear stress applied to a liquid and the rate of angular deformation within the liquid, having units of mass per length per time (g/cm sec).

Effective Diffusion Coefficient

The constant of proportionality in Fick's Second Law which is dependent on tortuosity, porosity, and moisture content and properties of the diffusing compound, having units of squared length per time (cm^2/sec). See tortuosity, porosity, moisture content, Fick's Second Law.

Excavation Zone

The zone excavated of native materials into which the UST is emplaced and then filled with backfill material. Depth of the excavation zone is between 10 and 15 feet and is covered by a concrete pad in areas of heavy traffic.

Fick's First Law

An equation relating the flux of molecules to the concentration gradient, with the proportionality constant being the diffusion coefficient. See Fick's Second Law, diffusion, effective diffusion coefficient.

Fick's Second Law

An equation relating the rate of change of concentration with time due to diffusion to the rate of change in concentration gradient with distance from the source of concentration. See Fick's first Law, diffusion, effective diffusion coefficient.

Henry's Law

The relationship between the partial pressure of a compound in the vapor phase over a liquid and the compound's equilibrium concentration in the liquid, through a constant of proportionality known as Henry's Law Constant. Generally used for low solution concentrations. See partial pressure.

Heterogeneity

The variation in a property of a porous medium as a function of location. Heterogeneity may be due to grain size trends, stratigraphic contacts, faults, and vertical bedding.

Moisture Content

The amount of water lost from the soil upon drying to a constant weight, expressed as the volume of water per unit bulk volume of the soil. For a fully saturated medium, moisture content equals the porosity; in the vadose zone, moisture content ranges between zero and the porosity value for the medium. See porosity, vadose zone, saturated zone.

Organic Matter Content

The fraction of soil, sediment, or porous medium composed of organic matter. In natural systems, this material consists primarily of the decay products of plants and animals.

Partial Pressure

The equilibrium vapor pressure exerted on the atmosphere by a component of a liquid mixture. See Henry's Law.

Pea Gravel

A well-sorted, clean, and well-rounded sediment (gravel) of diameter between 3/8 and 1/2 inch which is commonly used as backfill material. See backfill.

Phreatic Surface

The surface of water in an unconfined aquifer on which the fluid pressure in the voids is at atmospheric pressure, also termed the water table.

Piezometric Surface

The hydraulic head of water in a confined aquifer as defined by the elevation head and the pressure head at a particular location.

Porosity

The void fraction of a porous medium of rock or sediment, usually occupied by water and/or air. See also moisture content.

Pressure Head

The component of hydraulic head resulting from the weight of overlying water at the point of measurement, and any other forces, such as water well injection, that may be inducing pressures.

Raoult's Law

The relationship between the partial pressure of a component in a liquid to the product of the mole fraction of the component in the liquid and the vapor pressure of the pure component.

Residual Oil Saturation

The amount of oil remaining in the voids of a porous medium below which oil is retained in an immobile state.

Respiration

The biological consumption of oxygen during the oxidation of organic compounds or material by aerobic bacteria.

Saturated Zone

The zone of a porous medium below the water table in which the voids are fully saturated with fluid and the pressure is greater than atmospheric. See water table.

Solubility

The amount of mass of a compound that will dissolve into a unit volume or mass of the solvent (usually water), or final solution, having units of mass per volume (g/cm^3).

Specific Yield

The volume of water released from storage per unit area of aquifer in response to a unit decline of water table in an unconfined aquifer, having units of volume per unit area per unit thickness ($cm^3/cm^2/cm$).

Surface Tension

The measure of interfacial tension due to molecular attractions between two fluids in contact or between a liquid in contact with a solid. Surface tension is measured in units of dyn/cm and varies with temperature.

Tortuosity

The ratio of the average length of pore passages to the length of the column of the porous medium. This is the definition commonly used for the flow of water in a porous medium. "Vapor diffusion tortuosity" is a similar property of a porous medium, expressions for which have been derived empirically. See Appendix J.

Unsaturated Zone

See vadose zone.

Vadose Zone

The zone of a porous medium where the voids are partially filled with water.

Vapor Pressure

The equilibrium pressure exerted on the atmosphere by the vapors of a pure liquid at a given temperature.

Viscosity

See dynamic viscosity.

Volatilization

The process of transfer of a chemical from the aqueous or other liquid phase to the air phase. Solubility, molecular weight, and vapor pressure of the liquid and the nature of the air-liquid/water interface affect the rate of volatilization. See solubility, vapor pressure.

Water Table

See phreatic surface.

Wettability

The tendency of a liquid to spread over a solid surface, which depends on the surface tension of the liquid.

APPENDIX B

DICTIONARY OF VARIABLES AND PARAMETERS

This appendix defines the physical and chemical parmeters and variables used in this report. Dimensions of each parameter or variable are provided. Values of constant parameters (i.e., atmospheric pressure, $P_a = 760$ mm Hg) are provided where appropriate. All dimensions are given in consistent S.I. units. In the report, other units are used for convenience and for ease of understanding the results. A table of units conversion factors is therefore provided at the end of this appendix.

Definitions

A,B,C	Antoine equation coefficients (dimensionless).
C	Gas-phase concentration of kth constituent of gasoline (cm^3/cm^3).
C_w	Water-phase concentration of kth constituent of gasoline (cm^3/cm^3).
C_o	Equilibrium gasoline vapor concentration (cm^3/cm^3).
D_e	Effective diffusion coefficient (cm^2/sec).
D_o	Air diffusion coefficient (cm^2/sec).
D_o^r	Reference air diffusion coefficient measure for a specific compound (cm^2/sec).
D_{25}	Air diffusion coefficient meausured at 25°C (cm^2/sec).
D_{ij}	Dispersion tensor element (cm^2/sec).
erfc(z)	Complementary error function on variable z (dimensionless).
F_k	Retardation coefficient of kth gasoline constituent (dimensionless).
h	Piezometric head (cm).

H_k Henry's Law constant for k^{th} gasoline constituent (dimensionless). Non-dimensional units obtained from ratio of weight per volume of air to weight of water (e.g., g/cm^3).

J_x Volume flux per unit area entering system at source ($ft^3/hr/ft^2$).

K Hydraulic conductivity (cm/sec).

$\bar{M}_v$ Average molecular weight of gasoline vapors (g/mol).

$\bar{M}_a$ Average molecular weight of air, $\bar{M}_a = 28.96$ g/mol.

$\bar{M}$ Average molecular weight of gasoline-air mixture (g/mol).

M_k Molecular weight of kth gasoline vapor constituent (g/mol).

P_a Atmospheric pressure, $P_a = 760$ mm Hg.

P_k Partial pressure of kth gasoline constituent (mm Hg).

P_k^* Pure chemical vapor pressure of kth gasoline constituent (mm Hg).

P_t Total sum of partial pressures of gasoline constituents (mm Hg).

Q Influx rate of gasoline-air mixture entering system (cm^3/sec).

R Universal gas constant, $R = 62,360$ mm Hg·cm^3/mol·deg K.

R_k Heterogenous reaction term for k^{th} gasoline constituent (dimensionless).

s Volumetric gas concentration (cm^3/cm^3).

s_w Volumetric water concentration (cm^3/cm^3).

S Scalar quantity used to scale gasoline liquid volumes.

S_s Specific storativity (cm^{-1}).

t Time (seconds or hours).

T Temperature (deg. C or deg. K).

T_b Boiling point temperature (deg. K).

V_b Molar volume of kth gasoline vapor constituent at its boiling point ($cm^3/g \cdot mol$).

V_l	Volume of liquid gasoline (cm^3).
V_v	Volume of gasoline-air vapor entering system (cm^3).
W_v	Mass of gasoline vapors (g).
x	Distance (cm).
x_k	Mole fraction of kth gasoline vapor constituent (dimensionless).
$\mu_{g,k}$	Dynamic gas viscosity of kth gasoline vapor constituent (g/cm $\cdot$ sec).
$\mu_{o,k}$	Dynamic gas viscosity calculated at a reference temperature (g/cm $\cdot$ sec).
μ_{20}	Dynamic gas viscosity at 20° C (gm/cm $\cdot$ sec).
ρ_b	Liquid density of kth gasoline constituent at its boiling point (g/cm^3).
ρ_g	Gas-phase density (g/cm^3).
ρ_l	Liquid-phase density (g/cm^3).
ρ_v	Vapor density of gasoline-air mixture (g/cm^3).
τ	Tortuosity coefficient (dimensionless).
Θ_a	Air-filled porosity (cm^3/cm^3).
Θ_w	Water-filled porosity (cm^3/cm^3).
Θ_t	Total porosity (cm^3/cm^3).

Units Conversion Table

1 foot = 30.48 centimeters

1 ft/hr = 8.4667 x 10^{-3} cm/sec

1 ft^2/hr = 0.258 cm^2/sec

CHEMICAL PROPERTY ESTIMATION EQUATIONS

This appendix lists the equations used to estimate values of physicochemical properties of the constitutive chemicals of the gasoline blends presented in this appendix. Equations used to calculate leaked liquid gasoline volume from hydrocarbon vapor concentrations appear as well in this appendix. Physicochemical terms appearing in this appendix are defined in Appendices A and B. References used in estimating the chemical properties are listed in Section 5 of this report.

Average Molecular Weight of Gasoline Vapors, $\bar{M}_v$ (g/mol):

$$\bar{M}_v = \sum_{k=1}^{N} x_k \cdot M_k = \sum_{k=1}^{N} (P_k/P_t) \cdot M_k \qquad \text{(Equation C-1)}$$

$$P_t = \sum_{k=1}^{N} P_k$$

where:

x_k mole fraction of kth gasoline vapor constituent [dim.].

M_k molecular weight of kth gasoline vapor constituent (g/mol).

P_k partial pressure of kth gasoline vapor constituent (mm Hg).

P_t total pressure of gasoline vapors (mm Hg).

N number of gasoline vapor constituents.

Volume Influx of Gasoline Vapors, V_v (cm^3):

$$V_v = C_o \cdot Q \cdot t \qquad \text{(Equation C-2a)}$$

where:

C_c equilibrium vapor concentration in air of gasoline vapors (cm^3/cm^3).

$$C_o = P_t / P_a$$

P_a atmospheric pressure, P_a = 760 mm Hg at sea level.

Q   average influx of gasoline-air mixture into system (cm^3/sec).

t   duration of leak (seconds).

Mass of Gasoline Vapors, W_v (g):

$$W_v = \bar{M} \cdot V_v \cdot P_a/(T \cdot R)$$ (Equation C-3a)

where:

T   system temperature (°K)

R   universal gas constant, R = 62,360 mm $Hg \cdot cm^3/mol \cdot °K$.

Liquid Gasoline Volume, V_l (cm^3):

$$V_l = W_v/\rho_l$$ (Equation C-3b)

ρ_l gasoline liquid density, (g/cm^3)

Gasoline-Air Vapor Density, ρ_v (g/cm^3) at equilibrium concentration:

a. Average molecular weight of gasoline, $\bar{M}_v$, see Equation C-1 above.

b. Average molecular weight of air, $\bar{M}_a$:

Element	% Composition	Molecular Weight (g/mol)
N_2	78.084	28.0134
O_2	20.946	31.9988
Ar	0.934	39.9480
CO_2	0.033	44.0100
Total	100.000	$\bar{M}_a$ = 28.9641 g/mol

c. Average molecular weight of gasoline-air mixture, $\bar{M}$ (g/mol):

$$\bar{M} = (P_t/P_a) \cdot \bar{M}_v + (P_a - P_t) \cdot \bar{M}_a/P_a \qquad \text{(Equation C-4a)}$$

d. Vapor density of gasoline-air mixture, ρ_v (g/cm^3):

$$\rho_v = P_a \cdot \bar{M}/(T \cdot R) \qquad \text{(Equation C-4b)}$$

Air Diffusion Coefficient, D_o [cm^2/sec]:

a. Correction of air diffusion coefficient to any temperature from 25°C.

$$D_o = D_{25} \cdot (T/298.15°K)^{1.75} \qquad \text{(Equation C-5a)}$$

T   temperature (°K)

D_o air diffusion coefficient at temperature T (cm^2/sec).

D_{25} air diffusion coefficient at 25°C (cm^2/sec).

b. Calculation of air diffusion coefficient from a measured reference air diffusion coefficient for a structurally similar compound.

$$D_o = D_\alpha^r \cdot (M_r/M)^{1/2} \qquad \text{(Equation C-5b)}$$

where:

D_o^r air diffusion coefficient measured for a reference compound (cm^2/sec).

M   molecular weight of compound of interest (g/mol).

M_r molecular weight of the reference compound (g/mol).

Pure Chemical Vapor Pressure, P_k^* (mm Hg):

$$P_k^* = \exp(A - (B/(T + C))) \qquad \text{(Equation C-6)}$$

where:

T   temperature (°K)

A,B,C Antoine equation coefficients for a compound of interest.

Partial Pressure Over Gasoline Liquid, P_k (mm Hg):

$$P_k = x_k \cdot P_k^*$$ (Equation C-7)

where:

P_k partial pressure of a compound over gasoline liquid (mm Hg)

x_k mole fraction of kth gasoline vapor constituent (dimensionless).

Henry's Law Constant, H_k:

Temperature dependence of Henry's Law Constants.

Note: following equation assumes no significant change in solubility over temperature range of interest.

$$H_{k,T2} = H_{k,T1} \cdot (P_{T2}/P_{T1})$$ (Equation C-8)

where:

H_k Henry's Law Constant for a compound at a given temperature (dimensionless).

Pure Chemical Vapor Density, $\rho_{v,1}$ (g/m^3):

$$\rho_{v,1} = P_k \cdot M_k /(T \cdot R)$$ (Equation C-9)

Estimation of Liquid Density, ρ_1 (g/cm^3):

$$\rho_1 = M_1 \cdot \rho_b \cdot \{3 - 2 \cdot [T/(T_b + 273.15°K)]\}^{0.29}$$ (Equation C-10)

where:

T_b boiling point temperature (°C).

ρ_b liquid density at the boiling point (mol/cm^3).

Liquid Mole Fraction, x_k [dimensionless]:

$$x_k = (\%w_k/M_k) \cdot [1/{\textstyle\sum_{k=1}^{N}} (\%w_k/M_k)]$$
(Equation C-11)

where:

$\%w_k$ percentage composition of gasoline mixture of the kth constituent

---

Vapor Concentration of a Gasoline Constituent over Pure Gasoline Liquid, $C_{g,k}$ (parts per million):

$$C_{g,k} = (P_k/P_t) \times 10^6$$
(Equation C-12)

Gas Vapor Viscosity, $\mu_{g,k}$ (g/cm · sec):   (Equation C-13)

$$\mu_{g,k} = (27.0 \cdot M_k^{1/2} \cdot T^{3/2})/((T + 1.47 \cdot T_b) \cdot V_b^{2/3}$$

where:

$\mu_{g,k}$ gas vapor dynamic viscosity (g/cm · sec).

V_b molar volume at boiling point of kth constituent (cm^3/g · mol).

Temperature-dependence of gas viscosity:

$$\mu_g = \mu_{20} \cdot (T/293.15°K)$$
(Equation C-14)

μ_{20} gas vapor dynamic viscosity at 20°C (g/cm · sec).
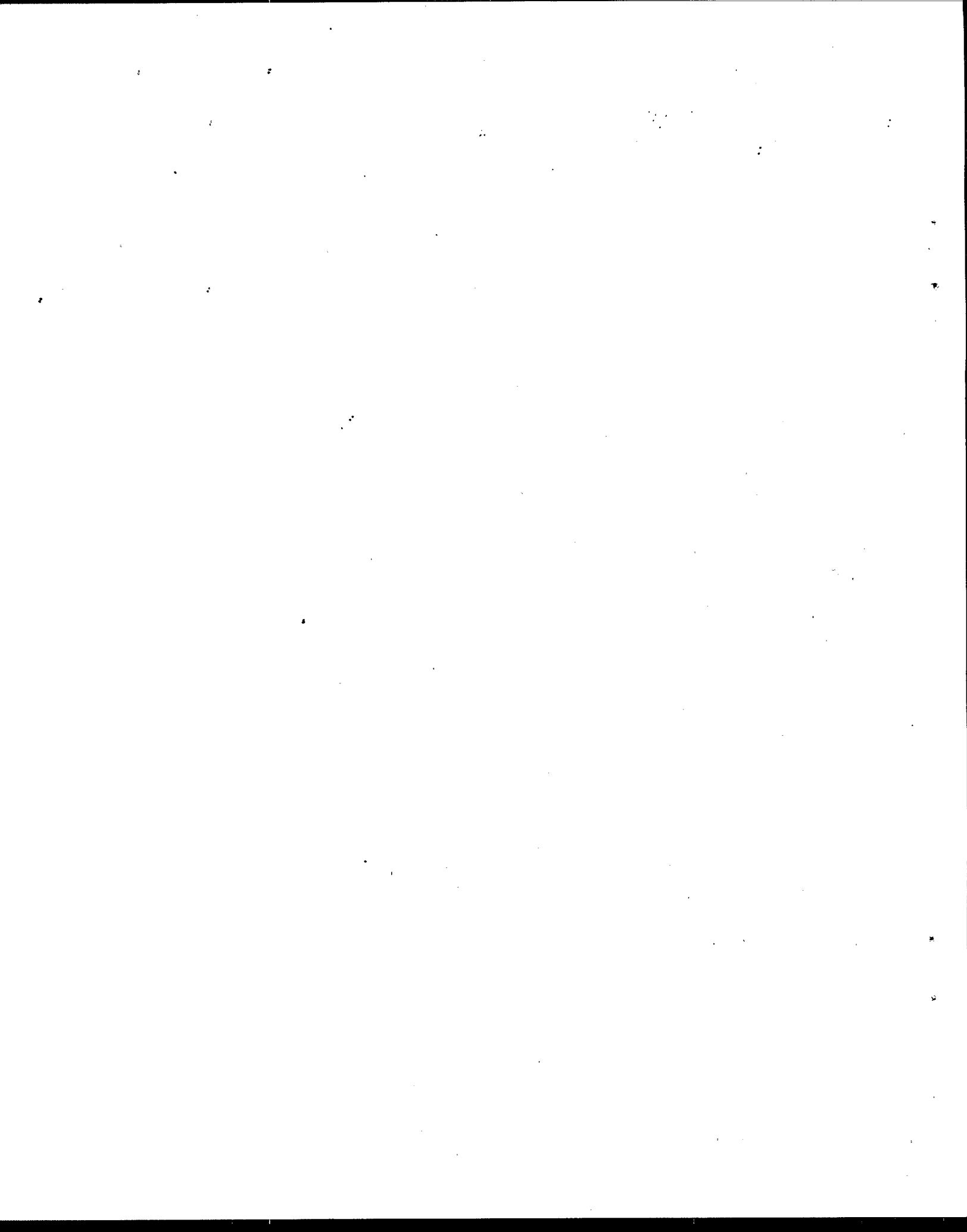
APPENDIX D
PHYSIOCOCHEMICAL PROPERTIES OF REPRESENTATIVE GASOLINE BLENDS

Tables of Properties

This appendix contains tables of the physiocochemical properties of the chemical constituents of four gasoline blends. The first blend is a representative gasoline devised by Warren Lyman of CDM for this project. The other three blends were proposed by K. Stetzenbach of the Environmental Research Center at the University of Nevada at Las Vegas in a recent memo (1987), a copy of which is included at the end this appendix.

Values of physicochemical properties of the constitutive chemicals of each blend are provided for 20°, 10°, and 0° C. The physiocochemical properties reported for each blend are:

Property	Reference
– Percent composition	Arthur D. Little, Inc., 1987.
– Liquid phase mole fraction	Equation C–11.
– Pure chemical vapor density	Equation C–9.
– Concentration over liquid gasoline	Equation C–12
– Henry's Law constants	Mackay and Shiu, 1981.
– Gram molecular weight	Reid, Prausnitz, and Sherwood, 1977.
– Air diffusion coefficient	Lugg, 1968.; CDM, 1986.
– Partial pressure over gasoline	Equation C–7.
– Boiling point	Reid, Prausnitz, and Sherwood, 1977.
– Gas viscosity	Perry and Chilton, 1973.

Average gasoline blend properties are reported for:

- Average molecular weight of gasoline vapors (Equation C-1).
- Average molecular weight of gasoline vapor-air mixture
- Vapor density of gasoline vapor-air mixture (Equation C-4).
- Average air diffusion coefficient
- Average liquid density
- Average gas density

References that appear in Section 5 of this report were used to prepare the tables in this appendix.

LIST OF TABLES FOR APPENDIX D

Comparison to "Standard Gasoline Vapor Mixture"

The vapor mixture of the CDM synthotic gasoline blend was compared against the gasoline vapor mixture suggested by K. Stetzenbach (1987) of this appendix. Assuming the vapor mixture given by Stetzenbach is for 10° C, the percentages of the vapor mixture on a constituent basis are:

	CDM Gasoline Vapor Mixture	Stetzenbach Vapor Mixture
isopentane	39%	30%
isobutane	27%	19%
n-pentane	6%	19%
n-butane	9%	30%
toluene	0.4%	1%
m-xylene	0.1%	1%
others	18.5%	0%
sum	100%	100%

This comparison shows that the Stetzenbach gasoline vapor mixture contains more n-pentane and n-butane and less isopentane and isobutane than the CDM gasoline vapor mixture. If the vapor rercentages are grouped into the C_4 and C_5 alkanes and aromatic compounds, the comparison becomes:

	CDM Gasoline Vapor Mixture	Stetzenbach Vapor Mixture
C_4 alkanes	36%	49%
C_5 alkanes	45%	49%
aromatics	0.5%	2%
others	18.5%	0%
sum	100%	100%

This comparison indicates that the CDM gasoline vapor mixture and the Stetzenbach vapor mixture are similar.

Table D-1

CHEMICAL PROPERTY ESTIMATION FOR SYNTHETIC
GASOLINE AND CONSTITUENTS AT 20 DEGREES C.

REPRESENTATIVE CHEMICAL	PERCENT COMPOSITION	GRAM MOL. WEIGHT (GM/MOL)	LIQ. PHASE MOL FRACT.	AIR DIFFUSION COEFFICIENT (CM^2/SEC)	LIQUID DENSITY (GM/CM^3)	PURE CHEMICAL VAPOR PRESSURE (mm Hg)	PARTIAL PRESSURE OVER GASOLINE (mm Hg)	PURE CHEMICAL VAPOR DENSITY (GM/M^3)	CONCENTRATION OVER LIQUID GASOLINE (ppm)	BOILING POINT (deg. K)	HENRY'S LAW CONSTANT (dim.)	GAS VISCOSITY (uPOISE)
Isobutane	2	58.12	0.0326	0.0911	0.5570	2252.75	73.5178	7162.14	96733.9	261.25	4304.39	70.01
n-Butane	1	58.12	0.0163	0.0911	0.5790	1555.33	25.3788	4944.83	33393.1	272.65	3404.37	70.90
Isopentane	14	72.15	0.1840	0.0817	0.6200	574.89	105.7925	2268.97	139200.7	300.95	4792.93	68.91
n-Pentane	3	72.15	0.0394	0.0817	0.6260	424.38	16.7346	1674.92	22019.2	309.15	4299.67	63.85
n-Octane	1	114.23	0.0083	0.0598	0.7030	10.46	0.0869	65.37	114.3	398.75	9330.24	61.06
Benzene	3	78.11	0.0364	0.0905	0.8850	75.20	2.7390	321.31	3604.0	353.25	18.07	72.22
Toluene	5	92.14	0.0515	0.0824	0.8670	21.84	1.1237	110.05	1478.6	383.75	21.38	74.01
Xylene (m)	7	106.17	0.0625	0.0668	0.8640	6.16	0.3852	35.78	506.8	466.25	21.40	53.72
n-Hexane	9	86.18	0.0990	0.0711	0.6590	121.24	12.0080	571.57	15800.0	341.85	5663.95	58.50
2-Methylpentane	8	86.18	0.0880	0.0711	0.6530	171.50	15.0985	808.51	19866.4	333.35	5724.28	59.40
Cyclohexane	3	84.16	0.0338	0.0719	0.7790	77.55	2.6218	357.04	3449.7	353.85	594.42	70.52
n-Heptane	1.5	100.20	0.0142	0.0659	0.6840	35.55	0.5047	194.86	664.1	371.55	7412.91	54.20
2-Methylhexane	5	100.20	0.0473	0.0659	0.6790	51.90	2.4563	284.50	3232.0	363.15	11282.83	55.00
Methylcyclohexane	1	98.19	0.0097	0.0666	0.7707	36.21	0.3497	194.50	460.2	374.05	1300.19	56.00
2,4-Dimethylhexane	8	114.23	0.0664	0.0617	0.7000	23.32	1.5492	145.75	2038.4	382.55	9839.65	52.20
Ethylbenzene	2	106.17	0.0179	0.0733	0.8670	7.08	0.1264	41.09	166.3	409.25	24.76	54.00
1-Pentene	1.5	70.14	0.0203	0.0829	0.6400	530.80	10.7654	2036.57	14165.0	303.05	1394.40	66.50
2,2,4-Trimethylhexane	2	128.26	0.0148	0.0608	0.7173	11.30	0.1671	79.30	219.9	399.65	10969.52	49.78
2,2,5,5-Tetramethylhexane	1.5	142.29	0.0100	0.0577	0.7200	6.47	0.0647	50.35	85.1	410.55	39373.43	48.11
1,4-Diethylbenzene	5	134.22	0.0353	0.0594	0.8620	0.70	0.0246	5.11	32.4	456.85	40.43	47.60
1-Hexene	1.5	84.16	0.0169	0.0719	0.6730	149.97	2.5348	690.40	3335.3	336.55	1401.18	60.50
1,3,5-Trimethylbenzene	5	120.20	0.0394	0.0628	0.8650	1.73	0.0681	11.36	89.7	437.85	19822.78	50.20
C12-aliphatic	10	170.00	0.0558	0.0524	0.8600	0.08	0.0042	0.70	5.5	489.15		41.40
Total	100	102.20	1.0000		0.7373		274.1020		360660.5		5434.632	

Temperature = 293.15 deg. K
Pressure = 760 mm Hg
Gas Constant =
   0.06236 mm Hg*m^3/mol*K
Molecular Weight
of Air =   28.96 gm/mol
Average Molecular
Weight of Gasoline
Vapors =   69.48 gm/mol
Molecular weight
of Gasoline-Air
Mixture =   43.58 gm/mol

Vapor Density
of Gasoline-Air
Mixture =   1811.60 gm/m^3

Weighted average
 air diffusion
 coefficient =   0.0726 cm^2/sec
Weighted average
 liquid density   0.7182 gm/cm^3
Weighted average
 gas density   1041.63 gm/m^3

D-4

Table D-2

CHEMICAL PROPERTY ESTIMATION FOR SYNTHETIC
GASOLINE AND CONSTITUENTS AT 10 DEGREES C.

REPRESENTATIVE CHEMICAL	PERCENT COMPOSITION	GRAM MOL. WEIGHT (GM/MOL)	LIQ. PHASE MOL FRACT.	AIR DIFFUSION COEFFICIENT (CM^2/SEC)	LIQUID DENSITY (GM/CM^3)	PURE CHEMICAL VAPOR PRESSURE (mm Hg)	PARTIAL PRESSURE OVER GASOLINE (mm Hg)	PURE CHEMICAL VAPOR DENSITY (GM/M^3)	CONCENTRATION OVER LIQUID GASOLINE (ppm)	BOILING POINT (deg. K)	HENRY'S LAW CONSTANT (dim.)	GAS VISCOSITY (uPOISE)
Isobutane	2	58.12	0.0326	0.0657	0.5729	1647.77	53.7745	5423.76	70755.9	261.25	3259.64	67.62
n-Butane	1	58.12	0.0163	0.0657	0.5931	1112.75	18.1571	3662.69	23890.9	272.65	2521.65	68.68
Isopentane	14	72.15	0.1840	0.0769	0.6311	392.47	72.2231	1603.70	95030.4	300.95	3387.63	66.56
n-Pentane	3	72.15	0.0394	0.0769	0.6364	283.84	11.1925	1159.80	14727.0	309.15	2977.29	61.67
n-Octane	1	114.23	0.0083	0.0543	0.7096	5.63	0.0468	36.63	61.5	398.75	5200.06	59.98
Benzene	3	78.11	0.0364	0.0651	0.8957	45.53	1.6583	201.40	2182.0	353.25	11.32	69.76
Toluene	5	92.14	0.0515	0.0776	0.8758	12.43	0.6397	64.86	841.7	383.75	12.60	71.49
Xylene (a)	7	106.17	0.0625	0.0629	0.8701	3.26	0.2039	19.61	268.3	446.25	11.83	31.89
n-Hexane	9	86.18	0.0990	0.0669	0.6676	75.70	7.4976	349.48	9865.2	341.85	3461.34	56.50
2-Methylpentane	8	86.18	0.0880	0.0669	0.6620	109.55	9.6446	534.70	12690.2	333.35	3785.69	57.37
Cyclohexane	3	84.16	0.0338	0.0677	0.7884	47.51	1.6060	226.44	2113.2	353.85	376.99	68.11
n-Heptane	1.5	100.20	0.0142	0.0620	0.6914	20.66	0.2933	117.23	385.9	371.55	4459.78	52.35
2-Methylhexane	5	100.20	0.0473	0.0620	0.6867	30.94	1.4642	175.57	1926.5	343.15	6962.93	53.12
Methylcyclohexane	1	98.19	0.0097	0.0627	0.7789	21.45	0.2071	119.26	272.6	374.05	797.24	54.89
2,4-Dimethylhexane	8	114.23	0.0664	0.0581	0.7071	13.30	0.8833	86.03	1162.2	382.55	5808.15	50.42
Ethylbenzene	2	106.17	0.0179	0.0690	0.8748	3.77	0.0673	22.66	89.6	409.25	13.65	52.16
1-Pentene	1.5	70.14	0.0203	0.0780	0.6513	359.48	7.2909	1427.99	9593.3	303.05	977.71	64.23
2,2,4-Trimethylhexane	2	128.26	0.0148	0.0572	0.7240	6.18	0.0915	44.92	120.3	399.65	6214.17	48.00
2,2,5,5-Tetramethylhexane	1.5	142.29	0.0100	0.0543	0.7264	3.40	0.0340	27.37	44.7	410.55	21405.95	46.47
1,4-Diethylbenzene	5	134.22	0.0353	0.0559	0.8683	0.32	0.0113	2.43	14.9	456.85	19.24	45.98
1-Hexene	1.5	84.16	0.0169	0.0677	0.6821	94.87	1.6036	452.20	2110.1	336.55	917.75	58.44
1,3,5-Trimethylbenzene	5	120.20	0.0394	0.0591	0.8718	0.84	0.0333	5.74	43.8	437.85	9.02	48.49
C12-aliphatic	10	170.00	0.0558	0.0493	0.8656	0.03	0.0016	0.27	2.1	469.15	7742.54	39.99
Total	100	102.20	1.0000		0.7457		188.6252		248191.2		3202.673	

Temperature = 283.15 deg. K
Pressure = 760 mm Hg
Gas Constant = 0.06236 mm Hg*m^3/mol*K
Molecular Weight of Air = 28.96 gm/mol
Average Molecular Weight of Gasoline Vapors = 68.92 gm/mol
Molecular weight of Gasoline-Air Mixture = 38.88 gm/mol

Vapor Density of Gasoline-Air Mixture = 1673.38 gm/m^3
Weighted average air diffusion coefficient = 0.0684 cm^2/sec
Weighted average liquid density = 0.7271 gm/cm^3
Weighted average gas density = 736.25 gm/m^3

Table D-4

CHEMICAL PROPERTY ESTIMATION FOR STETZENBACH LOW REID
VAPOR PRESSURE GASOLINE AND CONSTITUENTS AT 20 DEGREES C.

REPRESENTATIVE CHEMICAL	PERCENT COMPOSITION	GRAM MOL. WEIGHT (GM/MOL)	LIQ. PHASE MOL FRACT.	AIR DIFFUSION COEFFICIENT (CM^2/SEC)	LIQUID DENSITY (GM/CM^3)	PURE CHEMICAL VAPOR PRESSURE (mm Hg)	PARTIAL PRESSURE OVER GASOLINE (mm Hg)	PURE CHEMICAL VAPOR DENSITY (GM/M^3)	CONCENTRATION OVER LIQUID GASOLINE (ppm)	BOILING POINT (deg. K)	HENRY'S LAW CONSTANT (dim.)	GAS VISCOSITY (uPOISE)
Isobutane	3	58.12	0.0485	0.0911	0.5570	2252.75	109.1671	7162.14	143640.9	261.25	4304.39	70.01
a-Butane	3	58.12	0.0485	0.0911	0.5790	1535.33	75.3702	4944.83	99171.3	272.65	3404.37	70.90
Isopentane	5	72.15	0.0651	0.0817	0.6200	574.89	37.4029	2268.97	49214.3	300.95	4792.93	68.91
a-Pentane,	5	72.15	0.0651	0.0817	0.6260	424.38	27.6103	1674.92	36329.4	309.15	4299.67	63.85
a-Octane	14	114.23	0.1151	0.0598	0.7030	10.46	1.2038	65.37	1583.9	398.75	9333.36	61.06
Benzene	2	78.11	0.0240	0.0905	0.8850	75.20	1.8076	321.31	2378.5	353.25	18.07	72.22
Toluene	15	92.14	0.1528	0.0624	0.8670	21.84	3.3372	110.05	4391.0	383.75	21.38	74.01
Xylene (a)	10	106.17	0.0884	0.0668	0.8640	6.16	0.5447	35.78	716.7	466.25	21.60	53.72
a-Hexane	5	86.18	0.0545	0.0711	0.6590	121.24	6.6040	571.57	8689.5	341.85	5663.95	58.50
2-Methyldecane	5	156.31	0.0300	0.0604	0.7400	0.26	0.0078	2.22	10.3	462.30	5139.23	43.70
2,2,4-Trimethylpentane	5	114.23	0.0411	0.0707	0.6920	38.72	1.5911	241.93	2093.5	372.40	12421.53	53.10
a-Heptane	5	100.20	0.0468	0.0659	0.6840	35.55	1.6655	194.86	2191.4	371.55	7412.51	54.20
2-Methyl-2-butene	5	70.14	0.0669	0.0787	0.6620	384.13	25.7076	1473.82	33825.8	304.30	1147.76	66.40
2,3-Dimethyl-1-butene	5	84.16	0.0558	0.0719	0.6741	205.21	11.4458	944.73	15060.3	328.80	1915.01	61.40
1,2,4-Trimethylbenzene	8	120.20	0.0625	0.0689	0.9770	1.45	0.0904	9.51	119.0	442.50	17.77	56.00
1,1-Dimethyl-2-phenylethane	5	134.22	0.0350	0.0651	0.8530	1.32	0.0463	9.72	60.9	445.90	97.45	48.40
Total	100	99.58	1.0000		0.7473		303.6022		399476.6		3553.339	

Temperature = 293.15 deg. K
Pressure = 760 mm Hg
Gas Constant =
    0.06236 mm Hg*m^3/mol*K
Molecular Weight
of Air = 28.96 gm/mol
Average Molecular
Weight of Gasoline
Vapors = 65.09 gm/mol
Molecular weight
of Gasoline-Air
Mixture = 43.39 gm/mol

Vapor Density
of Gasoline-Air
Mixture =   1804.06 gm/m^3

Weighted average
 air diffusion
 coefficient =   0.0746 cm^2/sec
Weighted average
 liquid density   0.7323 gm/cm^3
Weighted average
 gas density   1081.05 gm/m^3

Table D-5

CHEMICAL PROPERTY ESTIMATION FOR STETZENBACH LOW REID
VAPOR PRESSURE GASOLINE AND CONSTITUENTS AT 10 DEGREES C.

REPRESENTATIVE CHEMICAL	PERCENT COMPOSITION	GRAM MOL. WEIGHT (GM/MOL)	LIQ. PHASE MOL FRACT.	AIR DIFFUSION COEFFICIENT (CM^2/SEC)	LIQUID DENSITY (GM/CM^3)	PURE CHEMICAL VAPOR PRESSURE (mm Hg)	PARTIAL PRESSURE OVER GASOLINE (mm Hg)	PURE CHEMICAL VAPOR DENSITY (GM/M^3)	CONCENTRATION OVER LIQUID GASOLINE (ppm)	BOILING POINT (deg. K)	HENRY'S LAW CONSTANT (dim.)	GAS VISCOSITY (uPOISE)
Isobutane	3	58.12	0.0485	0.0857	0.5728 *	1647.77	79.8502	5423.76	105066.0	261.25	3259.64	67.42
n-Butane	3	58.12	0.0485	0.0857	0.5931	1112.75	53.9232	3662.69	70951.6	272.65	2521.64	68.48
Isopentane	5	72.15	0.0651	0.0769	0.6311	392.47	25.5344	1603.70	33597.9	300.95	3387.63	66.56
n-Pentane	5	72.15	0.0651	0.0769	0.6344	283.84	18.4665	1159.80	24298.0	309.15	2977.29	61.67
n-Octane	14	114.23	0.1151	0.0563	0.7096	5.63	0.6480	36.43··	852.7	398.75	5201.79	58.98
Benzene	2	78.11	0.0240	0.0851	0.8957	45.53	1.0944	201.40	1440.1	353.25	11.32	69.76
Toluene	15	92.14	0.1528	0.0776	0.8758	12.43	1.8997	64.86	2499.5	383.75	12.60	71.49
Xylene (m)	10	106.17	0.0994	0.0629	0.8701	3.26	0.2883	19.61	379.4	416.25	11.03	51.89
n-Hexane	5	86.18	0.0545	0.0669	0.6676	75.70	4.1234	369.48	5425.5	341.85	3461.35	56.50
2-Methyldecane	5	156.31	0.0300	0.0568	0.7453	0.11	0.0032	0.96	4.3	442.30	2206.63	42.21
2,2,4-Trimethylpentane	5	114.23	0.0411	0.0665	0.6995	23.02	0.9461	148.94	1244.9	372.40	12869.22	51.29
n-Heptane	5	100.20	0.0468	0.0620	0.6914	20.66	0.9678	117.23	1273.4	371.55	4459.53	52.35
2-Methyl-2-butene	5	70.14	0.0669	0.0741	0.6735	254.75	17.0493	1011.96	22433.3	304.30	798.08	44.13
2,3-Dimethyl-1-butene	5	84.16	0.0558	0.0677	0.6837	132.47	7.3885	631.38	9721.7	328.00	1279.84	59.31
1,2,4-Trimethylbenzene	8	120.20	0.0625	0.0649	0.8838	0.70	0.0438	4.77	57.6	442.50	8.91	54.09
1,1-Dimethyl-2-phenylethane	5	134.22	0.0350	0.0613	0.8595	0.64	0.0223	4.84	29.3	445.90	48.53	46.75
Total	100	99.58	1.0000		0.7557		212.2491		279275.2		2425.497	

Temperature = 283.15 deg. K
Pressure = 760 mm Hg
Gas Constant = 0.06236 mm Hg·m^3/mol·K
Molecular Weight of Air = 28.96 gm/mol
Average Molecular Weight of Gasoline Vapors = 64.55 gm/mol
Molecular weight of Gasoline-Air Mixture = 38.90 gm/mol

Vapor Density of Gasoline-Air Mixture = 1674.35 gm/m^3
Weighted average air diffusion coefficient = 0.0702 cm^2/sec
Weighted average liquid density 0.7413 gm/cm^3
Weighted average gas density 775.97 gm/m^3

D-8

Table D-6

CHEMICAL PROPERTY ESTIMATION FOR SIETZENBACH LOW REID
VAPOR PRESSURE GASOLINE AND CONSTITUENTS AT 0 DEGREES C.

REPRESENTATIVE CHEMICAL	PERCENT COMPOSITION	GRAM MOL. WEIGHT (GM/MOL)	LIQ. PHASE MOL FRACT.	AIR DIFFUSION COEFFICIENT (CM^2/SEC)	LIQUID DENSITY (GM/CM^3)	PURE CHEMICAL VAPOR PRESSURE (mm Hg)	PARTIAL PRESSURE OVER GASOLINE (mm Hg)	PURE CHEMICAL VAPOR DENSITY (GM/M^3)	CONCENTRATION OVER LIQUID GASOLINE (ppm)	BOILING POINT (deg. K)	HENRY'S LAW CONSTANT (dim.)	GAS VISCOSITY (uPOISE)
Isobutane	3	58.12	0.0485	0.0805	0.5974	1174.26	56.9039	4006.63	74873.3	261.25	2607.97	65.23
n-Butane	3	58.12	0.0485	0.0805	0.6044	774.09	37.5118	2841.24	49357.7	272.63	1818.42	66.06
Isopentane	5	72.15	0.0651	0.0722	0.6418	289.30	16.8703	1098.34	22197.8	300.95	2320.11	64.21
n-Pentane	5	72.15	0.0651	0.0722	0.6465	183.40	11.9321	776.84	15700.1	309.15	1994.20	59.69
n-Octane	14	114.23	0.1151	0.0528	0.7161	2.86	0.3288	19.16	432.7	398.75	2734.13	56.89
Benzene	2	78.11	0.0240	0.0800	0.9961	26.31	0.6352	120.79	833.1	353.25	6.79	67.29
Toluene	15	92.14	0.1528	0.0728	0.8844	6.72	1.0272	36.36	1331.6	383.75	7.04	68.96
Xylene (m)	10	106.17	0.0884	0.0590	0.8761	1.63	0.1438	10.14	189.3	444.25	6.12	50.05
n-Hexane	5	86.18	0.0545	0.0628	0.6759	45.32	2.4687	229.31	3248.3	341.65	2272.33	54.51
2-Methyldecane	5	156.31	0.0300	0.0634	0.7505	0.04	0.0012	0.37	1.6	442.30	863.72	40.72
2,2,4-Trimethylpentane	5	114.23	0.0411	0.0625	0.7067	13.08	0.5375	87.71	707.2	372.40	13331.63	49.48
n-Heptane	5	100.20	0.0468	0.0583	0.6986	11.42	0.5349	67.17	703.8	371.55	2835.01	50.59
2-Methyl-2-butene	5	70.14	0.0648	0.0696	0.6846	163.10	10.9152	671.59	14362.2	304.30	523.01	61.87
2,3-Dimethyl-1-butene	5	84.16	0.0558	0.0636	0.6930	82.31	4.5909	406.67	6040.6	328.80	824.34	57.21
1,2,4-Trimethylbenzene	8	120.20	0.0625	0.0609	0.8905	0.32	0.0198	2.23	26.0	442.50	4.17	52.18
1,1-Dimethyl-2-phenylethane	5	134.22	0.0350	0.0576	0.8659	0.28	0.0100	2.25	13.1	445.90	22.52	45.10
Total	100	99.58	1.0000		0.7639		144.4293		190038.6		1701.357	

Temperature = 273.15 deg. K
Pressure = 760 mm Hg
Gas Constant = 0.08236 mm Hg*m^3/mol*K

Vapor Density of Gasoline-Air Mixture = 1589.39 gm/m^3

Weighted average air diffusion coefficient = 0.0659 cm^2/sec
Weighted average liquid density = 0.7500 gm/cm^3
Weighted average gas density = 542.81 gm/m^3

Molecular Weight of Air = 28.96 gm/mol
Average Molecular Weight of Gasoline Vapors = 64.02 gm/mol
Molecular weight of Gasoline-Air Mixture = 35.62 gm/mol

Table D-7

CHEMICAL PROPERTY ESTIMATION FOR STETZENBACH HIGH REID
VAPOR PRESSURE GASOLINE AND CONSTITUENTS AT 20 DEGREES C.

REPRESENTATIVE CHEMICAL	PERCENT COMPOSITION	GRAM MOL. WEIGHT (GM/MOL)	LIQ. PHASE MOL FRACT.	AIR DIFFUSION COEFFICIENT (CM^2/SEC)	LIQUID DENSITY (GM/CM^3)	PURE CHEMICAL VAPOR PRESSURE (mm Hg)	PARTIAL PRESSURE OVER GASOLINE (mm Hg)	PURE CHEMICAL VAPOR DENSITY (GM/M^3)	CONCENTRATION OVER LIQUID GASOLINE (ppm)	BOILING POINT (deg. K)	HENRY'S LAW CONSTANT (dim.)	GAS VISCOSITY (uPOISE)
Isobutane	5	58.12	0.0754	0.0911	0.5570	2252.75	169.8184	7142.14	223445.3	261.25	4304.39	70.01
n-Butane	10	58.12	0.1508	0.0911	0.5790	1555.33	234.4892	4944.83	308538.4	272.65	3404.37	70.90
Isopentane	5	72.15	0.0607	0.0817	0.6200	574.89	34.9099	2268.97	45934.1	300.95	4792.93	68.91
n-Pentane	5	72.15	0.0607	0.0817	0.6260	424.38	25.7701	1674.92	33909.0	309.15	4299.67	63.85
n-Octane	5	114.23	0.0384	0.0598	0.7030	10.46	0.4013	65.37	528.0	398.75	9333.36	61.06
Benzene	2	78.11	0.0224	0.0905	0.8850	75.20	1.6872	321.31	2220.0	353.25	18.07	72.22
Toluene	15	92.14	0.1426	0.0924	0.8670	21.84	3.1148	110.05	4098.4	383.75	21.38	74.01
Xylene (m)	10	106.17	0.0825	0.0668	0.8640	6.16	0.5084	35.78	669.0	446.25	21.60	53.72
n-Hexane	5	86.18	0.0508	0.0711	0.6590	121.24	6.1638	571.57	8110.3	341.85	5463.95	58.50
2-Methyldecane	5	156.31	0.0280	0.0404	0.7400	0.26	0.0073	2.22	9.6	462.30	5139.23	43.70
2,2,4-Trimethylpentane	5	114.23	0.0384	0.0707	0.6920	38.72	1.4850	241.93	1954.0	372.40	12421.53	53.10
n-Heptane	5	100.20	0.0437	0.0459	0.6840	35.55	1.5545	194.86	2045.3	371.53	7412.51	54.20
2-Methyl-2-butene	5	70.14	0.0625	0.0787	0.6620	384.13	23.9941	1473.82	31571.2	304.30	1147.76	46.40
2,3-Dimethyl-1-butene	5	84.16	0.0521	0.0719	0.6741	205.21	10.6830	944.73	14056.5	328.80	1915.01	41.40
1,2,4-Trimethylbenzene	8	120.20	0.0583	0.0689	0.8770	1.45	0.0844	9.51	111.0	442.50	17.77	56.00
1,1-Dimethyl-2-phenylethane	5	134.22	0.0326	0.0651	0.8530	1.32	0.0432	9.72	56.8	445.90	97.45	49.40
Total	100	94.53	1.0000		0.7357		514.7144		677255.9		3161.221	

Temperature = 293.15 deg. K
Pressure = 760 mm Hg
Gas Constant =
   0.06236 mm Hg·m^3/mol·K
Molecular Weight
  of Air = 28.96 gm/mol
Average Molecular
 Weight of Gasoline
 Vapors = 61.88 gm/mol
Molecular weight
 of Gasoline-Air
 Mixture = 51.26 gm/mol

Vapor Density
 of Gasoline-Air
 Mixture = 2130.88 gm/m^3

Weighted average
 air diffusion
 coefficient = 0.0778 cm^2/sec
Weighted average
 liquid density 0.7129 gm/cm^3
Weighted average
 gas density 1742.30 gm/m^3

Table D-8

CHEMICAL PROPERTY ESTIMATION FOR STETZENBACH HIGH REID
VAPOR PRESSURE GASOLINE AND CONSTITUENTS AT 10 DEGREES C.

REPRESENTATIVE CHEMICAL	PERCENT COMPOSITION	GRAM MOL. WEIGHT (GM/MOL)	LIQ. PHASE MOL FRACT.	AIR DIFFUSION COEFFICIENT (CM^2/SEC)	LIQUID DENSITY (GM/CM^3)	PURE CHEMICAL VAPOR PRESSURE (mm Hg)	PARTIAL PRESSURE OVER GASOLINE (mm Hg)	PURE CHEMICAL VAPOR DENSITY (GM/M^3)	CONCENTRATION OVER LIQUID GASOLINE (ppm)	BOILING POINT (deg. K)	HENRY'S LAW CONSTANT (dim.)	GAS VISCOSITY (uPOISE)
Isobutane	5	58.12	0.0754	0.0857	0.5728	1647.77	124.2135	5423.76	163438.8	261.25	3259.44	67.62
n-Butane	10	58.12	0.1508	0.0857	0.5931	1112.75	167.7640	3662.69	220742.0	272.65	2521.46	68.40
Isopentane	5	72.15	0.0607	0.0769	0.6311	392.47	23.8325	1603.70	31358.6	300.95	3387.63	66.56
n-Pentane	5	72.15	0.0607	0.0769	0.6364	283.84	17.2357	1159.80	22678.5	309.15	2977.29	61.67
n-Octane	5	114.23	0.0384	0.0563	0.7096	5.63	0.2160	36.43	284.2	398.75	5201.79	58.98
Benzene	2	78.11	0.0224	0.0851	0.8957	45.53	1.0215	201.40	1344.1	353.25	11.32	69.76
Toluene	15	92.14	0.1426	0.0776	0.8758	12.43	1.7730	64.86	2333.0	383.75	12.60	71.49
Xylene (a)	10	106.17	0.0825	0.0629	0.8701	3.26	0.2691	19.61	354.1	464.25	11.83	51.89
n-Hexane	5	86.18	0.0508	0.0669	0.6676	75.70	3.8486	369.48	5063.9	341.85	3461.35	56.50
2-Methyldecane	5	156.31	0.0280	0.0568	0.7453	0.11	0.0030	0.96	4.0	442.30	2204.63	42.21
2,2,4-Trimethylpentane	5	114.23	0.0384	0.0665	0.6995	23.02	0.8830	148.94	1161.9	372.40	12860.22	51.29
n-Heptane	5	100.20	0.0437	0.0620	0.6914	26.66	0.9033	117.23	1188.5	371.55	4459.53	52.35
2-Methyl-2-butene	5	70.14	0.0625	0.0741	0.6735	254.75	15.9130	1011.96	20938.1	304.30	788.08	64.13
2,3-Dimethyl-1-butene	5	84.16	0.0521	0.0677	0.6837	132.47	6.8961	631.38	9073.8	328.60	1279.84	59.31
1,2,4-Trimethylbenzene	8	120.20	0.0593	0.0649	0.8838	0.70	0.0409	4.77	53.8	442.50	8.91	54.09
1,1-Dimethyl-2-phenylethane	5	134.22	0.0326	0.0613	0.8595	0.64	0.0208	4.84	27.3	445.90	48.53	46.75
Total	100	94.53	1.0000		0.7448		364.8339		480044.7		2269.126	

Temperature = 283.15 deg. K
Pressure = 760 mm Hg
Gas Constant = 0.06236 mm Hg*m^3/mol*K
Molecular Weight of Air = 28.96 gm/mol
Average Molecular Weight of Gasoline Vapors = 61.55 gm/mol
Molecular weight of Gasoline-Air Mixture = 44.61 gm/mol

Vapor Density of Gasoline-Air Mixture = 1919.95 gm/m^3
Weighted average air diffusion coefficient = 0.0732 cm^2/sec
Weighted average liquid density 0.7228 gm/cm^3
Weighted average gas density 1271.83 gm/m^3

Table D-9

CHEMICAL PROPERTY ESTIMATION FOR STETTENBACH HIGH REID
VAPOR PRESSURE GASOLINE AND CONSTITUENTS AT 0 DEGREES C.

REPRESENTATIVE CHEMICAL	PERCENT COMPOSITION	GRAM MOL. WEIGHT (GM/MOL)	LIQ. PHASE MOL FRACT.	AIR DIFFUSION COEFFICIENT (CM^2/SEC)	LIQUID DENSITY (GM/CM^3)	PURE CHEMICAL VAPOR PRESSURE (mm Hg)	PARTIAL PRESSURE OVER GASOLINE (mm Hg)	PURE CHEMICAL VAPOR DENSITY (GM/M^3)	CONCENTRATION OVER LIQUID GASOLINE (ppm)	BOILING POINT (deg. K)	HENRY'S LAW CONSTANT (dia.)	GAS VISCOSITY (uPOISE)
Isobutane	5	58.12	0.0754	0.0805	0.5876	1174.26	88.5187	4006.65	116471.9	261.25	2407.97	65.23
n-Butane	10	58.12	0.1508	0.0805	0.6046	774.09	116.7055	2641.24	153559.9	272.65	1818.42	66.06
Isopentane	5	72.15	0.0607	0.0722	0.6418	259.30	15.7459	1098.34	20718.3	300.95	2320.11	64.21
n-Pentane	5	72.15	0.0607	0.0722	0.6445	183.40	11.1368	776.84	14653.7	309.15	1994.20	59.49
n-Octane	5	114.23	0.0384	0.0528	0.7161	2.86	0.1096	19.16	144.2	398.75	2736.13	56.89
Benzene	2	78.11	0.0224	0.0800	0.9061	26.34	0.5910	120.79	777.6	353.25	6.79	67.29
Toluene	15	92.14	0.1426	0.0728	0.8844	6.72	0.9588	36.36	1261.5	383.75	7.06	68.96
Xylene (m)	10	106.17	0.0825	0.0590	0.8761	1.63	0.1343	10.14	176.7	466.25	6.12	50.05
n-Hexane	5	86.18	0.0508	0.0628	0.6759	45.32	2.3042	229.31	3031.8	341.85	2272.33	54.51
2-Methyldecane	5	156.31	0.0280	0.0534	0.7505	0.04	0.0011	0.37	1.5	462.30	863.72	40.72
2,2,4-Triaethylpentane	5	114.23	0.0384	0.0625	0.7067	13.06	0.5016	87.71	660.1	372.40	13331.03	49.48
n-Heptane	5	100.20	0.0437	0.0583	0.6986	11.42	0.4992	67.17	656.9	371.55	2555.01	50.50
2-Methyl-2-butene	5	70.14	0.0625	0.0696	0.6946	163.10	10.1877	671.59	13404.9	304.30	523.01	61.97
2,3-Dimethyl-1-butene	5	84.16	0.0521	0.0636	0.6930	82.31	4.2849	406.67	5638.0	328.80	824.34	57.21
1,2,4-Triaethylbenzene	8	120.20	0.0583	0.0609	0.8905	0.32	0.0185	2.23	24.3	442.50	4.17	52.18
1,1-Diaethyl-2-phenylethane	5	134.22	0.0326	0.0576	0.8659	0.28	0.0093	2.25	12.2	445.90	22.52	45.10
Total	100	94.53	1.0000		0.7536		251.7070		331193.6		1663.579	

Temperature = 273.15 deg. K
Pressure = 760 mm Hg
Gas Constant =
   0.06236 mm Hg•m^3/mol•K
Molecular Weight
of Air = 28.96 gm/mol
Average Molecular
Weight of Gasoline
Vapors = 61.23 gm/mol
Molecular weight
of Gasoline-Air
Mixture = 39.65 gm/mol

Vapor Density
of Gasoline-Air
Mixture = 1769.05 gm/m^3

Weighted average
  air diffusion
  coefficient = 0.0688 cm^2/sec
Weighted average
  liquid density 0.7323 gm/cm^3
Weighted average
  gas density 904.87 gm/m^3

Table D-10

CHEMICAL PROPERTY ESTIMATION FOR STETZENBACH HIGH
OCTANE GASOLINE AND CONSTITUENTS AT 20 DEGREES C.

REPRESENTATIVE CHEMICAL	PERCENT COMPOSITION	GRAM MOL. WEIGHT (GM/MOL)	LIQ. PHASE MOL. FRACT.	AIR DIFFUSION COEFFICIENT (CM^2/SEC)	LIQUID DENSITY (GM/CM^3)	PURE CHEMICAL VAPOR PRESSURE (mm Hg)	PARTIAL PRESSURE OVER GASOLINE (mm Hg)	PURE CHEMICAL VAPOR DENSITY (GM/M^3)	CONCENTRATION OVER LIQUID GASOLINE (ppm)	BOILING POINT (deg. K)	HENRY'S LAW CONSTANT (dim.)	GAS VISCOSITY (uPOISE)
Isobutane	5	58.12	0.0772	0.0911	0.5570	2252.75	173.9957	7162.14	228941.7	261.25	4304.39	70.01
n-Butane	5	58.12	0.0772	0.0911	0.5790	1555.33	120.1286	4944.83	158064.0	272.65	3404.37	70.90
Isopentane	5	72.15	0.0622	0.0817	0.6200	574.89	35.7687	2268.97	47064.0	300.95	4792.93	68.91
n-Pentane	5	72.15	0.0622	0.0817	0.6260	424.38	26.4040	1674.92	34742.1	309.15	4299.67	63.05
n-Octane	5	114.23	0.0393	0.0598	0.7030	10.46	0.4111	65.37	541.0	398.75	9333.36	61.04
Benzene	2	78.11	0.0230	0.0905	0.8850	75.20	1.7287	321.31	2274.6	353.25	18.07	72.22
Toluene	25	92.14	0.2436	0.0824	0.8670	21.84	5.3190	110.05	6998.6	383.75	21.38	74.01
Xylene (a)	10	106.17	0.0846	0.0668	0.8640	6.16	0.5209	35.78	685.4	416.25	21.60	53.72
n-Hexane	5	86.18	0.0521	0.0711	0.6590	121.24	6.3155	571.57	8309.8	341.85	5443.95	58.50
2-Methyldecane	5	156.31	0.0287	0.0404	0.7400	0.26	0.0075	2.22	9.8	462.30	5139.23	43.70
2,2,4-Trimethylpentane	5	114.23	0.0393	0.0707	0.6920	38.72	1.5215	241.93	2002.0	372.40	12421.53	53.10
n-Heptane	0	100.20	0.0000	0.0659	0.6840	35.55	0.0000	194.86	0.0	371.55	7412.51	54.20
2-Methyl-2-butene	5	70.14	0.0640	0.0787	0.6620	384.13	24.5844	1473.82	32347.9	304.30	1147.76	66.40
2,3-Dimethyl-1-butene	5	84.16	0.0533	0.0719	0.6741	205.21	10.9457	944.73	14402.3	328.80	1915.01	61.40
1,2,4-Trimethylbenzene	8	120.20	0.0598	0.0689	0.8770	1.45	0.0865	9.51	113.8	442.50	17.77	56.00
1,1-Dimethyl-2-phenylethane	5	134.22	0.0334	0.0651	0.8530	1.32	0.0443	9.72	58.2	445.90	97.45	48.40
Total	100	95.83	1.0000		0.7593		407.7819		536355.2		2646.039	

Temperature = 293.15 deg. K
Pressure = 760 mm Hg
Gas Constant =
   0.06236 mm Hg*m^3/mol*K
Molecular Weight
of Air = 28.96 gm/mol
Average Molecular
Weight of Gasoline
Vapors = 63.00 gm/mol
Molecular weight
of Gasoline-Air
Mixture = 47.22 gm/mol

Vapor Density
of Gasoline-Air
Mixture =   1963.20 gm/m^3

Weighted average
 air diffusion
 coefficient =   0.0778 cm^2/sec
Weighted average
 liquid density   0.7395 gm/cm^3
Weighted average
 gas density   1405.23 gm/m^3

Table D-11

CHEMICAL PROPERTY ESTIMATION FOR STETZENBACH HIGH
OCTANE GASOLINE AND CONSTITUENTS AT 10 DEGREES C.

REPRESENTATIVE CHEMICAL	PERCENT COMPOSITION	GRAM MOL. WEIGHT (GM/MOL)	LIQ. PHASE MOL FRACT.	AIR DIFFUSION COEFFICIENT (CM^2/SEC)	LIQUID DENSITY (GM/CM^3)	PURE CHEMICAL VAPOR PRESSURE (mm Hg)	PARTIAL PRESSURE OVER GASOLINE (mm Hg)	PURE CHEMICAL VAPOR DENSITY (GM/M^3)	CONCENTRATION OVER LIQUID GASOLINE (ppm)	BOILING POINT (deg. K)	HENRY'S LAW CONSTANT (dim.)	GAS VISCOSITY (uPOISE)
Isobutane	5	58.12	0.0772	0.0857	0.5728	1647.77	127.2690	5423.76	167459.2	241.25	3259.44	67.62
n-Butane	5	58.12	0.0772	0.0857	0.5931	1112.75	85.9454	3662.69	113086.0	272.65	2521.66	69.40
Isopentane	5	72.15	0.0622	0.0769	0.6311	392.47	24.4188	1603.70	32130.0	300.95	3397.63	66.54
n-Pentane	5	72.15	0.0622	0.0769	0.6364	283.84	17.6597	1159.80	23236.4	309.15	2977.29	61.67
n-Octane	5	114.23	0.0393	0.0563	0.7096	5.63	0.2213	36.43	291.2	399.75	5201.79	58.98
Benzene	2	78.11	0.0230	0.0851	0.8957	45.53	1.0466	201.40	1377.1	353.25	11.32	69.76
Toluene	25	92.14	0.2436	0.0776	0.8759	12.43	3.0278	64.86	3983.9	383.75	12.60	71.49
Xylene (m)	10	106.17	0.0846	0.0629	0.8701	3.26	0.2757	19.61	362.8	464.25	11.83	51.89
n-Hexane	5	86.18	0.0521	0.0669	0.6676	75.70	3.9432	369.48	5188.5	341.85	3661.35	56.50
2-Methyldecane	5	156.31	0.0287	0.0568	0.7453	0.11	0.0031	0.96	4.1	442.30	2204.63	42.21
2,2,4-Trimethylpentane	5	114.23	0.0393	0.0665	0.6995	23.02	0.9048	148.94	1190.5	372.40	12860.22	51.29
n-Heptane	0	100.20	0.0000	0.0620	0.6914	20.66	0.0000	117.23	0.0	371.55	4459.53	52.35
2-Methyl-2-butene	5	70.14	0.0640	0.0741	0.6735	254.75	16.3044	1011.96	21453.2	304.30	788.08	64.13
2,3-Dimethyl-1-butene	5	84.16	0.0533	0.0677	0.6837	132.47	7.0657	631.38	9297.0	328.80	1279.84	59.31
1,2,4-Trimethylbenzene	8	120.20	0.0598	0.0649	0.8838	0.70	0.0419	4.77	55.1	442.50	8.91	54.09
1,1-Dimethyl-2-phenylethane	5	134.22	0.0334	0.0613	0.8595	0.64	-0.0213	4.84	28.0	445.90	48.53	46.73
Total	100	95.03	1.0000		0.7682		288.1485		379142.9		1931.617	

Temperature = 283.15 deg. K
Pressure = 760 mm Hg
Gas Constant =
    0.06236 mm Hg*m^3/mol*K
Molecular Weight
of Air = 28.96 gm/mol
Average Molecular
Weight of Gasoline
Vapors = 62.58 gm/mol
Molecular weight
of Gasoline-Air
Mixture = 41.71 gm/mol

Vapor Density
of Gasoline-Air
Mixture = 1795.18 gm/m^3

Weighted average
air diffusion
coefficient = 0.0732 cm^2/sec
Weighted average
liquid density = 0.7491 gm/cm^3
Weighted average
gas density = 1021.28 gm/m^3

D-14

Table D-12

CHEMICAL PROPERTY ESTIMATION FOR STETZENBACH HIGH
OCTANE GASOLINE AND CONSTITUENTS AT 0 DEGREES C.

REPRESENTATIVE CHEMICAL	PERCENT COMPOSITION	GRAM MOL. WEIGHT (GM/MOL)	LIQ. PHASE MOL FRACT.	AIR DIFFUSION COEFFICIENT (CM^2/SEC)	LIQUID DENSITY (GM/CM^3)	PURE CHEMICAL VAPOR PRESSURE (mm Hg)	PARTIAL PRESSURE OVER GASOLINE (mm Hg)	PURE CHEMICAL VAPOR DENSITY (GM/M^3)	CONCENTRATION OVER LIQUID GASOLINE (ppm)	BOILING POINT (deg. K)	HENRY'S LAW CONSTANT (dim.)	GAS VISCOSITY (uPOISE)
Isobutane	5	58.12	0.0772	0.0805	0.5876	1174.26	90.6961	4006.65	119337.0	261.25	2407.97	85.23
n-Butane	5	58.12	0.0772	0.0805	0.6044	774.09	59.7892	2641.24	78668.6	272.65	1818.42	66.06
Isopentane	5	72.15	0.0622	0.0722	0.6418	259.30	16.1332	1098.34	21227.9	300.95	2320.11	66.21
n-Pentane	5	72.15	0.0622	0.0722	0.6465	183.40	11.4108	776.84	15014.2	309.15	1994.20	59.49
n-Octane	5	114.23	0.0393	0.0528	0.7161	2.86	0.1123	19.16	147.8	398.75	2734.13	56.89
Benzene	2	78.11	0.0230	0.0800	0.9061	26.34	0.6055	120.79	796.7	353.25	6.79	67.29
Toluene	25	92.14	0.2436	0.0728	0.8844	6.72	1.6373	36.36	2154.3	383.75	7.06	60.96
Xylene (o)	10	106.17	0.0946	0.0590	0.8761	1.63	0.1376	10.14	181.0	446.25	6.12	50.85
n-Hexane	5	86.18	0.0521	0.0628	0.6759	45.32	2.3608	229.31	3106.4	341.85	2272.33	54.51
2-Methyldecane	5	156.31	0.0287	0.0534	0.7505	0.04	0.0012	0.37	1.5	462.30	863.72	40.72
2,2,4-Trimethylpentane	5	114.23	0.0393	0.0625	0.7067	13.08	0.5140	87.71	476.3	372.40	13331.03	49.60
n-Heptane	0	100.20	0.0000	0.0583	0.6986	11.42	0.0000	67.17	0.0	371.55	2555.01	50.90
2-Methyl-2-butene	5	70.14	0.0640	0.0696	0.6846	163.10	10.4383	671.59	13734.7	304.30	523.01	61.87
2,3-Dimethyl-1-butene	5	84.16	0.0533	0.0636	0.6930	82.31	4.3903	406.67	5776.7	328.80	824.34	57.21
1,2,4-Trimethylbenzene	8	120.20	0.0598	0.0609	0.8905	0.32	0.0189	2.23	24.9	442.50	4.17	52.18
1,1-Dimethyl-2-phenylethane	5	134.22	0.0334	0.0576	0.8659	0.28	0.0095	2.25	12.5	445.90	22.52	45.10
Total	100	95.83	1.0000		0.7768		198.2539		260860.5		1450.274	

Temperature = 273.15 deg. K
Pressure = 760 mm Hg
Gas Constant = 0.06236 mm Hg*m^3/mol*K
Molecular Weight of Air = 28.96 gm/mol
Average Molecular Weight of Gasoline Vapors = 62.18 gm/mol
Molecular weight of Gasoline-Air Mixture = 37.62 gm/mol

Vapor Density of Gasoline-Air Mixture = 1678.72 gm/m^3
Weighted average air diffusion coefficient = 0.0687 cm^2/sec
Weighted average liquid density 0.7583 gm/cm^3
Weighted average gas density 723.66 gm/m^3

The vapor mixture of the CDM synthetic gasoline blend was compared against the gasoline vapor mixture suggested by K. Stetzenbach (1987) of this appendix. Assuming the vapor mixture given by Stetzenbach is for 10° C, the percentages of the vapor mixture on a constituent basis are:

	CDM Gasoline Vapor Mixture	Stetzenback Vapor Mixture
isopentane	39%	30%
isobutane	27%	19%
n-pentane	6%	19%
n-butane	9%	30%
toluene	0.4%	1%
m-xylene	0.1%	1%
others	18.5%	0%
sum	100%	100%

This comparison shows that the Stetzenbach gasoline vapor mixture contains more n-pentane and n-butane and less isopentane and isobutane than the CDM gasoline vapor mixture. If the vapor percentages are grouped into the C_4 and C_5 alkanes and aromatic compounds, the comparison becomes:

	CDM Gasoline Vapor Mixture	Stetzenbach Vapor Mixture
C_4 alkanes	36%	49%
C_5 alkanes	45%	49%
aromatics	0.5%	2%
others	18.5%	0%
sum	100%	100%

This comparison indicates that the CDM gasoline vapor mixture and the Stetzenbach vapor mixture are similar.

ENVIRONMENTAL RESEARCH CENTER

UNIVERSITY OF NEVADA, LAS VEGAS
4505 MARYLAND PARKWAY • LAS VEGAS, NEVADA 89154 • (702) 739-3382

MEMORANDUM

TO: Philip Durgin
FROM: Klaus Stetzenbach *KS*
DATE: September 24, 1987
SUBJECT: Standard Gasoline

In my memorandum to you on September 10, 1987, I presented components and concentrations for consideration of several standard gasolines. Subsequently, I have discussed this with Rick Johnson, Dave Kreamer, Gwen Eklund, Henry Kerfoot and Jim Stuart. From these discussions it was decided that:

1)   There is a need for at least three types of standard gasolines; a low Reid vapor pressure (RVP), a high RVP, and a high octane.

2)   Small volumes of calibration standards should be made at a central location, but larger volumes for experimental use should be mixed by the user.

3)   If a researcher wishes to add extra components, the hexane, heptane, or octane concentrations should be reduced. All other components should remain at their original concentrations.

4)   For instrumental standardization purposes, it will be acceptable to use a standard mixture of fewer components provided that the standardization mixture has been calibrated against one of the standard gasolines.

A table containing components and their concentrations for three standard gasolines is attached.

KS/
Attachment

STANDARD GASOLINE MIXTURES

COMPONENT		CONCENTRATION (%)	
	LOW RVP	HIGH RVP	HIGH OCTANE
2-methylpropane	3	5	5
butane	3	10	5
2-methylbutane	5	5	5
pentane	5	5	5
hexane	5	5	5
heptane	5	5	--
2,2,4 trimethylpentane	5	5	5
octane	14	5	5
2-methyldecane	5	5	5
2-methyl-2-butene	5	5	5
2,3-dimethyl-1-butene	5	5	5
benzene	2	2	2
toluene	15	15	25
xylene(s) *	10	10	10
1,2,4-trimethylbenzene	8	8	8
1,1-dimethyl-2-phenylethane	5	5	5
% aliphatics	50	50	40
% olefins	10	10	10
% aromatics	40	40	50
% C4 & C5	16	25	20

*   can be any mixture of xylenes, but concentration
    of each isomer must be specified.

ENVIRONMENTAL RESEARCH CENTER

UNIVERSITY OF NEVADA, LAS VEGAS
4505 MARYLAND PARKWAY • LAS VEGAS, NEVADA 89154 • (702) 739-3382

MEMORANDUM

TO: Philip Durgin
FROM: Klaus Stetzenbach
DATE: September 29, 1987
SUBJECT: Standard Gasoline Vapor Mixture

Based on the data from the references listed in my memo to you of September 10, 1987, I recommend that a standard gasoline vapor contain the compounds listed below. These are the same set of compounds that will be used by Radian in their testing of the gasoline vapor monitors.

STANDARD GASOLINE VAPOR MIXTURE

COMPONENT	CONCENTRATION (%)
2-methylpropane	19
butane	30
2-methylbutane	30
pentane	19
toluene	1
xylene(s) *	1

* can be any mixture of xylenes, but the concentration of each isomer must be specified.

EVALUATION OF AIR-WATER PHASE EXCHANGE ON DIFFUSION OF HYDROCARBON VAPORS

Development

The potential for loss of hydrocarbon vapors to vadose zone water was evaluated with a consideration of a retardation factor, F, which is based on Henry's Law. This retardation factor has the effect of linearly scaling the effective diffusion coefficient, reducing diffusive transport because of losses to the water phase. Aromatic hydrocarbons with high Henry's Law constant values (e.g., benzene, toluene, xylene) would be expected to experience higher losses to exchange with water than the low-molecular weight alkanes (e.g., isopentane, isobutane, n-butane) which have lower Henry's Law constant values. As a result, it would be expected that the aromatic hydrocarbons would be retarded relative to the alkanes in a diffusive transport simulation. The effect on diffusive transport of exchange between air and water as governed by Henry's Law was investigated by formulating an expression to include Henry's Law into the diffusion equation.

The governing equation for vapor diffusion is given in Equation H-1 of Appendix H. Dividing each term by the air-filled porosity produces:

$$\partial C/\partial t = \partial/\partial x_i \left[D_{e,ij} \left(\partial C/\partial x_j \right) \right] + \left(\partial s/\partial t \right)/\theta_a \qquad \text{(Equation E-1)}$$

where:

C	vapor concentration (cm^3/cm^3)
t	time (seconds)
x_i	distance in i^{th} direction (cm)
$D_{e,ij}$	effective diffusion coefficient (cm^2/sec)
$\partial s/\partial t$	vapor source/sink term ($cm^3/cm^3/sec$)
θ_a	air-filled porosity (cm^3/cm^3)

The source/sink term can be expanded to:

$$\partial s/\partial t = \partial s/\partial C \cdot \partial C/\partial t \qquad \text{(Equation E-2)}$$

To describe the partitioning term, $\partial s/\partial C$, Henry's Law can be introduced:

$$C = H_k \cdot C_w \qquad \text{(Equation E-3)}$$

where: H_k Henry's Law constant (dimensionless)
C_w concentration in water (cm^3/cm^3)

Using Henry's Law, an expression for the rate of partitioning into the water phase can be obtained by defining the "sink" (water) concentration, according to volume, and then differentiating with respect to vapor concentration:

$$s_w = \theta_w \cdot C/H_k \qquad \text{(Equation E-4)}$$

$$\partial s_w/\partial C = \theta_w/H_k = -\partial s/\partial C \qquad \text{(Equation E-5)}$$

where:

s_w volumetric water concentration (cm^3/cm^3)
θ_w water-filled porosity (cm^3/cm^3)

Equation E-5 is based on the assumptions that partitioning is instantaneous, linear, and reversible.

Substituting Equation E-5 into Equation E-1, and defining a retardation coefficient, F_k, for vapor-water partitioning, produces:

$$F_k \cdot \partial C/\partial t = \partial/\partial x_i [D_{e,ij}(\partial C/\partial x_j)] \qquad \text{(Equation E-6)}$$

$$F_k = 1 + (\theta_w/\theta_a)/H_k \qquad \text{(Equation E-7)}$$

This is the same equation solved by the DYNFLOW UST model (see Appendix H) except that the effective diffusion coefficient should be scaled by the retardation factor to account for gas-liquid phase exchange. The expression for the retardation factor (Equation E-7) is corroborated by G. Robbins (1987).

Discussion

The effect of low Henry's Law constant values (e.g., benzene, toluene, xylene) in equation 9 is to make the value of F greater than 1, thereby reducing the effective diffusion coefficients for these hydrocarbons. By contrast, large values of H for compounds such as isopentane will result in F values close to 1, indicating little or no effect on diffusive transport by the loss of these compounds to the water phase by exchange governed by Henry's Law.

Calculations performed with Equation E-7 show that, except in the case of benzene (i.e., H = 11), the effect of gas-liquid phase exchange on the effective diffusion coefficient is negligible. These calculations were made for the native soils of simulation run number 6 to maximize the effect of gas-liquid phase exchange since this simulation modeled the largest moisture content of any of the simulations performed. For the purposes of the DYNFLOW UST simulation, this analysis shows that the effect of losses of hydrocarbon vapors to the water phase in the vadose zone on diffusive transport can be safely neglected.

TABLE E-1

Example Calculation of Retardation Coefficient

Gasoline Component or Blend	H Henry's Law Coefficient (dimensionless)	F Retardation Coefficient (dimensionless)
CDM Synthetic Gasoline Blend	3,203	1.00
Isopentane	3,388	1.00
Isobutane	3,260	1.00
Benzene	11	1.49

Note: All values in this table are for 10° C

Assumptions: θ_t = Total Porosity = 45%

θ_a = Air Filled Porosity = 7%

Represents "Wet Clay" native soil as in Simulation Run Number 6 (See Appendix K)

CALCULATION OF EQUILIBRIUM GASOLINE VAPOR-AIR MIXTURE DENSITY

This appendix presents the equations used for calculation of the equilibrium vapor density of the gasoline vapor-air mixture. A sample calculation for equilibrium vapor density is presented also in this Appendix.

Vapor density of gasoline vapor-air mixture, ρ_v:

$$\rho_v = \bar{M} \cdot P_a / (T \cdot R) \qquad \text{(Equation F-1)}$$

where:

$\bar{M}$ average molecular weight of gasoline vapor-air mixture (g/mol)

R universal gas constant (62,630 mm Hg $\cdot$ cm^3/mol $\cdot$ °K)

T temperature (°K)

P_a atmospheric pressure (mm Hg)

---

2. Average molecular weight of gasoline vapor-air mixture, $\bar{M}$:

$$\bar{M} = (P_t / P_a) \cdot M_v + ((P_a - P_t) / P_a) \cdot M_a \qquad \text{(Equation F-2)}$$

where:

P_t equilibrium vapor pressure of gasoline vapor (mm Hg)

M_a average molecular weight of air, $M_a = 28.96$ (g/mol)

M_v average molecular weight of gasoline vapors (g/mol)

The following is an example calculation of the density of a gasoline vapor-air mixture. From Table D-1 of Appendix D, and using Equation F-2:

M_v = 69.48 g/mol

T = 293.15 °K

R = 62,360 mm Hg · cm^3/(mol · °K)

M_a = 28.96 g/mol

P_t = 274 mm Hg

$\bar{M}$ = (274/760) · 69.48 + ((760-274)/760) · 28.96

$\bar{M}$ = 43.57 g/mol

ρ_v = (43.57 · 760/(293.15 · 62,360)

ρ_v = 1.811 x 10^{-3} g/cm^3

The calculated gasoline vapor-air mixture vapor density from this sample calculation indicates that the gasoline vapor-air mixture is about 50% denser than air (e.g., air density ≈ 1.2 x 10^{-3} g/m^3).

APPENDIX G

CALCULATION OF
THE LIQUID VOLUME OF LEAKED GASOLINE

This appendix presents the methodology for calculating the liquid volume of leaked gasoline, using the simulation results from the DYNFLOW diffusion-based model of vapor transport from an UST leak. A sample calculation is also provided.

At the end of each simulation time step, DYNFLOW prints a "mass balance" table that includes all inflows and outflows from the model for the UST leak simulations. The only gasoline vapor inflow was at the simulated leak, which was represented as a fixed concentration. Thus, for each simulation run, DYNFLOW produced a time history of inflow rate versus simulation time. An example of this, for simulation run number 1 ("average conditions"), is listed in Table G-1. Note that the inflow rates are those printed directly by DYNFLOW, corresponding to a leak concentration of "100" representing 100 percent of equilibrium concentration.

To compute the volume of gasoline that has leaked, incremental and cumulative volumes of diffused gasoline vapors at the end of each time step were computed, as shown in Table G-1. The incremental leaked volume was calculated as follows:

$$V_{i,100} = [(Q_{i,100} + Q_{i-1,100})/2] \cdot \Delta t_i \qquad \text{(Equation G-1)}$$

where: $V_{i,100}$ incremental leak volume of gasoline vapors (ft^3);

$Q_{i,100}$ simulated influx rate for time step i (ft^3/hr);

Δt_i length of time step i (hours);

100 subscript referring to "100 per cent" concentration.

The cumulative volume was computed at each simulation time by adding all previous incremental volumes:

$$V_{v,100} = \sum_{i=1}^{N} V_{i,100}$$ (Equation G-2)

where: N   number of simulation time steps

The cumulative volumes were then converted from "100 percent" of equilibrium concentration equivalents to estimated gasoline vapor volumes by multiplying by the equilibrium vapor concentration and air-filled porosity:

$$V_v = V_{v,100} \cdot C_o \cdot \theta_a / 100$$ (Equation G-3)

where: C_o equilibrium vapor concentration in air of gasoline vapors (ft^3/ft^3)

          θ_a air filled porosity (ft^3/ft^3)

The air-filled porosity is included because the DYNFLOW simulations were performed with a unit storage coefficient. The concentrations predicted by DYNFLOW are correct, and they are based on reasonably-estimated effective diffusion coefficients that incorporate porosity; but, the inflows need to be corrected for the available space for vapors to occupy.

For the example in Table G-1, the total volume of leaked vapors at the end of two days was estimated as follows:

$$V_v \text{ (at 2 days)} = 656 \cdot 0.284 \cdot 0.20/100 \text{ ft}^3$$
$$= 0.37 \text{ ft}^3 = 10,551 \text{ cm}^3$$

The next step was to compute the mass of these gasoline vapors:

$$W_v = \bar{M} \cdot V_v \cdot P_a / (T \cdot R) \qquad \text{(Equation G-4)}$$

where:

W_v — mass of gasoline vapors (g)

$\bar{M}$ — average gram molecular weight of gasoline-air mixture (g/mol)

R — universal gas constant ($62,360$ mm Hg $\cdot$ cm^3/mol $\cdot$ °K)

T — temperature (°K)

P_a — atmospheric pressure (mm Hg)

From the example:

$$W_v = 38.88 \cdot 10,551 \cdot 760/(283.15 \cdot 62,360) = 17.7 \text{ g}$$

Knowing the mass of gasoline vapors, the corresponding volume of liquid gasoline was calculated using:

$$V_1 = W_v/\rho_1 \qquad \text{(Equation G-5)}$$

where:

V_1 — leaked volume of liquid gasoline (cm^3)

ρ_1 — gasoline liquid density (g/cm^3)

Completing the example, and converting cubic centimeters to gallons:

$$V_1 = 17.7/0.7271 = 24.3 \text{ cm}^3 = 0.01 \text{ gallons}$$

This is the estimated minimum volume of leaked gasoline after a simulated leak duration of two days, using the conditions from simulation run number 1 ("average conditions").

G-3

The cumulative volume of leaked gasoline, V_1, can be calculated from the cumulative volume of gasoline vapor, $V_{v,100}$, through a scalar quantity, air-filled porosity, and saturation vapor concentration.

$$V_1 = V_{v,100} \cdot C_o \cdot \Theta_a \cdot S$$

where:

S   scalar quantity

at $0°$ C, $S = 1.61 \times 10^{-4}$

at $10°$ C, $S = 1.72 \times 10^{-4}$

at $20°$ C, $S = 1.89 \times 10^{-4}$

TABLE G-1

Example Time History of DYNFLOW-Simulated
Vapor Volatilization Flux Rates and Volumes

Simulation Time at End of Time Step (hours)	Time Step Length (hours)	DYNFLOW Inflow Rate (ft^3/hr)	Volatilization Volume During Time Step (ft^3)	Cumulative Volatilization Volume (ft^3)
1	1	17.594	8.797	8.797
2	1	16.229	16.912	25.709
3	1	15.630	15.930	41.639
4	1	15.237	15.434	57.073
5	1	14.952	15.095	72.168
6	1	14.750	14.851	87.019
9	3	14.313	43.595	130.614
12	3	14.033	42.520	173.134
18	6	13.689	83.166	256.300
24	6	13.473	81.486	337.786
30	6	13.320	80.379	418.165
36	6	13.205	79.575	497.740
42	6	13.174	79.137	576.877
48	6	13.081	78.765	655.642

Note: All rates and volumes in this table correspond to simulation of the volatilization as 100 percent of equilibrium vapor concentration.

The volatilization rates are from Simulation Run Number 1 ("average conditions"), as listed in Table N-8.

APPENDIX H

ANALOGY OF DIFFUSION AND CONFINED GROUND WATER FLOW

This appendix presents the mathematical justification for using DYNFLOW to perform diffusion simulations with a computer model which solves the confined ground water flow equation. A description of DYNFLOW, its development, usage, validation, and availability also is presented in the appendix.

GOVERNING EQUATIONS

The governing differential equation for vapor diffusion in three dimensions can be expressed as:

$$\theta_a \cdot \partial C/\partial t = \theta_a \cdot \partial/\partial x_i [D_{\bullet,ij}(\partial C/\partial x_j)] + \partial s/\partial t, \quad i = 1,2,3$$

(Equation H-1)

where:

C	vapor concentration (ft^3/ft^3 of gas)
t	time (hours)
$D_{\bullet,ij}$	effective diffusion coefficient tensor (ft^2/hr)
x_i	distance in direction i (ft)
θ_a	air-filled porosity (ft^3/ft^3)
$\partial s/\partial t$	vapor source term ($ft^3/ft^3/hr$)

Similarly, the equation for confined ground water flow is:

$$S_s \cdot \partial h/\partial t = \partial/\partial x_i [K_{ij}(\partial h/\partial x_j)] + Q, \quad i = 1,2,3 \qquad \text{(Equation H-2)}$$

where:

h	aquifer piezometric head (ft)
S_s	aquifer specific storativity (ft^{-1})
K_{ij}	hydraulic conductivity tensor (ft/hr)
Q	hydraulic source term ($ft^3/hr/ft^3$)

By analogy, the two equations can be made identical by letting:

$$D_{e,ij} \equiv K_{ij}/S_s \qquad \text{(Equation H-3)}$$

$$C \equiv h \qquad \text{(Equation H-4)}$$

$$(\partial s/\partial t)/\theta_a \equiv Q/S_s \qquad \text{(Equation H-5)}$$

In fact, K_{ij}/S_s is referred to as the "aquifer diffusivity" in ground water hydrology.

This analogy means that any computer program that simulates three-dimensional confined ground water flow can be used to solve the vapor diffusion equation. In this work assignment, CDM's three-dimensional program called DYNFLOW was used.

For sake of convenience, the term S_s was set equal to unity. This meant that the hydraulic conductivity values in all simulation runs were equal to the effective diffusion coefficients.

To interpret the fluxes computed by DYNFLOW at source or sink boundary condition locations (such as the point used to simulate the UST leak as a constant concentration), the air-filled porosity was multiplied by the computed "water" flux, giving a simulated flux of vapor product (ft^3/hr). This was cross-checked by taking the simulated concentration distribution and computing the volume of vapor product occupying the pore spaces, and comparing it to the integral of the fluxes over time.

DYNFLOW SIMULATION MODEL

DYNFLOW is a three-dimensional, finite element groundwater flow code, developed and applied at CDM. DYNFLOW uses the finite element formulation and allows the user to mix 3-D, 2-D, 1-D, planar, and pond elements. The code also has flexible capabilities for changing boundary conditions, geometries in all three dimensions, and model time-stepping during the course of a simulation run.

The present version of DYNFLOW evolved from work performed over the last
decade. The original research for the model was conducted at the
Massachusetts Institute of Technology in the mid 1970's. Many of the
personnel involved in this original development work subsequently joined
CDM as full-time employees, including the work assignment manager, who is a
co-author of DYNFLOW. These people, while at CDM, were involved in
numerous groundwater flow and groundwater contamination studies (including
many related to RCRA and CERCLA) and continued to make refinements and
improvements on the original models to enhance both their usefulness and
their ability to accurately represent real-world behavior.

The current versions of DYNFLOW and DYNTRACK have been applied by CDM at
numerous sites under our current OERR contract; they have been used in
performing RI/FS work at many sites. In addition, DYNFLOW and DYNTRACK
have formed the basis of CDM's involvement in enforcement-related efforts.

For one of these projects, OWPE commissioned the International Ground Water
Modeling Center (IGWMC) of the Holcomb Research Institute at Butler
University to review the DYNFLOW and DYNTRACK simulation codes. IGWMC's
Report of Findings (May 3, 1985) provides a formal acknowledgment of the
code's theoretical and scientific appropriateness.

CDM will license an executable version of DYNFLOW to any interested party,
for a licensing fee that is commensurate with the extensive research and
development time that CDM has invested in the program. (For public sector
entities, this fee is often waived.) The availability of licensing
arrangements puts DYNFLOW in the public sector. This, in addition to the
code verification performed by the International Ground Water Modeling
Center, makes DYNFLOW a robust and publicly-defensible numerical simulation
program.

A complete Users Manual is available for DYNFLOW (CDM, 1984). It contains
sections on theory, program structure, command language, computer
implementation, and code verification. Details on the verification
simulation runs can be provided.

APPENDIX I

ANALYTICAL VERIFICATION OF THE DYNFLOW-BASED DIFFUSION MODEL

This appendix presents an analytical verification of the DYNFLOW diffusion model. The analytical verification describes theory, methodology, simulation input, simulation results, and conclusions.

A simple, one-dimensional diffusion problem was constructed to verify the performance of the DYNFLOW diffusion model. The diffusion equation solved in this exercise was:

$$\partial C / \partial t \;=\; D_e \cdot \partial^2 C / \partial x^2 \qquad\qquad \text{(Equation I-1)}$$

where:

C vapor concentration (ft^3/ft^3)

D_e effective soil diffusion coefficient (ft^2/hr)

t time (hr)

x horizontal distance from source (ft)

The grid was constructed as two parallel rows of elements, each row 2 feet wide, for a total lateral width of 4 feet. The vertical thickness was 2 feet, giving a cross-section area of 8 square feet. The longitudinal length of the grid was 18 feet, and so the volume was 144 cubic feet.

Boundary conditions were no-flow boundaries on the sides, top, and bottom of the numerical grid used to solve this differential equation. It was assumed that no vapors were present within the system prior to initiation of simulation. With the initiation of simulation, the nodes on one end of the numerical grid were set at constant concentration values with time. The numerical simulations were made with an effective soil diffusion coefficient of $D_e = 0.1348 \; ft^2/hr$, which was assumed to be constant and isotropic.

Two grid densities for the numerical model were selected to examine the effect of spatial discretization on the numerical results. The fine numerical grid utilized 6 levels separated by a 0.4 foot of vertical distance; nodes along the longitudinal horizontal axis were separated by a 0.4 foot of horizontal distance. The coarse numerical grid utilized 2 levels separated by 2 feet of vertical distance; nodes along the longitudinal horizontal axis were separated by 2 feet of horizontal distance.

The analytical solution to the diffusion equation used the same diffusion coefficient value and is solved with:

$$C/C_o = erfc(x/(4 \cdot D_\bullet \cdot t)^{1/2})$$ (Equation I-2)

where:

C	vapor concentration at distance x from the source (ft^3/ft^3)
C_o	source vapor concentration (ft^3/ft^3)
$erfc(z)$	complementary error function, with argument z.

A good fit between the numerical solution results for the fine grid and the analytical solution at time t = 6 hours was found (Figure I-1). A poorer fit, however, between the coarse grid numerical results and the analytical solution resulted at time t = 6 hours (Figure I-2).

At time t = 96 hours, results from the fine and coarse numerical grid simulations showed good agreement with the analytical solution (Figures I-3 and I-4).

As a second verification measure, the influxes calculated by the DYNFLOW diffusion model were compared to fluxes computed for the analytical solution. The analytical fluxes were computed from:

$$J_x = -D_\bullet \cdot \partial[C/C_o]/\partial x$$ (Equation I-3)

I-2

where:

J_x volume flux per unit area entering system at source
($ft^3/hr/ft^2$)

To determine the gradient, $\partial C/\partial x$, near the source, Equation I-2 was evaluated at progressively smaller values of x. In the limit as x approached zero, the calculated gradient approached the gradient at the source. This estimate of the gradient very near the source was multiplied by $D_e = 0.1348$ ft^2/hr to evaluate J_x. This analytical value for J_x was compared against the flux values generated by DYNFLOW, as shown in Table 1-1.

This analysis shows that the flux computed by DYNFLOW for the fine grid agrees with the analytical calculation of flux at both simulation times. The coarse grid flux at 96 hrs also corresponds to the analytical flux at 96 hrs. Some discrepancy, due to the discretization of the coarse grid, is apparent at the earlier time.

The grid used for the UST simulations described in this report had a spacing of 1 foot in the backfill zone. This spacing falls between the fine and coarse grids used in this appendix.

Based on the results of the verification test, it was determined that the DYNFLOW diffusion model produces results that accurately match analytic solutions. More importantly, it was determined that a 1-foot spacing is adequate for the simulation of vapor diffusion from an UST leak.

Addendum

Further proof of verification for the use of DYNFLOW, and for the method of calculating liquid leaked volume, was obtained by simulating the one-dimensional case to steady-state and computing the cumulative influx volume. This volume should equal the available storage space in the DYNFLOW grid, or 144 cubic feet. Multiplication by the air-filled porosity, as described in Appendix G, would give the volume of vapors in the system.

The simulation to steady-state produced good agreement between simulated results and the grid volume: DYNFLOW simulated about 152 cubic feet of total inflow, using the coarse test grid. These results further enhance the verification of DYNFLOW and they support the methods outlined in Appendix G and Appendix H for computing liquid volume equivalents based on DYNFLOW simulation results.

TABLE I-1

COMPARISON OF DYNFLOW AND ANALYTIC SOLUTION OF VAPOR INFLUX

Simulation Time (hour)	Analytic Solution	One-Dimensional Vapor Influx ($ft^3/hr/ft^2$) DYNFLOW RESULTS	
		Fine Grid	Coarse Grid
6	0.085	0.083	0.060
96	0.021	0.021	0.020
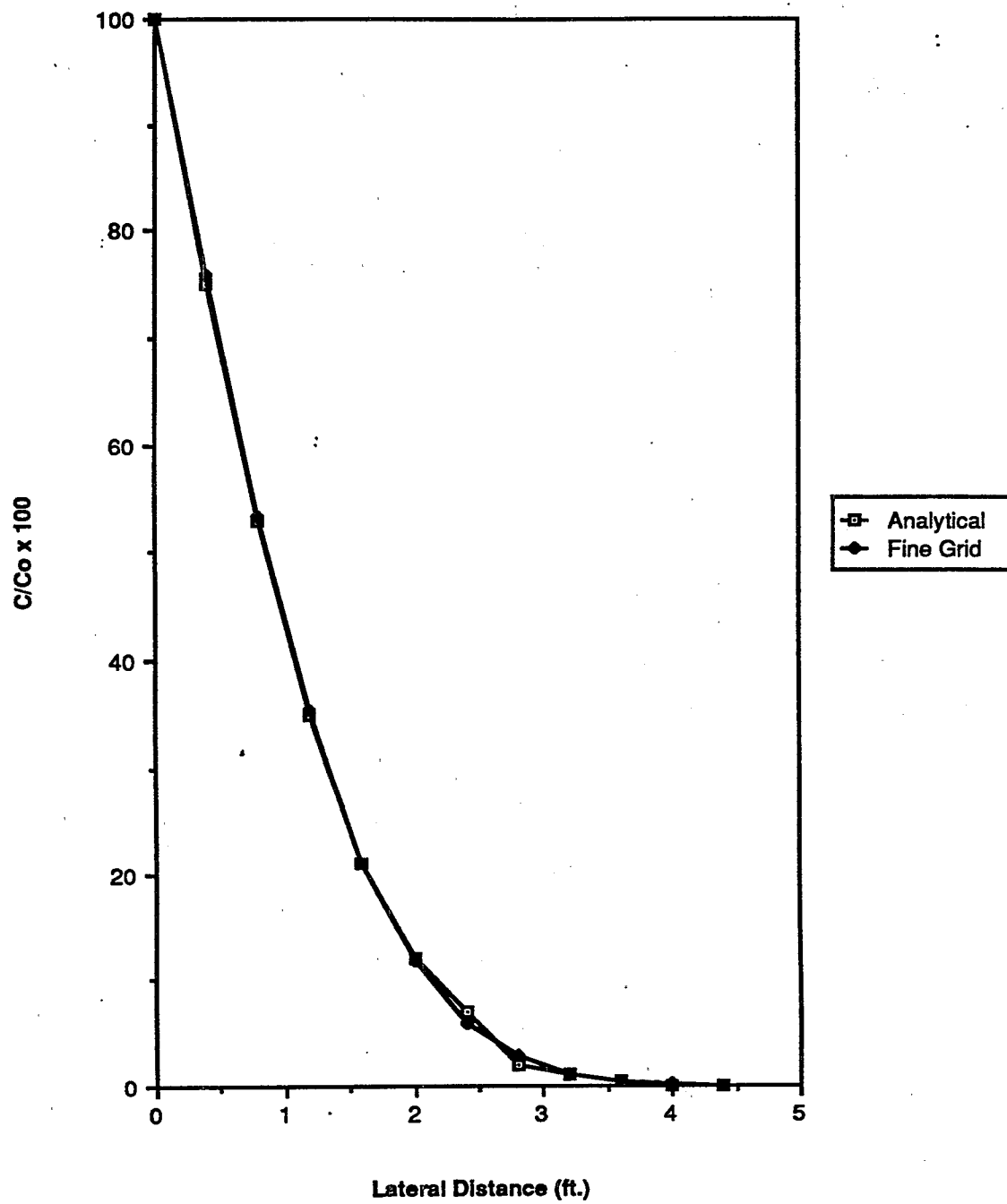
FIGURE I-1. Analytic vs. DYNFlOW (fine grid) at 6 hours.
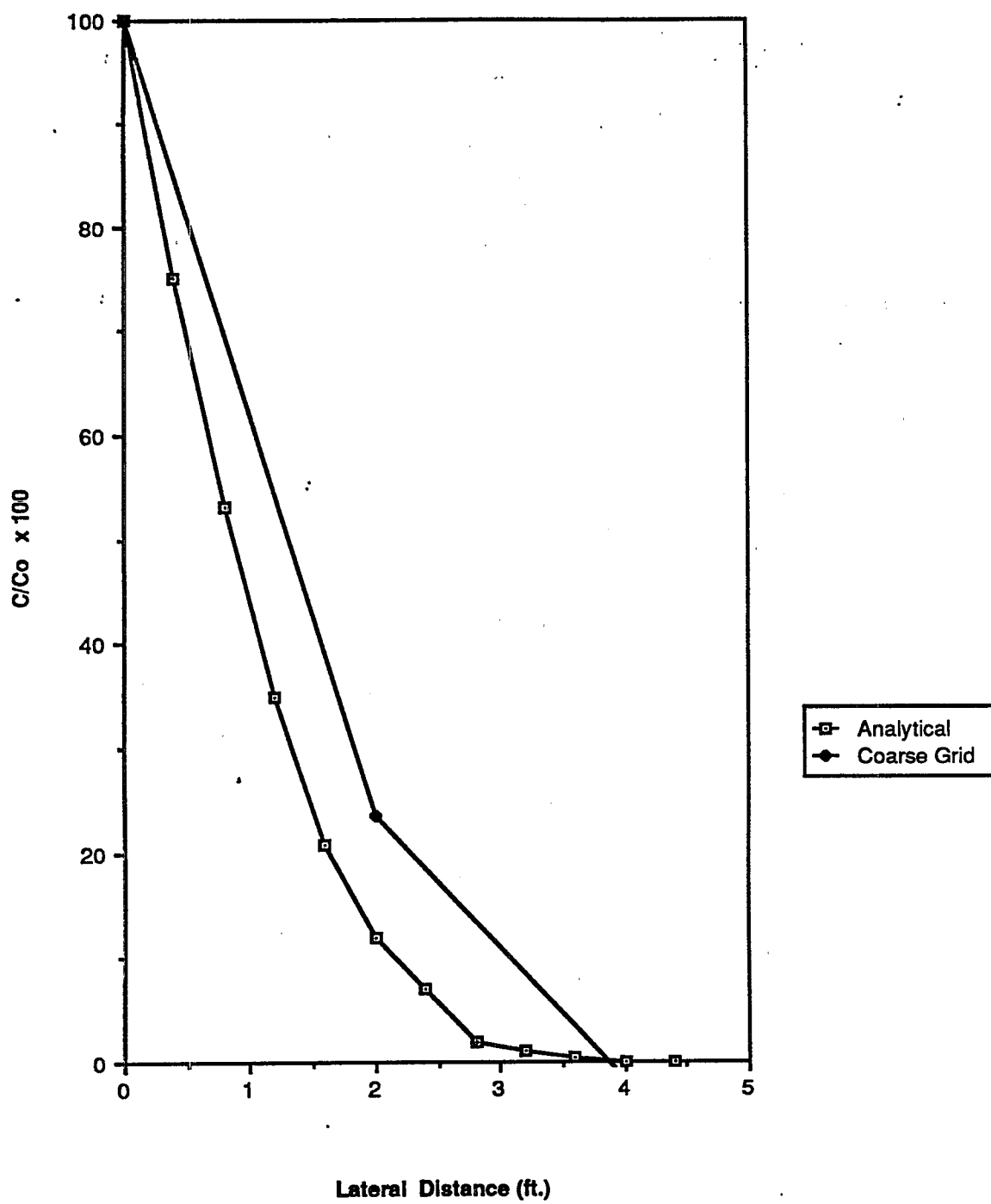
FIGURE I-2. Analytic vs. DYNFLOW (coarse grid) at 6 hours.
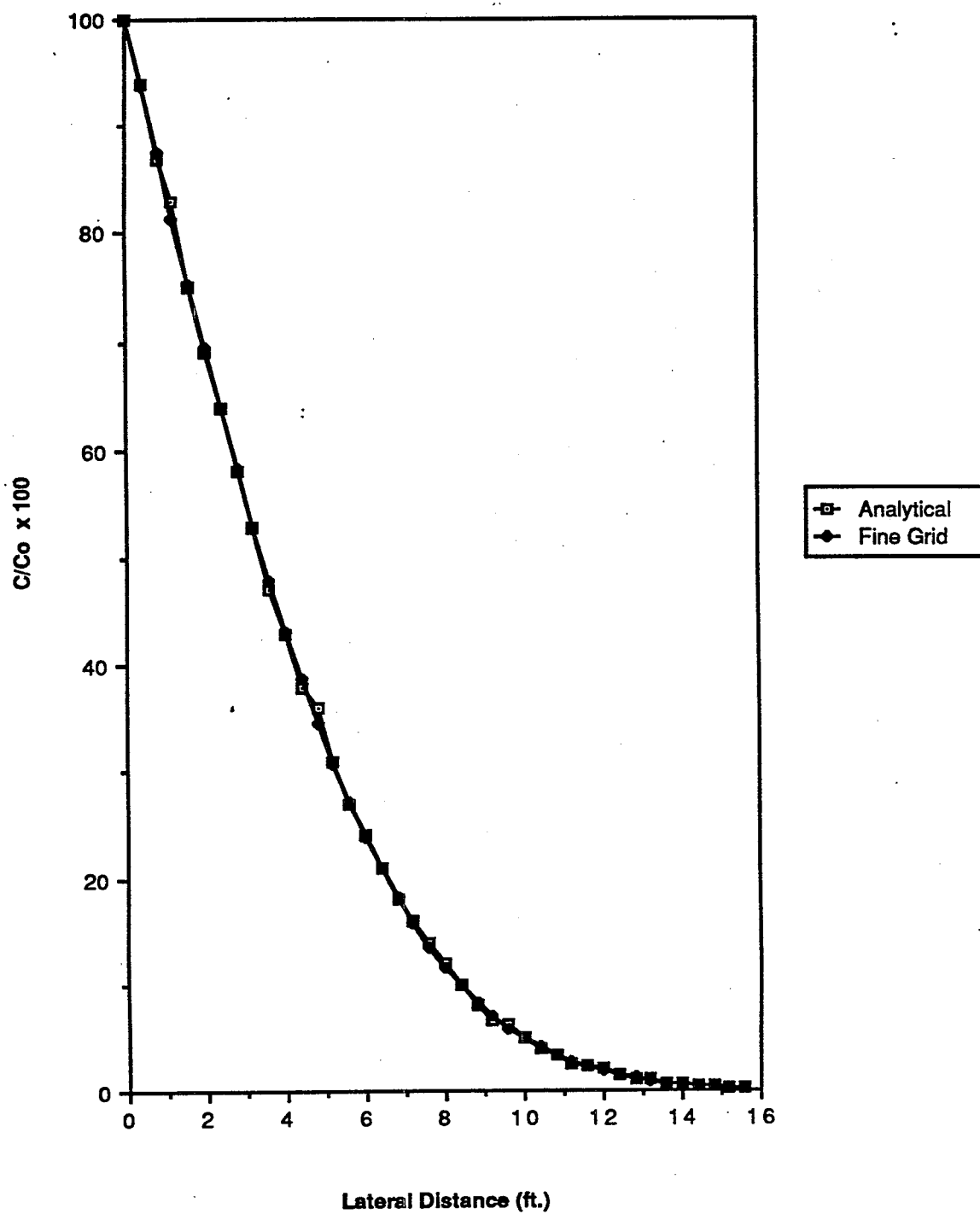
FIGURE I-3. Analytic vs. DYNFLOW (fine grid) at 96 hours.
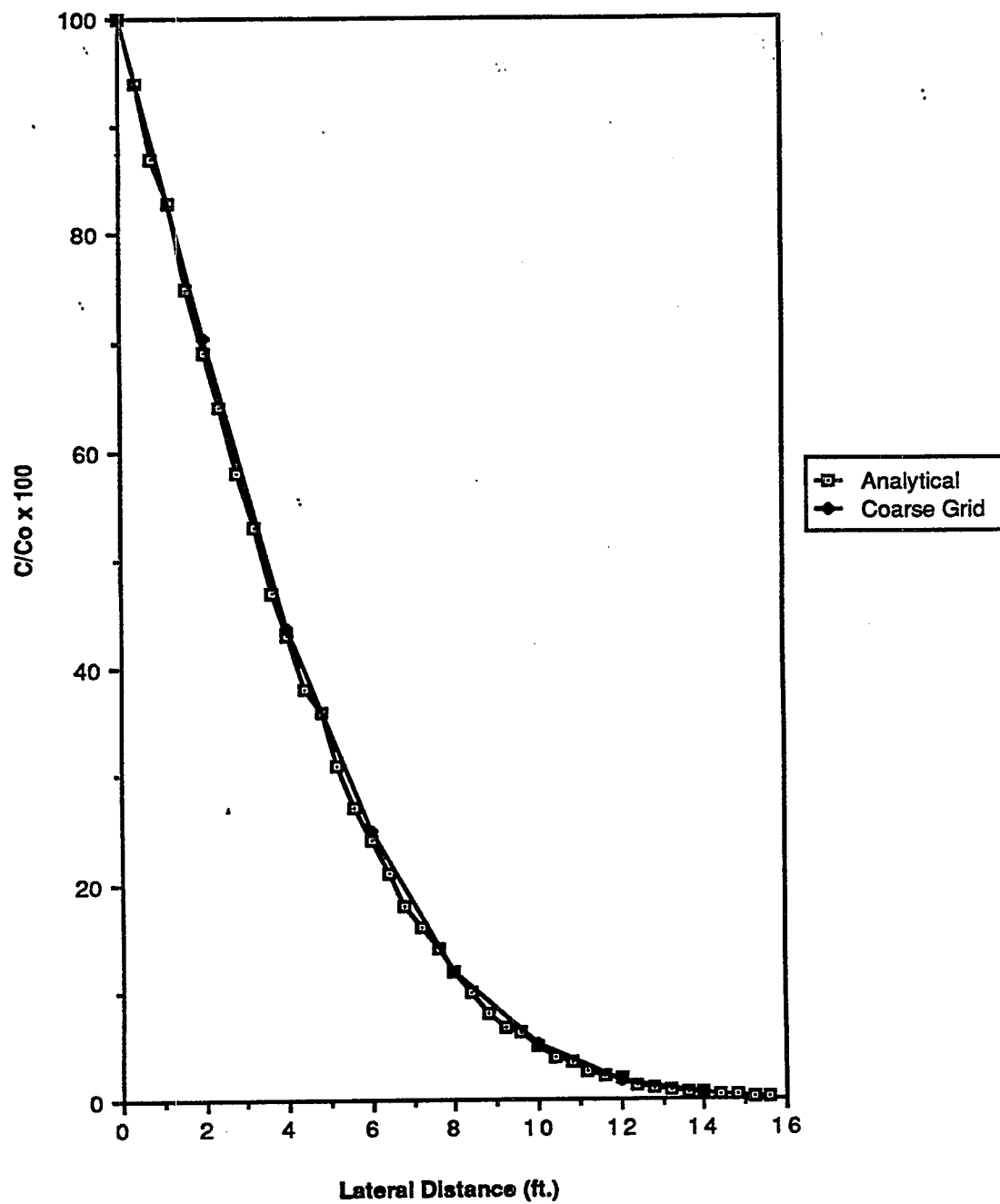
FIGURE I - 4. Analytic vs. DYNFLOW (coarse grid) at 96 hours.

APPENDIX J

VAPOR DIFFUSION TORTUOSITY AND EFFECTIVE SOIL DIFFUSION EQUATIONS

This appendix describes how air diffusion coefficients from Appendix D were scaled by values of vapor diffusion tortuosity. The result is an effective soil diffusion coefficient. Values of air diffusion coefficients, effective soil diffusion coefficients, and the vapor diffusion tortuosity coefficients used in making the UST vapor transport in simulations are presented in Appendix K.

Values for the vapor diffusion tortuosity factor were derived using an expression presented in Millington (1959):

$$\tau = \theta_a^{1/3} \cdot (\theta_a/\theta_\tau)^2 \qquad \text{(Equation J-1)}$$

where:

τ vapor diffusion tortuosity coefficient (dimensionless),
     $0 \leq \tau \leq 1$

θ_a air-filled porosity (cm^3/cm^3), $0 \leq \theta_a \leq \theta_t$

θ_t total porosity (cm^3/cm^3),
     $\theta_a \leq \theta_t \leq 1$

Although there exist many other expressions for vapor diffusion tortuosity (Buckingham, 1904; Penman, 1940; Alberton, 1979), recent research suggests that the Millington formulation is physically realistic (C. Bruell, U. Lowell, personal communication, 1987). Because of this, the Millington expression was used to calculate vapor diffusion tortuosity coefficients used in the DYNFLOW diffusion simulations.

Air diffusion coefficients, D_o, for the hydrocarbon vapors (see Appendix D) were scaled with the vapor diffusion tortuosity coefficient to obtain a diffusion coefficient suitable for modeling diffusion in a porous medium:

$$D_e = \tau \cdot D_o \qquad \text{(Equation J-2)}$$

where:

D_e effective soil diffusion coefficient (cm^2/sec)

D_o air diffusion coefficient (cm^2/sec)

Care should be taken in referring to the "effective diffusion coefficient," because when this coefficient is placed in the governing equation (see Equation H-1 in Appendix H), it is multiplied by the air-filled porosity, θ_a. For this reason, Equation J-2 does not include the air-filled porosity.

References for the equations presented above appear in Section 5 of this report.

APPENDIX K

SIMULATION MATRIX

This appendix presents tables of simulation parameters used in the modeling of diffusive transport of hydrocarbon vapors. Table K-1 contains parameters for the excavation zone/backfill, and Table K-2 is for the native soils.

The parameters required to calculate the effective soil diffusion coefficients (see Appendix J) are presented for both excavation zone backfill and native soils. Values of total porosity and moisture content were varied to simulate and assess the sensitivity of diffusion results to these properties.

Each of the six reported simulations were performed with a paved, impervious ground surface. Simulation Run Number 7 was the same as Number 1, except an open surface was simulated, with concentrations there fixed at zero, to represent free discharge of vapors at the surface.

Run Number 1 was taken to be the "average" situation that was used for plotting and analyzing "average" condition results in Sections 3 and 4 of this report. Runs 2 through 6 represent increasing moisture contents and decreasing air-filled porosities. These are hypothetical conditions which may be considered worse than average and were used solely to simulate the sensitivity of results to those conditions.

TABLE K-1

Simulation Properties of Backfill Materials

Simulation Run Number

Backfill Material	1 Dry Gravel	2 Dry Gravel	3 Moist Sand	4 Moist Sand	5 Wet Sand	6 Wet Sand	7 Dry Gravel
Total Porosity	0.20	0.20	0.30	0.30	0.40	0.40	0.20
Air-Filled Porosity	0.14	0.14	0.11	0.11	0.10	0.10	0.14
Water Filled Porosity	0.06	0.06	0.19	0.19	0.30	0.30	0.06
Saturation	0.30	0.30	0.63	0.63	0.75	0.75	0.30
Water Content	3%	3%	8%	8%	12%	12%	3%
Vapor Diffusion Tortuosity	0.25	0.25	0.07	0.07	0.03	0.03	0.25
Effective Diffusion Coefficient (cm^2/sec)	0.017	0.017	0.005	0.005	0.002	0.002	0.017
Effective Diffusion Coefficient (ft^2/hr)	0.065	0.065	0.020	0.020	0.008	0.008	0.065
Surface Conditon	Paved	Paved	Paved	Paved	Paved	Paved	Open

TABLE K-2

Simulated Native Soil Conditions

Simulation Number

Native Soil Material	1 Dry Silty Sand	2 Moist Silty Sand	3 Moist Sand	4 Wet Silty Sand	5 Wet Sand	6 Wet Clay	7 Dry Silty Sand
Total Porosity	0.20	0.20	0.30	0.20	0.40	0.45	0.20
Air-Filled Porosity	0.14	0.10	0.11	0.05	0.10	0.07	0.14
Water-Filled Porosity	0.06	0.10	0.19	0.15	0.30	0.38	0.06
Saturation	0.30	0.50	0.63	0.75	0.75	0.84	0.30
Water Content	3%	4%	8%	6%	12%	15%	3%
Vapor Diffusion Tortuosity	0.25	0.12	0.07	0.02	0.03	0.01	0.25
Effective Diffusion Coeficient (cm^2/Sec)	0.017	0.008	0.005	0.0015	0.002	0.0008	0.017
Effective Diffusion Coefficient (ft^2/hr)	0.065	0.031	0.020	0.006	0.008	0.003	0.065
Surface Condition	PAVED	PAVED	PAVED	PAVED	PAVED	PAVED	OPEN

APPENDIX L

MODFLOW VERIFICATION

This appendix presents the results of a simulation performed with MODFLOW, a computer program from the U.S. Geological Survey (McDonald and Harbaugh, 1984) that simulates three-dimensional groundwater flow. The purpose of this exercise was to reproduce simulation results produced by DYNFLOW with a groundwater flow program that is widely used throughout this country. MODFLOW is a modular, three-dimensional, finite difference flow program developed at the U.S.G.S. It uses a block-centered finite difference scheme, with solution by a strongly implicit procedure.

Physical dimensions of the MODFLOW diffusion model were the same as those used for the DYNFLOW diffusion model. The model was 44' wide, 10' long, and 24' deep. The tank dimensions were 12' by 6', surrounded by 2' of backfill. Half of the tank, backfill, and surrounding soils were simulated to reduce computational cost and time. This slicing was performed along the longitudinal symmetry axis through the tank.

Boundary conditions of the model were no-flow on the top, bottom, and sides. The tank sides were also treated as no-flow boundaries.

It was assumed that there was no background concentration within the system. Once the leak was initiated, a constant concentration node represented a constant source over time of vaporizing product. This point source was placed at the bottom of one end of the tank.

The diffusion properties of the native soil and backfill used in the DYNFLOW and MODFLOW simulations were 0.1348 ft^2/hr and 0.038 ft^2/hr, respectively. Simulations were performed with 4 time steps of 6 hours each, for a total simulation period of 24 hours.

L-1

Simulation results from DYNFLOW and MODFLOW were compared by plotting concentration-distance profiles. These concentration profiles were drawn for the two simulation times: 6 and 24 hours. Figures L-1 and L-2 are horizontal distance-concentration profiles drawn from the point source away from the tank, along the symmetry boundary, at a depth of 8 feet. A second profile was taken vertically through the entire thickness of the model, one foot away from the source, and the results plotted as Figures L-3 and L-4.

These profiles show close agreement between the results produced by DYNFLOW and MODFLOW. Generally, however, DYNFLOW produced slightly higher concentration values than MODFLOW, especially near the source. This minor discrepancy is probably due to differences in the grid set-up, geometric specification of the leak, and model interpolation procedures.

The rate of mass influx entering the system was simulated by both DYNFLOW and MODFLOW for each simulation time step. These mass influxes, plotted in Figure L-5, show fairly close agreement. MODFLOW, however, consistently produced about 5 percent more mass influx than DYNFLOW. This discrepancy is probably due to the difference in source geometry. In DYNFLOW, the point source was at the edge of the simulated tank. In MODFLOW, the leak was at the center of a 1 foot cubic "block" embedded in the tank.

Both models produced similar results, with minor differences due to the slight differences in numerical approximations. Closer agreement could have been reached by adjusting the MODFLOW source geometry to put the simulated leak at the edge of the UST; however, this was determined to be beyond the objectives of the MODFLOW-DYNFLOW comparison.

Another observation is that representation of the UST and the leakage source was easier to accomplish, and much smoother geometrically, with DYNFLOW than with MODFLOW. The leak was placed exactly at the edge of the UST in the DYNFLOW model; whereas, with MODFLOW, the leak had to be embedded in the tank. A node point-oriented application of MODFLOW could have alleviated this problem. With respect to tank geometry, MODFLOW could only produce a jagged, "blocked" approximation of a circle. The DYNFLOW

model, even though it was at the same 1 foot spacing, had triangular edges that simulated the cylinder much more closely, especially at the bottom of the tank where the leak was simulated.

Finally, note that the time-stepping scheme in MODFLOW uses an implicit technique with lumped storage, whereas DYNFLOW uses a Crank-Nicholson (trapezoidal) technique with proportional storage. Given the relatively small time steps, the differences here are probably small relative to the differences caused by the source and tank representation. In any event, these differences cannot be readily separated from the others.

In conclusion, it is clear that either program could be used to address this problem. For the given application, however, the DYNFLOW results are considered to be more defensible.
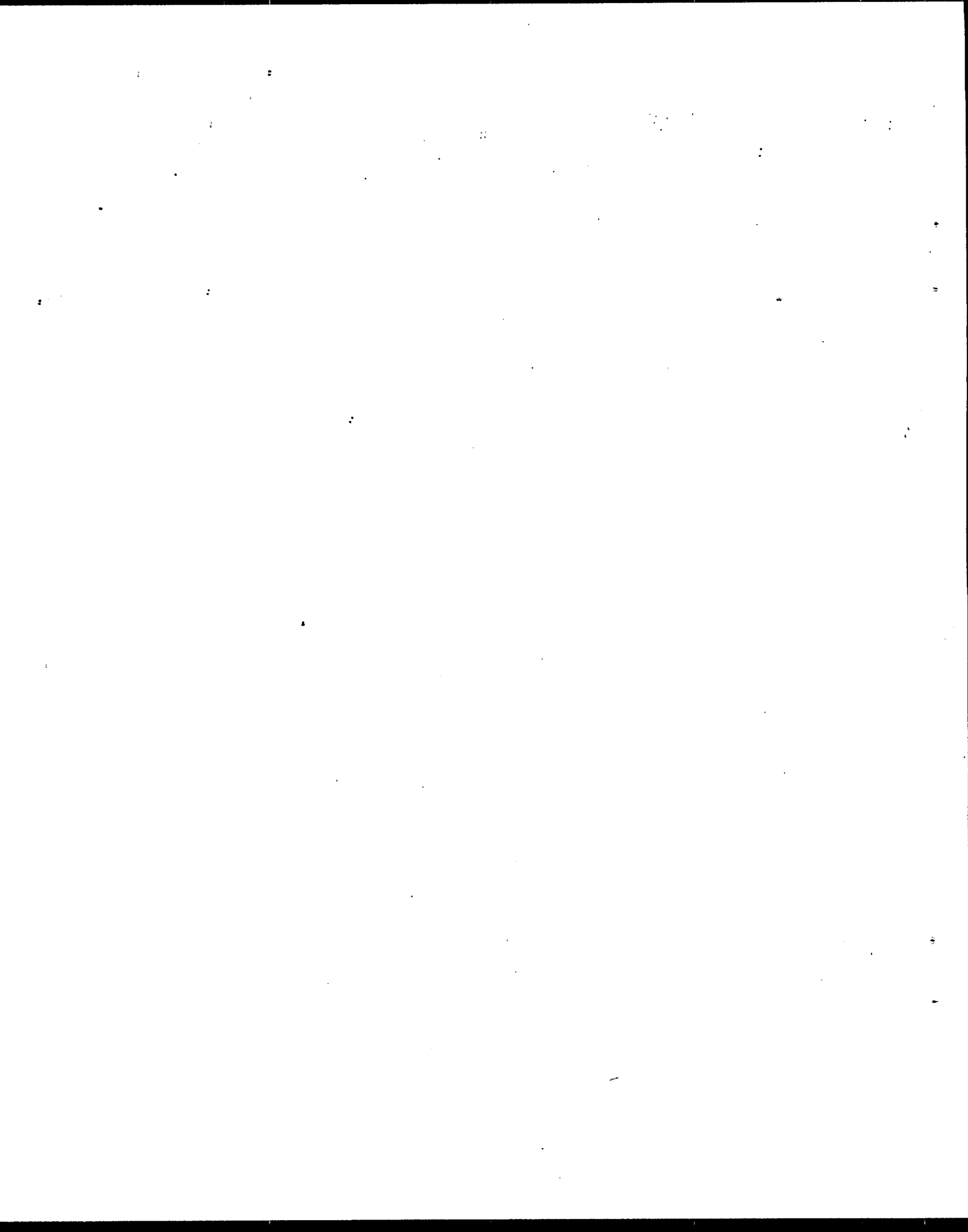
APPENDIX M

DYNFLOW COMMAND FILES

This Appendix contains listings of the command files used to make the simulation runs described in Appendix K. The simulation runs were made using the "iterative solver" version of DYNFLOW Release 4.0, called "DYNFLOW4B."

Not presented herein are the contents of the computer file ("KEEP.SAV") containing the specifications of grid information and lateral boundary conditions for the simulations. Sufficient information is provided in the body of this report. Also, listings of lateral boundary conditions and grid information are stored and available in CDM's project files.

```
REST                                                KEEP.SAV
TITLE
RUN #1 FROM FINAL REPORT 2/88, UST W.A. 1-4, 7400-104-MV-ANLY
RUN1.LOG AS OUTPUT; RUN1.CFI, KEEP.SAV AS INPUT
100% SOURCE AT LEVEL7 NODE 61.  UNITS ARE IN FEET AND HOURS.
!
!--- BACKFILL
PROP
2,  0.065, 0.065,  0.065,  1.0,  0.0,  0.0,
!--- NATIVE SOIL
PROP
1,  0.065, 0.065, 0.065,  1.0, 0.0, 0.0,
!
INIT   0.0
INIT  100.      LEVELSING     7     NODE SING    61
FIX             LEVELSING     7     NODE SING    61
!
ITER   1.
DT     1.
GOTIL  6.
DT     3.
GOTIL  12.
DT     6.
GOTIL  24.
SAVE                                              R1D01.SAV
DT     6.
GOTIL  84.
SAVE                                              R1D03.SAV
DT     6.
GOTIL  168.
SAVE                                              R1D07.SAV
DT     24.
GOTIL  252.
SAVE                                              R1D10.SAV
DT     24.
GOTIL  336.
SAVE                                              R1D14.SAV
DT     24.
GOTIL  420.
SAVE                                              R1D17.SAV
DT     24.
GOTIL  504.
SAVE                                              R1D21.SAV
DT     24.
GOTIL  588.
SAVE                                              R1D24.SAV
DT     24.
GOTIL  672.
SAVE                                              R1D28.SAV
XCFI
```

```
REST                                                        KEEP.SAV
TITLE
RUN #2 FROM FINAL REPORT 2/88, UST W.A. 1-4, 7400-104-MV-ANLY
RUN2.LOG AS OUTPUT; RUN2.CFI, KEEP.SAV AS INPUT
100% SOURCE AT LEVEL7 NODE 61.  UNITS ARE IN FEET AND HOURS.
!
!-- BACKFILL
PROP
2,  0.065, 0.065,  0.065,  1.0,  0.0,  0.0,
!-- NATIVE SOIL
PROP
1,  0.031, 0.031, 0.031,  1.0, 0.0, 0.0,
!
INIT    0.0
INIT   100.       LEVELSING      7      NODE SING     61
FIX               LEVELSING      7      NODE SING     61
!
ITER    1.
DT      1.
GOTIL   6.
DT      3.
GOTIL   12.
DT      6.
GOTIL   24.
SAVE                                                    R2D01.SAV
DT      6.
GOTIL   84.
SAVE                                                    R2D03.SAV
DT      6.
GOTIL   168.
SAVE                                                    R2D07.SAV
DT      24.
GOTIL   252.
SAVE                                                    R2D10.SAV
DT      24.
GOTIL   336.
SAVE                                                    R2D14.SAV
DT      24.
GOTIL   420.
SAVE                                                    R2D17.SAV
DT      24.
GOTIL   504.
SAVE                                                    R2D21.SAV
DT      24.
GOTIL   588.
SAVE                                                    R2D24.SAV
DT      24.
GOTIL   672.
SAVE                                                    R2D28.SAV
XCFI
```

```
REST                                              KEEP.SAV
TITLE
RUN #3 FROM FINAL REPORT 2/88, UST W.A. 1-4, 7400-104-MV-ANLY
RUN3.LOG AS OUTPUT; RUN3.CFI, KEEP.SAV AS INPUT
100% SOURCE AT LEVEL7 NODE 61.  UNITS ARE IN FEET AND HOURS.
!
!---- BACKFILL
PROP
2,  0.02, 0.02,  0.02,  1.0,  0.0,  0.0,
!---- NATIVE SOIL
PROP
1,  0.02, 0.02, 0.02,  1.0, 0.0, 0.0,
!
INIT    0.0
INIT    100.     LEVELSING    7     NODE SING    61
FIX              LEVELSING    7     NODE SING    61
!
ITER    1.
DT      1.
GOTIL   6.
DT      3.
GOTIL   12.
DT      6.
GOTIL   24.
SAVE                                              R3D01.SAV
DT      6.
GOTIL   84.
SAVE                                              R3D03.SAV
DT      6.
GOTIL   168.
SAVE                                              R3D07.SAV
DT      24.
GOTIL   252.
SAVE                                              R3D10.SAV
DT      24.
GOTIL   336.
SAVE                                              R3D14.SAV
DT      24.
GOTIL   420.
SAVE                                              R3D17.SAV
DT      24.
GOTIL   504.
SAVE                                              R3D21.SAV
DT      24.
GOTIL   588.
SAVE                                              R3D24.SAV
DT      24.
GOTIL   672.
SAVE                                              R3D28.SAV
XCFI
```

```
REST                                                          KEEP.SAV
TITLE
RUN #4 FROM FINAL REPORT 2/88, UST W.A. 1-4, 7400-104-MV-ANLY.
RUN4.LOG AS OUTPUT; RUN4.CFI, KEEP.SAV AS INPUT
100% SOURCE AT LEVEL7 NODE 61.   UNITS ARE IN FEET AND HOURS.
!
!—— BACKFILL
PROP
2,  0.02, 0.02,  0.02,  1.0,  0.0,  0.0,
!—— NATIVE SOIL
PROP
1,  0.006, 0.006, 0.006,  1.0, 0.0, 0.0,
!
INIT    0.0
INIT  100.        LEVELSING     7       NODE SING    61
FIX               LEVELSING     7       NODE SING    61
!
ITER   1.
DT     1.
GOTIL  6.
DT     3.
GOTIL  12.
DT     6.
GOTIL  24.
SAVE                                                    R4D01.SAV
DT     6.
GOTIL  84.
SAVE                                                    R4D03.SAV
DT     6.
GOTIL  168.
SAVE                                                    R4D07.SAV
DT     24.
GOTIL  252.
SAVE                                                    R4D10.SAV
DT     24.
GOTIL  336.
SAVE                                                    R4D14.SAV
DT     24.
GOTIL  420.
SAVE                                                    R4D17.SAV
DT     24.
GOTIL  504.
SAVE                                                    R4D21.SAV
DT     24.
GOTIL  588.
SAVE                                                    R4D24.SAV
DT     24.
GOTIL  672.
SAVE                                                    R4D28.SAV
XCFI
```

```
REST                                                    KEEP.SAV
TITLE
RUN #5 FROM FINAL REPORT 2/88, UST W.A. 1-4, 7400-104-MV-ANLY
RUN5.LOG AS OUTPUT; RUN5.CFI, KEEP.SAV AS INPUT
100% SOURCE AT LEVEL7 NODE 61.  UNITS ARE IN FEET AND HOURS.
!
!--- BACKFILL
PROP
2,  .008, .008,  .008,  1.0,  0.0,  0.0,
!--- NATIVE SOIL
PROP
1,  .008, .008, .008,  1.0, 0.0, 0.0,
!
INIT   0.0
INIT   100.       LEVELSING    7      NODE SING    61
FIX               LEVELSING    7      NODE SING    61
!
ITER   1.
DT     1.
GOTIL  6.
DT     3.
GOTIL  12.
DT     6.
GOTIL  24.
SAVE                                               R5D01.SAV
DT     6.
GOTIL  84.
SAVE                                               R5D03.SAV
DT     6.
GOTIL  168.   .
SAVE                                               R5D07.SAV
DT     24.
GOTIL  252.
SAVE                                               R5D10.SAV
DT     24.
GOTIL  336.
SAVE                                               R5D14.SAV
DT     24.
GOTIL  420.
SAVE                                               R5D17.SAV
DT     24.
GOTIL  504.
SAVE                                               R5D21.SAV
DT     24.
GOTIL  588.
SAVE                                               R5D24.SAV
DT     24.
GOTIL  672.
SAVE                                               R5D28.SAV
XCFI
```

```
REST
TITLE
RUN #6 FROM FINAL REPORT 2/88, UST W.A. 1-4, 7400-104-MV-ANLY
RUN6.LOG AS OUTPUT; RUN6.CFI, KEEP.SAV AS INPUT
100% SOURCE AT LEVEL7 NODE 61.  UNITS ARE IN FEET AND HOURS.
!
!-- BACKFILL
PROP
2,  0.008, 0.008,  0.008,  1.0,  0.0,  0.0,
!-- NATIVE SOIL
PROP
1,  0.003, 0.003, 0.003,  1.0, 0.0, 0.0,
!
INIT   0.0
INIT   100.      LEVELSING     7     NODE SING    61
FIX              LEVELSING     7     NODE SING    61
!
ITER   1.
DT     1.
GOTIL  6.
DT     3.
GOTIL  12.
DT     6.
GOTIL  24.
SAVE                                                   R6D01.SAV
DT     6.
GOTIL  84.
SAVE                                                   R6D03.SAV
DT     6.
GOTIL  168.    .
SAVE                                                   R6D07.SAV
DT     24.
GOTIL  252.
SAVE                                                   R6D10.SAV
DT     24.
GOTIL  336.
SAVE                                                   R6D14.SAV
DT     24.
GOTIL  420.
SAVE                                                   R6D17.SAV
DT     24.
GOTIL  504.
SAVE                                                   R6D21.SAV
DT     24.
GOTIL  588.
SAVE                                                   R6D24.SAV
DT     24.
GOTIL  672.
SAVE                                                   R6D28.SAV
XCFI
```

```
REST                                                    KEEP.SAV
TITLE:
RUN #7 FROM FINAL REPORT 2/88, UST W.A. 1-4, 7400-104-MV-ANLY
RUN7.LOG AS OUTPUT; RUN7.CFI, KEEP.SAV AS INPUT
100% SOURCE AT LEVEL7 NODE 61.   UNITS ARE IN FEET AND HOURS.
!
!—— BACKFILL
PROP
2,  0.065, 0.065,  0.065,  1.0,  0.0,  0.0,
!—— NATIVE SOIL
PROP
1,  0.065, 0.065, 0.065,  1.0,  0.0,  0.0,
!
INIT   0.0
INIT  100.      LEVELSING      7      NODE SING     61
FIX             LEVELSING      7      NODE SING     61
FIX             LEVELSING     15      NODE ALL
!
ITER   1.
DT     1.
GOTIL  6.
DT     3.
GOTIL  12.
DT     6.
GOTIL  24.
SAVE                                                    R7D01.SAV
DT     6.
GOTIL  84.
SAVE                                                    R7D03.SAV
DT     6.
GOTIL  168.
SAVE                                                    R7D07.SAV
DT     24.
GOTIL  252.
SAVE                                                    R7D10.SAV
DT     24.
GOTIL  336.
SAVE                                                    R7D14.SAV
DT     24.
GOTIL  420.
SAVE                                                    R7D17.SAV
DT     24.
GOTIL  504.
SAVE                                                    R7D21.SAV
DT     24.
GOTIL  588.
SAVE                                                    R7D24.SAV
DT     24.
GOTIL  672.
SAVE                                                    R7D28.SAV
XCFI
```

APPENDIX N

TABULAR DYNFLOW RESULTS

This Appendix contains tables of DYNFLOW simulation results for the scenarios that were described in Appendix K. Presented are concentration time histories and vapor influx time histories. All results are in terms of "100 per cent" equilibrium vapor concentration at the leakage source, and they can therefore be transformed into estimated concentrations and leak volumes according to the methods and equations described in the report and in Appendix G.

List of Tables

TABLE N-1

TIME HISTORY OF SIMULATED VAPOR CONCENTRATIONS FOR RUN NUMBER 1

DYNFLOW Concentrations Expressed as Percent of Source Concentration

Simulation Day	Nearby Sensors		Intermediate Sensors		Distant Sensors	
	Deep #1	Shallow #2	Deep #3	Shallow #4	Deep #5	Shallow #6
1	5.314	0.010	0.	0.	0.	0.
3.5	9.154	0.355	0.372	0.	0.	0.
7	10.688	0.952	0.974	0.132	0.010	0.
10.5	11.500	1.471	1.367	0.308	0.049	0.012
14	11.986	1.918	1.674	0.505	0.101	0.039
17.5	12.227	2.167	1.908	0.682	0.154	0.067
21	12.537	2.311	2.040	0.801	0.191	0.093
24.5	12.482	2.461	2.158	0.924	0.230	0.127
28	12.603	2.609	2.265	1.038	0.270	0.167

TABLE N-2

TIME HISTORY OF SIMULATED VAPOR CONCENTRATIONS FOR RUN NUMBER 2

DYNFLOW Concentrations Expressed as Percent of Source Concentration

Simulation Day	Nearby Sensors		Intermediate Sensors		Distant Sensors	
	Deep #1	Shallow #2	Deep #3	Shallow #4	Deep #5	Shallow #6
1	5.405	0.001	0.002	0.	0.	0.
3.5	10.141	0.364	0.382	0.010	0.001	0.
7	12.557	1.046	1.124	0.133	0.013	0.001
10.5	13.812	1.687	1.747	0.362	0.053	0.009
14	14.623	2.221	2.217	0.588	0.105	0.032
17.5	15.183	2.701	2.603	0.842	0.172	0.072
21	15.601	3.091	2.922	1.084	0.243	0.121
24.5	15.961	3.485	3.191	1.349	0.322	0.198
28	16.248	3.809	3.425	1.576	0.398	0.274

TABLE N-3

TIME HISTORY OF SIMULATED VAPOR CONCENTRATIONS FOR RUN NUMBER 3

DYNFLOW Concentrations Expressed as Percent of Source Concentration

Simulation Day	Nearby Sensors		Intermediate Sensors		Distant Sensors	
	Deep #1	Shallow #2	Deep #3	Shallow #4	Deep #5	Shallow #6
1	1.799	0.	0.	0.	0.	0.
3.5	5.550	0.008	0.001	0.	0.	0.
7	7.766	0.121	0.112	0.001	0.	0.
10.5	8.935	0.308	0.307	0.008	0.	0.
14	9.673	0.503	0.508	0.028	0.	0.
17.5	10.136	0.671	0.689	0.058	0.002	0.
21	10.530	0.841	0.862	0.099	0.004	0.
24.5	10.900	1.046	1.027	0.151	0.009	0.001
28	11.095	1.181	1.165	0.202	0.018	0.002
					0.029	0.004

TABLE N-4

TIME HISTORY OF SIMULATED VAPOR CONCENTRATIONS FOR RUN NUMBER 4

DYNFLOW Concentrations Expressed as Percent of Source Concentration

Simulation Day	Nearby Sensors		Intermediate Sensors		Distant Sensors	
	Deep #1	Shallow #2	Deep #3	Shallow #4	Deep #5	Shallow #6
1	1.804	0.	0.	0.	0.	0.
3.5	5.708	0.008	0.003	0.	0.	0.
7	8.544	0.105	0.103	0.	0.	0.
10.5	10.308	0.277	0.306	0.009	0.	0.
14	11.558	0.519	0.559	0.030	0.001	0.
17.5	12.492	0.724	0.800	0.059	0.004	0.
21	13.252	0.986	1.078	0.111	0.010	0.001
24.5	13.874	1.231	1.345	0.174	0.019	0.002
28	14.384	1.454	1.575	0.245	0.029	0.004

TABLE N-5

TIME HISTORY OF SIMULATED VAPOR CONCENTRATIONS FOR RUN NUMBER 5

DYNFLOW Concentrations Expressed as Percent of Source Concentration

Simulation Day	Nearby Sensors		Intermediate Sensors		Distant Sensors	
	Deep #1	Shallow #2	Deep #3	Shallow #4	Deep #5	Shallow #6
1	0.263	0.	0.	0.	0.	0.
3.5	2.677	0.	0.	0.	0.	0.
7	4.817	0.001	0.	0.	0.	0.
10.5	6.161	0.023	0.011	0.	0.	0.
14	7.081	0.063	0.052	0.	0.	0.
17.5	7.774	0.124	0.110	0.005	0.	0.
21	8.310	0.189	0.187	0.002	0.	0.
24.5	8.746	0.267	0.264	0.006	0.	0.
28	9.110	0.344	0.348	0.011	0.	0.

TABLE N-6

TIME HISTORY OF SIMULATED VAPOR CONCENTRATIONS FOR RUN NUMBER 6

DYNFLOW Concentrations Expressed as Percent of Source Concentration

Simulation Day	Nearby Sensors		Intermediate Sensors		Distant Sensors	
	Deep	Shallow	Deep	Shallow	Deep	Shallow
	#1	#2	#3	#4	#5	#6
1	0.267	0.	0.	0.		
3.5	2.682	0.	0.001	0.	0.	0.
7	4.884	0.001	0.	0.	0.	0.
10.5	6.387	0.019	0.011	0.	0.	0.
14	7.530	0.056	0.047	0.	0.	0.
17.5	8.439	0.108	0.104	0.	0.	0.
21	9.186	0.177	0.177	0.002	0.	0.
24.5	9.818	0.251	0.259	0.005	0.	0.
28	10.358	0.331	0.355	0.010	0.	0.

TABLE N-7

TIME HISTORY OF SIMULATED VAPOR CONCENTRATIONS FOR RUN NUMBER 7

DYNFLOW Concentrations Expressed as Percent of Source Concentration

Simulation Day	Nearby Sensors		Intermediate Sensors		Distant Sensors	
	Deep #1	Shallow #2	Deep #3	Shallow #4	Deep #5	Shallow #6
1	5.314	0.009	0.001	0.001	0.	0.
3.5	9.154	0.335	0.372	0.010	0.	0.
7	10.686	0.785	0.974	0.108	0.016	0.001
10.5	11.463	1.036	1.397	0.209	0.054	0.005
14	11.687	1.148	1.607	0.275	0.091	0.016
17.5	11.902	1.229	1.783	0.325	0.132	0.027
21	12.091	1.289	1.928	0.360	0.174	0.038
24.5	12.250	1.334	2.049	0.386	0.214	0.047
28	12.384	1.369	2.150	0.407	0.251	0.056

TABLE N-8

Time-Histories of DYNFLOW - Simulated Vapor Fluxes

Simulation Days	Inflow at Leak (cu. ft/hr)							Outflow through surface (cu. ft/hr)
	RUN 1	RUN 2	RUN 3	RUN 4	RUN 5	RUN6	RUN 7	
0.04	17.594	18.495	6.121	6.119	2.524	2.522	18.505	-0.001
0.08	16.229	16.858	5.878	5.862	2.550	2.545	16.860	-0.001
0.13	15.630	16.100	5.705	5.687	2.491	2.487	16.123	-0.001
0.17	15.237	15.616	5.473	5.473	2.436	2.433	15.627	-0.001
0.21	14.952	15.302	5.337	5.339	2.353	2.352	15.333	-0.001
0.25	14.750	15.008	5.229	5.232	2.311	2.309	15.061	-0.001
0.38	14.313	14.485	4.986	4.981	2.232	2.226	14.494	-0.003
0.50	14.033	14.151	4.858	4.841	2.144	2.156	14.180	-0.008
0.75	13.689	13.756	4.643	4.640	2.053	2.046	13.620	-0.007
1.00	13.473	13.484	4.523	4.518	1.988	1.981	13.552	-0.009
1.25	13.320	13.311	4.449	4.444	1.937	1.936	13.387	-0.009
1.50	13.205	13.168	4.386	4.378	1.903	1.900	13.286	-0.016
1.75	13.174	13.043	4.239	4.326	1.874	1.880	13.174	-0.028
2.00	13.081	12.938	4.301	4.282	1.850	1.859	13.080	-0.030
2.25	13.101	12.883	4.266	4.241	1.842	1.838	13.101	-0.053
2.50	13.034	12.806	4.228	4.210	1.824	1.820	13.034	-0.074
2.75	12.982	12.808	4.204	4.182	1.808	1.805	12.982	-0.104
3.00	12.935	12.744	4.182	4.157	1.795	1.791	12.935	-0.137
3.25	12.817	12.688	4.163	4.134	1.782	1.779	12.817	-0.170
3.50	12.961	12.637	4.159	4.114	1.765	1.768	12.961	-0.204
3.75	12.929	12.590	4.142	4.095	1.756	1.751	12.928	-0.235
4.00	12.887	12.489	4.127	4.089	1.747	1.742	12.887	-0.282
4.25	12.851	12.580	4.103	4.072	1.739	1.734	12.851	-0.331
4.50	12.691	12.551	4.091	4.056	1.732	1.727	12.691	-0.380
4.75	12.789	12.509	4.080	4.042	1.725	1.720	12.789	-0.446
5.00	12.654	12.471	4.084	4.024	1.719	1.713	12.654	-0.473
5.25	12.751	12.437	4.074	4.013	1.718	1.715	12.751	-0.547
5.50	12.615	12.406	4.064	3.994	1.712	1.708	12.616	-0.576
5.75	12.658	12.321	4.055	3.983	1.707	1.703	12.658	-0.661
6.00	12.655	12.281	4.043	3.972	1.702	1.697	12.655	-0.736
6.25	12.640	12.263	4.036	3.962	1.697	1.692	12.640	-0.815

TABLE N-8 (continued)

Time-Histories of DYNFLOW - Simulated Vapor Fluxes

Simulation Days	Inflow at Leak (cu. ft/hr)							Outflow through surface (cu. ft/hr)
	RUN 1	RUN 2	RUN 3	RUN 4	RUN 5	RUN6	RUN 7	
6.50	12.636	12.243	4.038	3.952	1.693	1.687	12.636	-0.887
6.75	12.623	12.225	4.032	3.943	1.688	1.683	12.623	-0.958
7.00	12.613	12.182	4.028	3.934	1.684	1.679	12.614	-1.027
8.00	12.548	12.167	3.999	3.917	1.672	1.656	12.549	-1.197
9.00	12.473	12.091	3.979	3.888	1.661	1.644	12.473	-1.347
10.00	12.481	12.048	3.967	3.862	1.646	1.637	12.769	-1.583
10.50	12.633	12.060	3.975	3.872	1.647	1.632	12.462	-1.721
11.50	12.442	11.982	3.935	3.829	1.643	1.623	12.422	-2.111
12.50	12.394	11.955	3.923	3.809	1.636	1.614	12.425	-2.299
13.50	12.385	11.924	3.962	3.805	1.629	1.607	12.413	-2.484
14.00	12.351	12.041	3.947	3.794	1.623	1.605	12.425	-2.532
15.00	12.480	11.881	3.899	3.772	1.614	1.592	12.406	-2.660
16.00	12.337	11.847	3.894	3.759	1.609	1.586	12.383	-2.841
17.00	12.315	11.819	3.888	3.745	1.605	1.587	12.390	-2.939
17.50	12.310	11.829	3.917	3.758	1.613	1.584	12.389	-2.984
18.50	12.308	11.792	3.879	3.730	1.609	1.579	12.376	-3.071
19.50	12.299	11.780	3.874	3.752	1.606	1.573	12.354	-3.212
20.50	12.302	11.756	3.921	3.743	1.602	1.567	12.361	-3.293
21.00	12.302	11.763	3.902	3.729	1.621	1.568	12.361	-3.325
22.00	12.290	11.719	3.916	3.724	1.591	1.561	12.349	-3.396
23.00	12.280	11.694	3.907	3.720	1.595	1.557	12.329	-3.508
24.00	12.282	11.688	3.899	3.710	1.586	1.553	12.336	-3.576
24.50	12.285	11.693	3.875	3.724	1.607	1.561	12.336	-3.602
25.50	12.272	11.668	3.856	3.696	1.589	1.555	12.326	-3.659
26.50	12.263	11.646	3.854	3.689	1.588	1.552	12.307	-3.753
27.50	12.263	11.642	3.854	3.665	1.583	1.549	12.314	-3.811
28.00	12.266	11.647	3.858	3.686	1.600	1.571	12.313	-3.833